

Hydrochar from In- dustrial Biosludge

Is there an application for
Fischer-Tropsch biosludge
hydrochar produced via hy-
drothermal carbonization
L.D. van der Loos

Hydrochar from Industrial Biosludge

Is there an application for Fischer-Tropsch
biosludge hydrochar produced via
hydrothermal carbonization

by

L.D. van der Loos

to obtain the degree of Master of Science
at the Delft University of Technology,
to be defended publicly on Thursday April 20, 2023 at 16:30 AM.

Student number: 4398556
Project duration: February 1, 2022 – April 20, 2023
Thesis committee: Dr. L. Cutz, TU Delft, daily supervisor
J. A. Pavez Jara, TU Delft, daily supervisor
Ir. G. Stockinger, Shell
Prof. dr. ir. W. de Jong, TU Delft, supervisor
Prof. dr. ir. M. de Kreuk, TU Delft, supervisor
Prof. dr. ir. R. Lindeboom, TU Delft, supervisor

This thesis is confidential and cannot be made public until April 20, 2028.

An electronic version of this thesis is available at <http://repository.tudelft.nl/>.

Abstract

One way to create a more circular system and reduce greenhouse gas emissions is by improving the utilization of secondary streams, including sludge such as Fischer-Tropsch biosludge that is discarded through the common practice of landfilling. Biochar, which has accumulated increased interest in recent times, has significant potential for decreasing carbon emissions. This master thesis was set up as an opportunity-based research project to understand the utilization of Fischer-Tropsch biosludge by the hydrothermal carbonisation process and characterizing of its product phases. A central composite surface response design was used to conduct experiments aimed at analyzing the impact of temperature and time on the characteristics of the phases. Three different levels of the factors have been used. Three phases have been identified: a gas phase, an aqueous phase, and a biochar phase. The high ash content and low surface area of the biochar made it difficult to determine a specific use case for the biochar. Yet, the aqueous phase has low ash and possible potential for biogas creation by anaerobic digestion. The gas phase is quantitatively not of significance. Stockpiling the biochar could sequester carbon credits and more research can be conducted to find a post- or pre-treatment to improve the biochar for a social-economically benefiting application.

Contents

1	Introduction	1
1.1	Background	1
1.2	Problem Statement	3
1.3	Research Gap	3
1.4	Research Question	4
1.5	Research Objective	4
1.6	Research Scope	5
1.7	Research Method	5
1.8	Report Outline	6
2	Literature Study Concerning Hydrochar	7
2.1	Literature Study Outline	7
2.2	Conversion Technologies	9
2.3	Sludge	9
2.3.1	Biosludge	10
2.4	Regulations	11
2.5	General Characteristics of Char, Hydrothermal Carbonization Aqueous and Gas Phase	12
2.5.1	Fixed Carbon and Volatile Mater.	12
2.5.2	Ash	13
2.5.3	Dewaterability: Bound and Free Water	14
2.5.4	Aqueous Phase	15
2.5.5	Gas Phase	16
2.6	Hydrochar Compared to Biochar	16
2.7	Hydrothermal Carbonization Parameter Influences	17
2.7.1	Reaction Mechanisms	17
2.7.2	Temperature	18
2.7.3	Residence Time	19
2.7.4	Severity	19
2.7.5	Solid Loading	20
2.7.6	Catalyst	20
2.8	Heavy Metals and Fertilizer Elements	20
2.8.1	Heavy Metals	21
2.8.2	Phosphorus	21
2.8.3	Morphology	21
2.9	Applications	22
2.9.1	Catalyst	22
2.9.2	Soil Amendment	22
2.9.3	Absorbent	24
2.9.4	Fuel	25
2.9.5	Battery	25
2.9.6	Anaerobic Digestion	25
2.10	Conclusion	26
3	Materials and Methods	27
3.1	Experimental Design	27
3.2	Material	27
3.3	Experiment Procedure for HTC	28
3.4	Analyses Methods	28
3.4.1	Mass Yields	29
3.4.2	Hydrochar and Aqueous Phase pH	29

3.4.3	Ammonia and COD Hach Kits	30
3.4.4	Inductively Coupled Plasma - Optical Emission Spectrometry	30
3.4.5	Ultimate Analysis	30
3.4.6	Proximate Analysis	30
3.4.7	Bomb Calorimetry	31
3.4.8	XRD and XRF	31
3.4.9	Surface Area	31
3.4.10	Leaching of Heavy Metals and Total Organic Carbon	31
3.4.11	Gas Chromatography - Mass Spectrometry Biogas	31
4	Experimental Results and Discussion	33
4.1	HTC Product Distribution.	33
4.2	Ultimate Analysis	34
4.3	Proximate Analysis	36
4.4	Hydrochar pH.	36
4.5	Bomb Calorimetry	37
4.6	ICP-OES Analysis	38
4.6.1	Aqueous Phase.	38
4.6.2	Biochar	40
4.7	Leaching of Heavy metals and Total Organic Carbon	42
4.8	Absorption	43
4.9	XRD of Biochars and XRF of Biochar Ashes	44
4.10	Aqueous Phase Analysis.	45
4.11	Gas Phase Analysis	47
4.12	Optimization	47
4.13	Mass Balance.	49
5	Conclusions	51
6	Recommendations	53
	Appendices	57
A	Raw Data, Statistics, and Model Equations	59
A.1	Aqueous Phase Literature	59
A.2	Model Equations	59
A.3	ICP-OES	60
A.3.1	Aqueous Phase.	60
A.3.2	Hydrochar.	60
A.3.3	Leaching	60
A.4	Dry Sludge	61
A.5	Mass Balance.	61

Glossary

- BC** biochar. 2, 6, 7, 9, 11–13, 16, 17, 22–24, 26, 34–38, 41, 43, 44, 46, 47, 49, 51–55
- BET** Brunauer–Emmett–Teller theory. 31, 43, 54
- CAPEX** capital expenditure. 19, 54
- COD** chemical oxygen demand. 4, 15, 20, 29, 30, 45, 46, 51, 54
- EBC** European Biochar Certificate. 2, 3, 11, 26, 35, 38
- ETPs** Effluent Treatment Plant. 1–3, 10
- EU** European Union. 11
- FC** fixed carbon. 4, 12, 13, 16, 20, 25, 26, 30, 36, 52
- GC-MC** Gas chromatography Mass Spectroscopy. 31, 54
- GHG** greenhouse gas. 1, 10, 17, 22, 55
- GTL** gas to liquid. 2, 3, 27
- HC** hydrochar. 1–7, 9, 11–14, 16–31, 33–36, 38, 39, 41, 42, 45–49, 51, 60, 61, 65, 66
- HHV** higher heating value. 20, 25, 26, 37, 38, 47, 51
- HM** heavy metals. 1, 3, 4, 7, 8, 10, 11, 13, 20, 21, 23, 25, 26, 28, 30, 31, 38, 39, 41, 42, 46, 47, 51, 53, 54, 60, 63
- HTC** hydrothermal carbonization. 1–5, 7, 9, 12–20, 23, 25–29, 33–38, 43, 46, 49, 51, 52, 54, 55, 59, 61, 66
- HTG** hydrothermal gasification. 9
- HTL** hydrothermal liquefaction. 9, 21, 26
- IBI** International Biochar Initiative. 2, 3, 11, 26, 38
- ICP-OES** inductively coupled plasma atomic emission spectroscopy. 30, 31, 38–44, 47, 48, 51, 53, 60, 63–66
- LCA** live cycle assessment. 25
- OFGs** oxygen-containing functional groups. 16, 24
- PAHs** Polycyclic Aromatic Hydrocarbons. 1, 3, 11, 23, 24
- PFR** persistent free radical. 16, 19
- SD** standard deviation. 33
- SSA** specific surface area. 16

TGA thermogravimetric analysis. 30

TOC Total Organic Carbon. 15, 42

VM volatile mater. 4, 12, 13, 16, 19, 23, 25, 26, 30, 36, 42

WAS waste activated sludge. 9, 10, 28

WHC water holding capacity. 11, 22, 23

XRD X-ray diffraction. 31

XRF X-ray fluorescence. 31, 44, 45

Introduction

Greenhouse gas (GHG) emissions must be reduced across many sectors in order to meet the United Nations' 2050 target. In terms of GHG emissions, incineration of sludge is considered the worst option, being around 2.5 times more polluting than reusing sludge as cement ingredient, which comes in second last place at around 89 tonnes of CO₂-equivalent per tonne sludge (Y.-C. Chen & Kuo, 2016). Unfortunately, incineration is the second method of disposal, and it is becoming more popular across Europe. (EurEau, 2021; Fytili & Zabaniotou, 2008). After incineration, it is estimated that approximately 30% of the solids remain as ash (Fytili & Zabaniotou, 2008). These ashes are disposed of in landfills where they can leach, and depending on the source of the sludge, it may be toxic due to the heavy metals (HM) content (Fytili & Zabaniotou, 2008). Aside from emissions, landfilling sludge emits an unpleasant odour that pollutes the surrounding air and may attract vectors that can spread contagious diseases (Garg, 2009).

Valorization of sludge can reduce the 1.57% of the total global GHG emissions Effluent Treatment Plant (ETPs) are emitting, increase circularity and create revenue (Lawal et al., 2021; L. Lu et al., 2018; Pandey & Prakash, 2019). Sludge can be utilised to create valuable products through sludge treatment options, such as composting, anaerobic digestion, pyrolysis, and hydrothermal carbonization (HTC) (Malool et al., 2022). These processes allow residual sludge to be converted into heat generation, carbon sequestration, absorbent, anaerobic digestion, or soil amendment products (Appels et al., 2008; Masoumi et al., 2021). Nonetheless, one of the main challenges of using industrial biosludge as feedstock is the high content of HM or other pollutants, such as Polycyclic Aromatic Hydrocarbons (PAHs), which can have a negative influence on the environment when handled carelessly.

The goal of this thesis is to assess if hydrochar (HC) from industrial biosludge processed by HTC complies with existing regulations and possesses the necessary characteristics to be used as a resource for applications in the energy storage and conversion field. To ensure that a product resulting from the HTC process is sustainable and legal for commercial use, it is crucial to compare its chemical composition to relevant regulations and evaluate its overall characteristics. By doing so, one can ensure that the product meets the necessary standards for safety, quality, and environmental impact. If this conversion path is feasible, it could create opportunities for de-carbonizing industries by utilizing industrial sludge in combination with HTC. This is an opportunity-based master thesis in which Shell provides biosludge from a Fischer-Tropsch process as a feedstock, combined with the expertise of the Process & Energy department and the Civil Engineering and Geosciences department from the TU Delft.

1.1. Background

The Paris Agreement, signed by United Nations Framework Convention on Climate Change parties, resulted in a commitment to reduce emissions, invest in clean technology, and eventually reverse climate change (UNFCCC, n.d.). Using industrial residual streams for manufacturing new products will help meet the Paris Agreement's targets by increasing circularity (Padhye et al., 2022; The Government of

Japan, 2019). The circular economy is a production and consumption model involving sharing, leasing, reusing, repairing, refurbishing, upcycling, and recycling existing materials and products (Geissdoerfer et al., 2017). A potential residual stream is sludge obtained from ETPs, where standard processing methods such as disposal or incineration consume energy, release harmful pollutants, and discard valuable nutrients (Usman et al., 2012). Creating new valuable products from industrial sludge can up-cycle sludge contributing to the circular economy, reducing ETPs emissions and waste, and creating sustainable substitutes for current fossil fuel-derived products.

Industrial and municipal ETPs produce an increasing amount of biosludge worldwide, which requires adequate processing or disposal to prevent detrimental environmental impact. Biosludge is the main residual stream obtained from ETPs consisting of circa 98% water, biological material and nutrients used in the treatment process (Mowla et al., 2013). It is estimated that the total wet amount of sludge in Europe, the United States of America and China was 240 million tonnes during the period 2007-2013 (Gao et al., 2020). Zooming in on upcoming economies like China; wastewater treatment capacity has more than doubled in the last decade, and sludge production is expected to increase by 15% per year, addressing the need for better treatment of sludge (X. Zhang et al., 2022). This increasing amount of sludge can harm the environment through CO₂ equivalent emissions, polluting water or arable land if not handled properly (W. Liu et al., 2021).

HC is produced by wet thermochemical conversion processes such as HTC and hydrothermal liquefaction. Compared to dry thermochemical processes such as pyrolysis, HTC provides higher mass yields using less energy input and less severe temperatures (Akbari et al., 2021; Heidari et al., 2019; L. Wang et al., 2014). Also, dry conversion technologies create biochar (BC), which is chemically different from HC.

By turning the increasing amount of sludge produced globally into a useful and profitable commodity, HC products made from biosludge could support the circular economy. These HC products made using HTC can play a pivotal role in four challenges:

1. (Re)storing carbon; reducing the atmospheric carbon.
2. Reducing landfilling and incineration; decreasing pollution.
3. Decrease energy use for disposal and drying of sludge; reducing energy usage of effluent treatment.
4. Implementation as a valuable product and reusing resources; socioeconomic profit to gain.

These four points let industrial biosludge contribute to the transition from a carbon-based economy to a more circular and sustainable economy by using HTC. Although HC is not widely available, it has shown potential as a soil amendment, adsorbent, a solid biofuel, or in energy storage as a green carbon alternative (Fang et al., 2018; Huezco et al., 2021; Monica et al., 2022; H. B. Sharma et al., 2021). Three factors are critical in developing an environmentally friendly and commercially viable HC product:

- (a) Compliance with regulation stated by authorities.
- (b) Residual gas and aqueous HTC streams must cause fewer complications than the gained benefits.
- (c) It has to be economically profitable.

No institutes are setting regulations for HC, but two institutes are setting standards for BC, among them the International Biochar Initiative (IBI) and European Biochar Certificate (EBC). These institutes aim to limit the risks of BC usage (IBI, 2015; Schmidt et al., 2022). The EBC is a voluntary industry standard in Europa but is already obligatory in Switzerland for agricultural products (Schmidt et al., 2022). Probably a similar regulation will become obliged for HC.

The biosludge used in this thesis comes from a gas to liquid (GTL) Fischer-Tropsch site from Shell. The gas feedstock (syngas) results from the partial oxidation of natural gas and oxygen. Syngas is a

mixture of carbon monoxide and hydrogen gas (Shell, 2022). This syngas is fed to a catalytic Fischer-Tropsch reactor to produce a waxy mixture of paraffinic hydrocarbons. Following the Fischer-Tropsch reactor, a hydrocracker unit cuts the paraffinic hydrocarbons into desired chain lengths, where the desired product fractions vary by global market demand. These products are then distilled into marketable oil products (F. Zhu et al., 2016). In addition, water is produced as a byproduct of the Fischer-Tropsch process. This water is contaminated with hydrocarbons and it is treated in one of the largest ETPs of its kind, capable of handling up to 45,000 cubic metres of water per day, equivalent to a city the size of Delft ("Pearl GTL - overview", n.d.). A Coagulation and a flocculation process using aerobic micro-organisms to digest paraffinic hydrocarbons are used to clean the effluent. The biosludge consists of the aerobic micro-organisms in combination with the coagulated particles.

Compared to municipal sludge, Fischer-Tropsch biosludge is not contaminated with pathogens, pharmaceuticals, microplastics, mercury, PAHs, polychlorinated biphenyl, perfluorinated surfactants, polycyclic musks, siloxanes, pesticides, phenols, nanoparticles, sweeteners, benzotriazoles, and personal care products (Fijalkowski et al., 2017; B. Sarkar et al., 2019). Nonetheless, the GTL sludge is high in HM concentration due to leaching of the catalyst, corrosion of process equipment, and dosing treatment such as coagulants and micronutrients used in ETPs. High HM concentration can inflict environmental harm and could not comply with IBI and EBC regulations.

1.2. Problem Statement

The standard practice for disposing of sludge is landfilling or dumping, which can have disastrous environmental consequences. For instance, in South Korea in 2005, 78% of the sludge was dumped in the ocean due to policies that prohibited sludge landfilling (Buta et al., 2021; Chung et al., 2020). This led to a major environmental disaster, causing severe marine pollution and raising concerns among the society on wildlife and water quality (Z. Chen et al., 2021; Garg, 2009). As a result, new policies were implemented in South Korea to restore sludge landfilling and significantly increase incineration (Chung et al., 2020). These countermeasures prevented further environmental damage. However, sludge incineration increased, releasing harmful pollutants such as CO₂, CH₄, and small amounts of H₂S (Marzbali et al., 2021). Additionally, landfilling practices increased, which does not contribute to a more circular economy.

Currently, the focus is on minimizing sludge to reduce the costs of handling, transportation, heating, and disposal, which can account for up to 50% of operating costs in ETPs (Appels et al., 2008). Due to the high moisture content (over 80%) and biological nature of biosludge, dewatering this feedstock mechanically is difficult or requires a significant amount of energy for vaporization. Reducing the cost of sludge processing and creating a useful product simultaneously can increase circularity and contribute to improving the environment.

1.3. Research Gap

Research on HC is getting more traction as it can play an important role in the 17 Sustainable Development Goals stated by the United Nations (Padhye et al., 2022). In 2013, the search term "hydrochar" in Scopus returned 32 papers, while in 2022, it returned around 500 papers. This is because HC can be produced from different feedstocks, using different operational conditions and used in a wide variety of applications. But if we focus only on the search term 'hydrothermal carbonization sludge' only 82 results were returned from Scopus in 2021.

Only a few studies have been conducted examining biosludge as a feedstock in combination with HTC. An even smaller percentage of these topics focus on industrial sludge as a feedstock and none have been reported on Fischer-Tropsch biosludge. Because HC is a complex product that differs depending on feedstock in structure and chemical composition, the results of the limited research on comparable sludge may differ. Furthermore, other metals may be present in greater concentrations in the sludge than in municipal sludge, which may affect yield, morphology, and regulatory allowance. The industrial origin of Fischer-Tropsch biosludge feedstock can provide new insights into the potential of the HTC pathway on industrial biosludge.

1.4. Research Question

As pointed out in section 1.1, compliance with regulations, less harm than benefits, and the economics favouring the process and product are necessary to produce a useful HC. Therefore the main research question is stated as follows:

Can hydrochar be made from industrial Fischer-Tropsch biosludge processed by HTC that complies with regulations and generates socioeconomic benefits?

To answer this question two sub-questions have to be answered. The first sub-questions assess the characteristics of the HC produced under changing process factors:

How does variation of temperature and residence time affect the characteristics of hydrochar and the aqueous phase?

Secondly, from these characteristics and in combination with regulations, the most potential use cases were selected for hydrochar by answering the question;

What are possible use cases for Fischer-Tropsch biosludge hydrochar?

1.5. Research Objective

The primary objectives of this research were as follows: (1) to provide a green method for upcycling industrial biosludge into a useful product compared to its current pathway of landfilling and incineration, (2) to produce a high-quality product that complies with regulations so that it can be allowed as a functional product:

1. Provide a method for transforming industrial biosludge into high-value products, supported by analytical data.
2. Determine the possible products that can be derived from HTC and ensure that they comply with product regulations.

The industrial sector shares a common goal of building a more sustainable future. However, this sector is often faced with the question of "how to be sustainable" and "how do all of these options compare?". It takes time to understand all the possibilities for processing industrial biosludge. This study presents one technological option for utilizing sludge.

The second goal is to determine which product applications are suitable for HC and whether they comply with regulations. While products may be sustainable, they could also have adverse effects on the environment if the downsides are not addressed. Regulations determine which concentrations are safe and which are not. Therefore, regulations are necessary to determine whether the HTC method produces an environmentally friendly product from a complex and heterogeneous material.

The research objectives need to be defined scientifically to provide specificity. Thus, the following specific objectives have been identified for this thesis;

- (a) Determine the effects of temperature and residence time on HC; yield, HM concentrations, pH, elemental composition, volatile mater (VM), fixed carbon (FC), ash, and leachability.
- (b) Determine the effect of temperature and residence time on the aqueous phase parameters; chemical oxygen demand (COD), pH, ammoniacal nitrogen, and HM concentrations.
- (c) Compare the experimental results with characteristics stated in the literature and regulations to qualitatively describe potential use-cases.

1.6. Research Scope

This research project aims to contribute to more sustainable waste management practices by repurposing Fischer-Tropsch biosludge through an environmentally-friendly process, and by identifying potential beneficial applications for the HC product. This is done by exploring the potential applications of Fischer-Tropsch biosludge through the HTC process, resulting in the production of HC and an aqueous stream. Although time constraints prevented the execution of use case tests, the characteristics of the HC were analyzed to identify potential applications. Three possible applications were considered: soil amendment, biocoal, and absorbent.

Figure 1.1 presents a synopsis of the research field, covering the path from biomass to product application. The figure differentiates between various feedstocks, reaction parameters, characterizations, and intended applications. The green-highlighted terms indicate the path that this thesis will cover within the research field. Although non-highlighted options will be addressed from time to time, they are outside the scope of this research. This is because different starting materials exhibit contrasting HC characteristics after HTC, which can undermine the obtained results and create confusion within the literature. A study on economics is not included in this figure as it is beyond the scope of this thesis.

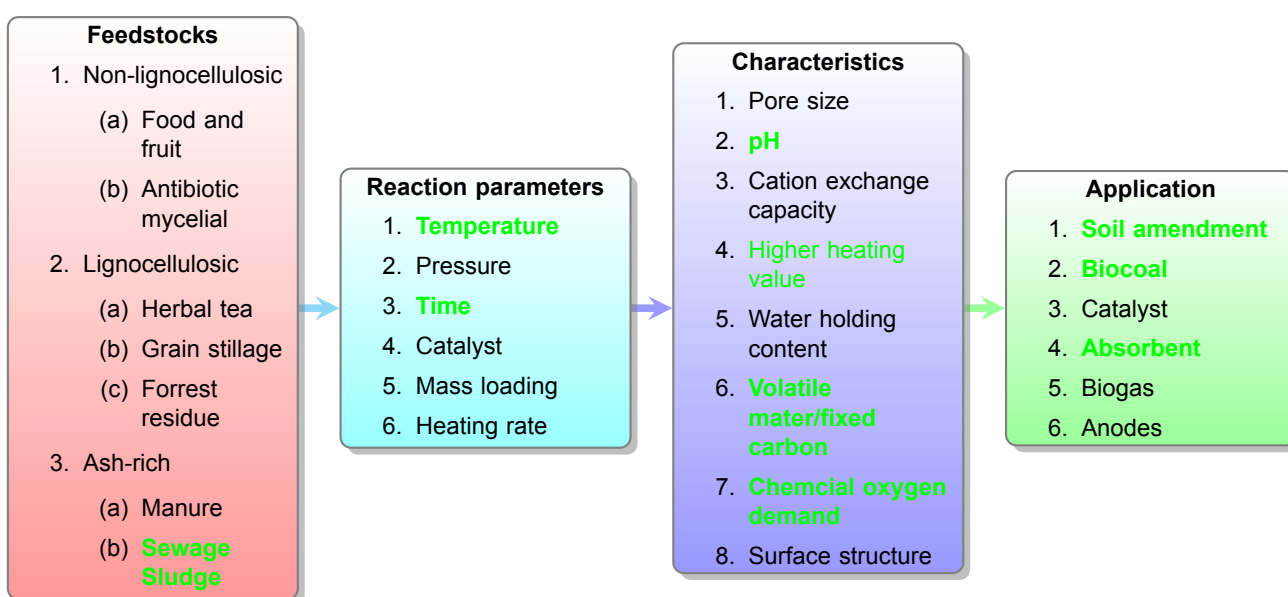


Figure 1.1: The hydrochar research space with some possible feedstock examples, different reaction parameters, product characteristics, and possible applications. Where all the bold green words are the chosen feedstock, reaction parameters, characteristics and application for this research.

Shell's commitment to circular economy principles aims to reduce greenhouse gas emissions and turn secondary streams into valuable resources. This research project aims to explore the potential of Shell's biosludge as a product instead of disposing of it in landfills. By repurposing biosludge through an environmentally-friendly process, this research can provide a blueprint for sustainable waste management to help reduce the carbon footprint of Shell's operations and other industrial biosludge streams.

1.7. Research Method

To obtain state-of-the-art knowledge about biosludge, the HTC, process, HC applications, and regulations; literature research was conducted. Before sample creation could start, an experimental design was established, and samples were created and stored accordingly. Once the data was collected, statistical analysis was performed to determine the effects of temperature and time on the chosen response variables. Finally, the results were compared with existing literature on HC regulations. The five deliverables of this project include a literature review, an experimental design, sample creation and storage, data analysis, and a comparison with existing literature and regulations. By completing these

deliverables, this research project aims to contribute to a better understanding of the potential applications of HC and to identify potential environmental implications. The aforementioned five deliverables are listed:

1. Literature study.
2. Design of experiments.
3. HC, liquid and gas phase creation and storage of aqueous and HC phases.
4. Analysing the phases and examining the obtained data.
5. Find a use case by comparing results with literature and regulations.

1.8. Report Outline

This thesis consists of six chapters. The literature review in chapter 2 covers the difference between HC and BC, the properties of the various HC phases, and how different parameters affect their characteristics. The experimental setup, including materials, equipment, and procedures, is detailed in chapter 3. The data obtained from the experiments and the discussion are presented and analyzed in chapter 4. The conclusions are presented in chapter 5. Finally, recommendations for future work are provided in chapter 6.

2

Literature Study Concerning Hydrochar

To understand how various biomass conversion technologies, differences in feedstock, and changes in reaction parameters interact with each other, a literature review was conducted. Additional aspects, such as regulations, HM, and BC for comparison with HC, are also explained in this chapter. Most of the literature used in this study is based on sludge unless the feedstock is otherwise specified. The contents of this chapter are summarized below:

1. section 2.1 describes the question needed to be answered from this literature study;
2. what distinguishes HTC as a more beneficial technology than alternatives in the field of biomass conversion is covered in section 2.2;
3. sludge definition and composition is described in section 2.3 ;
4. the different regulations that HC has to comply are explained in section 2.4;
5. HC key parameters can be found in section 2.5
6. in section 2.6, BC and HC are compared;
7. parameters affecting the HTC process are described in detail in subsection 2.7.1;
8. metals are an essential part of this research and their behaviour and influence on the phases are described in section 2.8;
9. finally, a conclusion is written in section 2.10.

2.1. Literature Study Outline

To ensure a focused literature study, it is essential to formulate clear research questions that guide the investigation. In this study, the primary research question was broken down into several sub-questions and sub-sub-questions to facilitate a systematic and comprehensive analysis. The structure of these questions is depicted in Figure 2.1, which is based on the research space presented in Figure 1.1. By addressing these questions, this study aims to provide a thorough understanding of the properties and characteristics of the different phases of HC and their relationship with the process parameters.

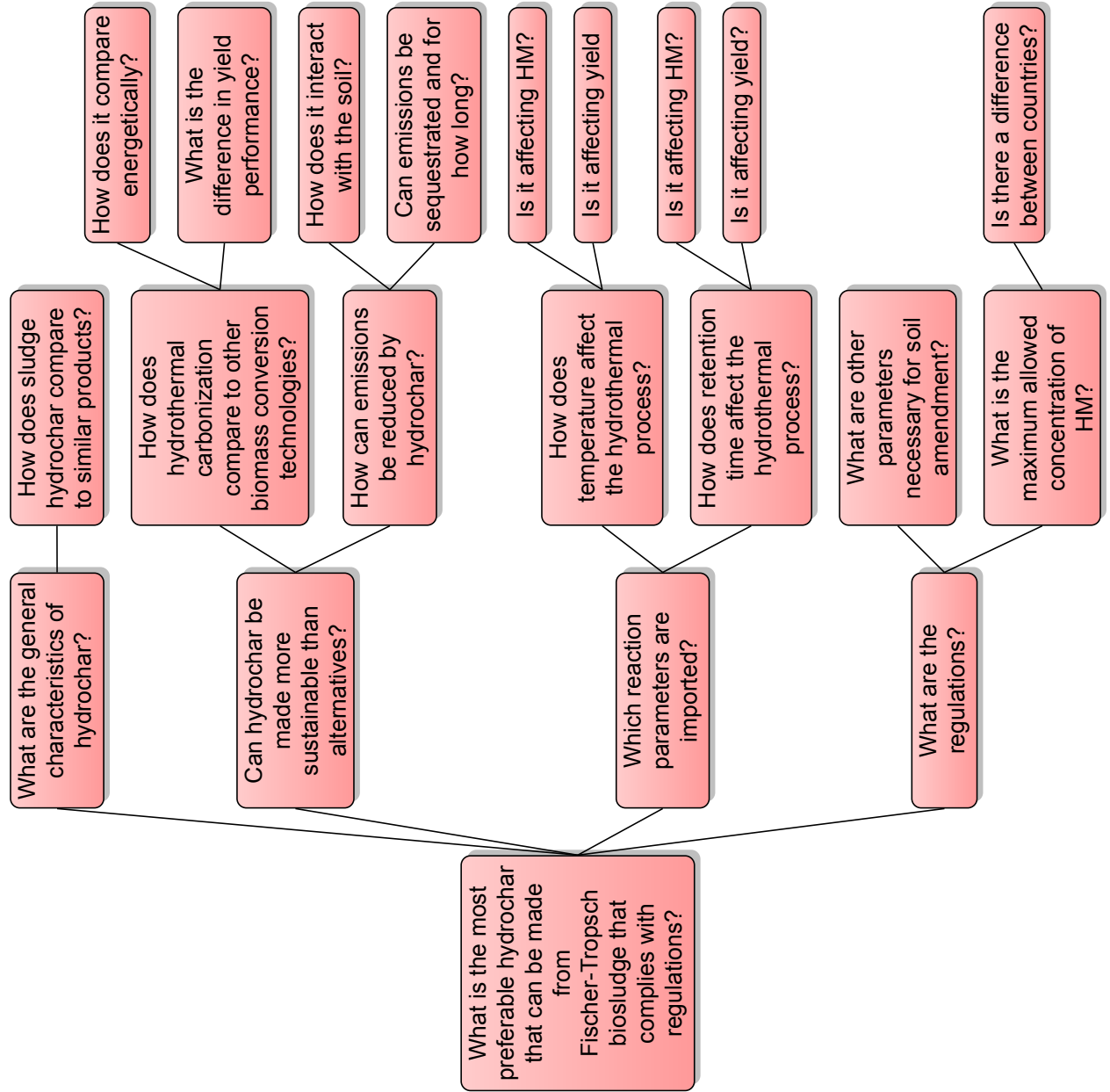


Figure 2.1: Decision tree setting out the research gaps to answer the main question and what question needs to be answered in the literature study.

2.2. Conversion Technologies

Various methods are available for converting biomass into valuable products, such as BC, syngas, bio-oil, and HC. HTC, hydrothermal liquefaction (HTL), and hydrothermal gasification (HTG) are effective with wet feedstocks, while pyrolysis is suitable for dry biomass (Khosravi et al., 2022; Ronsse et al., 2013). The composition of the end products is generally determined by the conditions in which these procedures apply heating and pressurizing biomass. Table 2.1 summarizes the main operating parameters, feedstocks, and products for various hydrothermal and thermal processes, where HTC and slow pyrolysis produce HC and BC, respectively. The primary product of HTC, which is produced in wet conditions, is HC, whereas slow pyrolysis produces BC due to the dry and oxygen-free environment (Khosravi et al., 2022).

Table 2.1: Thermal processes for converting biomass obtained from Khosravi et al. (2022)

Comparison of the thermal technologies for the production of hydrochar and biochar.							
Hydrothermal treatments				Pyrolysis			
	Hydrothermal carbonization	Hydrothermal liquefaction (HTL)	Hydrothermal gasification (HTG)	Slow pyrolysis	Intermediate pyrolysis	Fast pyrolysis	Flash pyrolysis
Temp.(°C)	180-375	200-400	350-700	300-700	300-500	500-1000	400-1000
Time	Minutes-hours	1-120 min	30s-30min	Hours-weeks	< 20 s	< 1 min	< 30 min
Pressure	autogenous pressure (2-6 Mpa)	10-25 MPa	20-50 Mpa	0.1 Mpa	0.1 Mpa	< 5 Mpa	< 0.5 Mpa
Main product	Hydrochar	Bio-oil	Syngas	Biochar	Bio-oil	Bio oil	Syngas
Feedstock	Dry Wet	Agricultural wastes, woody wastes, crop residue Fresh vegetable wastes, sewage sludge, animal wastes, algae		Agricultural wastes, woody wastes, crop residue Fresh vegetable wastes, sewage sludge, animal wastes, algae			
Reaction mechanism	Hydrolysis, dehydration, decarboxylation, condensation, polymerization, and aromatization			Dehydration, aromatization, decarboxylation, polymerization, intramolecular condensation, and rearrangement reactions			
Reference	Ilyas et al. (2019) Kambo and Dutta (2015) Z. Zhang et al. (2019)	Ilyas et al. (2019)	Libra et al. (2011) Kruse (2009)	Z. Zhang et al. (2019)	Funke et al. (2017)	Lee et al. (2020) Onay and Kockar (2003)	Onay and Kockar (2003)

The HTC process is a hydrothermal process that operates under comparatively mild temperatures (150-250°C) and with autogenous pressure using subcritical water as a medium to promote reactions that favour the formation of HC from various types of biomass feedstock (Gaur et al., 2020; Malool et al., 2022; Merzari et al., 2019). The subcritical water acts as a mild base and mild acid, and is less polar compared to water solvent, which enables the conversion of the feedstock into organic compounds, resulting in the formation of HC (Gaur et al., 2020). The process is well-suited for three types of biomass feedstocks, namely lignocellulosic materials (such as grain stillage and herbal tea waste), non-lignocellulosic materials (including food and fruit waste, and antibiotic mycelial residues), and ash-rich materials (such as livestock manure and sludge) (Zhuang et al., 2022). The main advantage of the HTC process is that it eliminates the need for pre-drying of wet feedstocks (Kambo & Dutta, 2015; Merzari et al., 2019). Also, the HTC process is slightly exothermic and uncatalyzed process has obtained yields ranging between 50-60% (Ekanthalu et al., 2021; Ischia & Fiori, 2021). After the process, the resulting products can be separated into an aqueous phase, HC, and gas fractions, which are considered sterile (Reza et al., 2016).

Slow pyrolysis is typically carried out at atmospheric pressure, in the absence of oxygen, and at temperatures between 300-700°C, although some studies have reported using temperatures up to 850°C (Ronsse et al., 2013; Staf & Buryan, 2016). However, slow pyrolysis has a relatively low yield, typically around 30% on a dry weight basis (Akbari et al., 2021; Mohammadi et al., 2019; Reißmann et al., 2018). Additionally, the feedstock must be pre-dried, which adds an energy-intensive step to the process (Khosravi et al., 2022; Ronsse et al., 2013).

2.3. Sludge

The choice of feedstock is a critical factor that affects both the yield and quality of BC and HC. However, the term sludge encompasses a broad spectrum of materials with vastly different chemical compositions (D. C. Li & Jiang, 2017). Although terms such as activated sludge, anaerobic sludge, freshwater sludge, digested sludge, primary sludge, secondary sludge, organic sludge, and waste activated sludge (WAS) are used to describe sludge, their compositions can vary significantly depending on their source and treatment (W. Wang et al., 2020; Y. Zhang et al., 2021). Different types of sludge can be ranked based on their energy content as follows: biosludge > anaerobically digested sludge > paper mill sludge > primary sludge (L. Wang, Chang, & Li, 2019). The specific benefits and challenges of different types

of sludge depend on their origin and pre-treatment steps. This thesis primarily focuses on biosludge, which is discussed in detail in subsection 2.3.1.

Previous studies showed significant variations in the elemental and proximate analyses of dry sludge, as demonstrated in Table 2.2. In a literature review by Tasca et al. (2019), the main elements and properties of sludge that underwent anaerobic digestion, primary sludge, or secondary sludge treatments were analyzed. While some studies differentiated between primary and secondary sludge and industrial sources, others did not. Secondary sludge was found to contain 13.9% oxygen (J. H. Zhang et al., 2014), whereas Escala et al. (2013) reported a higher oxygen content of 31.99%. Biosludge has a lower carbon content than primary sludge as bacteria have not yet converted compounds to CO₂ (Merzari et al., 2019). This is likely to be the case for the studies of Hunsom and Autthanit (2013) and Wen et al. (2011) that utilise textile industry sludge from India and municipal sludge from China, respectively. Furthermore, primary sludge lacks bacterial flocs and microorganisms compared to biosludge (Sun et al., 2021).

Table 2.2: Proximate and ultimate analysis of different sludge obtained from D. C. Li and Jiang (2017)

Reference	elemental analysis (wt%)					Chemical content (wt%)			Proximate analysis (wt%)			
	C	H	O	N	S	Protein	Lipid	Carbohydrate	Moisture	Volatile Matter	Fixed Carbon	Ash
Ma et al. 2017	40.5	4.51	48.5	5.48	1.01	26.29	27.26	22.88	3.59	53.93	6.23	36.25
Xie et al. 2014	53.24	7.39	33.25	6.12	–	–	–	–	4.53	68.57	16.42	15.01
Yu et al. 2016	25.27	4.2	16.23	3.05	–	–	–	–	6.57	44.45	3.3	45.68
Wang et al. 2011	37.45	5.84	–	2.9	1.32	–	–	–	–	45.62	7.12	46.41
Hunsom and Autthanit 2013	68.69	–	29.05	–	0.3	–	–	–	9.53	60.5	5.57	20.4
Trinh et al. 2013	28	3.4	10.3	4	0.9	–	–	–	7.3	38	7.9	46.8
Xie et al. 2014	53.24	7.39	33.25	6.12	–	–	–	–	4.53	68.57	16.42	15.01
Wen et al. 2011	66.7	9.2	14.3	9.3	0.5	–	–	–	6	49.4	30.7	13.9

The accurate quantification of N₂O, CH₄, and CO₂ emissions from ETPs is an ongoing endeavour that is crucial for assessing their environmental impact. While CO₂ emissions from ETPs are typically considered short-cycled and therefore not included in the overall GHG emissions calculation, the emissions of N₂O and CH₄ must be carefully identified and quantified. (Kampschreur et al., 2009).

HM concentrations in sludge are highly dependent on the topographical origin and industrial processes. Research conducted on sludge from China, Ireland, Italy, Russia, and Canada has revealed varying concentrations of zinc, cadmium, copper, nickel, lead, chromium, molybdenum, and strontium (Gao et al., 2020). For instance, Ireland and Italy have high lead shares in their HM matrix, while Ireland and Russia have strontium traces in their HM matrix (Gao et al., 2020). In addition, specific industrial processes are associated with particular HM appearance in sludge, as is shown in Table 2.3. Cadmium, lead, and mercury ions are the most harmful to living organisms, and petroleum refineries have cadmium and lead in their wastewater, as shown in Table 2.3 (Tran et al., 2017). Furthermore, textile mills, tanning industries, and power plant effluent typically have less complex HM matrix compositions, containing only chromium, which is the main additive in stainless steel (Kamerud et al., 2013; Tran et al., 2017). Where electroplating and metal surface modification processes account for most of the amounts of lead, zinc, cadmium, nickel, and copper found in effluents (Tran et al., 2017).

2.3.1. Biosludge

Biosludge, also known as activated sludge or WAS, is a byproduct of the wastewater treatment process using primary and secondary effluent treatment. Biosludge consists of carbohydrates, lipids, and protein molecules (Khosravi et al., 2022). This widely used practice in the developed world involves a two-stage process: aeration and sludge settlement (Scholz, 2006).

During the first stage, the wastewater is mixed with microorganisms, including bacteria, which are aerated to promote their growth and ability to break down and remove solids from the effluent. This process is known as activated sludge because the microorganisms become "activated" and able to perform their function effectively (Scholz, 2006).

Table 2.3: Heavy metals found in industries (Tran et al., 2017)

Industry	Al	As	Cd	Cr	Cu	Hg	Pb	Ni	Zn
Paper mills				x	x	x	x	x	x
Organic chemistry	x	x	x	x		x	x		x
Allies, chlorine		x	x	x		x	x		x
Fertilizers	x	x	x	x	x	x	x	x	x
Petroleum refinery	x	x	x	x	x		x	x	x
Steelworks		x	x	x	x	x	x	x	x
Aircraft	x		x	x	x	x		x	
Glass/cement				x					
Textile mills				x					
Tanning				x					
Power plants				x					

In the second stage, the mixture is allowed to settle, and the floc structure of the microorganisms coagulates and settles, resulting in the formation of biosludge. The clarified effluent stream obtained is free of solid particles and can be used as clean water (Scholz, 2006). However, the biosludge stream requires further processing to stabilize and reduce its volume before it can be safely disposed of or used for other purposes.

Overall, the biosludge produced from the activated sludge process is the main byproduct of wastewater treatment that requires proper handling and management to ensure environmental safety and sustainability.

2.4. Regulations

The potential uses of HC derived from biosludge could be beneficial, but regulations exist to minimize the risk of toxic elements entering the environment and food chain. However, currently, HC is not covered under existing regulations, and there is a need to develop specific guidelines for its use (Breulmann et al., 2017). In contrast, the IBI and the EBC have established regulations for the use of BC in various fields, including EBC-Feed, EBC-AgroOrganic, EBC-ConsumerMaterials, EBC-Agro, EBC-Urban, and EBC-BasicMaterials (Breulmann et al., 2017).

BC-Agro has specific limits for heavy metals, while EBC-AgroOrganic and EBC-Feed have even stricter thresholds due to their use as organic soil amendments and cattle food, respectively. The IBI combines the maximum allowed HM thresholds of multiple jurisdictions, including Australia, Canada, EU, UK, and the USA (IBI, 2015). Certification of a BC product requires values of organic contamination, such as PAHs, declaration of nutrient values for N, P, K, Mg, Ca, Fe, as well as physical properties, including dry matter, salt content, bulk density, water holding capacity (WHC), pH, and electrical conductivity (IBI, 2015; Schmidt et al., 2022).

In contrast, regulations and disposal methods for sludge vary significantly among different countries due to their respective histories and policies. The maximum allowable content of HM in sludge disposal varies between Germany and China, as shown in Table 2.4. Within the European Union (EU), there are also significant differences, with France allowing concentrations of Zn, Cu, and Cd, to be up to 10 times the amount that is allowed in the Netherlands (Inglezakis et al., 2014). Figure 2.2 shows the different end uses of sludge around the world. Some countries, such as Germany and the Netherlands, have banned the use of sludge in agriculture or landfill, leading to almost complete incineration of sludge in the Netherlands (Buta et al., 2021). Recently, Germany also prohibited this application, and Sweden is considering doing the same, as a consequence of EU Directive 86/278/CEE (Buta et al., 2021). However, such laws can lead to increased landfill or incineration practices, which are not sustainable solutions.

Table 2.4: Different Regulations on heavy metal application to land and in biochar.

Regulations	Heavy metals (mg/kg)									
	As	Cd	Cr	Cu	Pb	Hg	Ni	Zn	Mo	Co
China sewage sludge ordinance (2018)										
A(farmland, gardenplot, pastureland)	30	3	500	500	300	3	100	1200		
B(Otherland)	75	15	1000	1500	1000	15	200	3000		
China organic fertilizer standard (2012)	15	3	150		50	2				
German sewage sludge ordinance (1992)			900	800	900	8	200			
German fertilizer ordinance (2015)	40	1.5		70	150	1	80	1000		
USA 40 CFR Part 503	75	85	-	4300	840	57	420	7500		
European Biochar Certificate V10.1	13	1.5	90	100	120	1	50	400		
International Biochar Standards V2.1	13-100	1.4-39	93-1200	143-6000	121-300	5-75	34-100	200-700	1-25	34-100

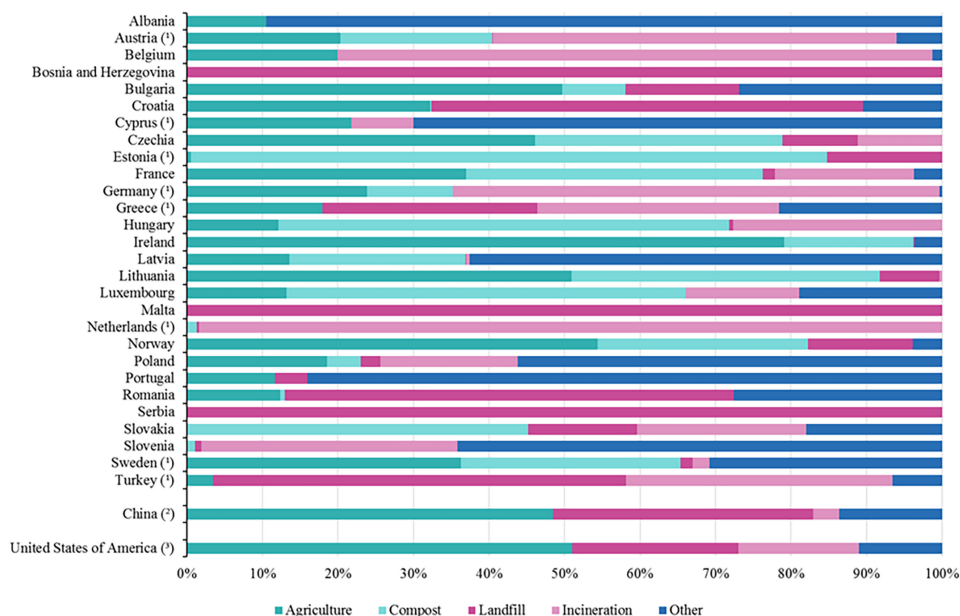


Figure 2.2: Different regulations impact the processing type of sludge as can be seen through the distinction of end-use. (1) 2016 data. (2) 2003 data. (3) 2019 data (Buta et al., 2021).

2.5. General Characteristics of Char, Hydrothermal Carbonization Aqueous and Gas Phase

HC and BC, collectively referred to as "char" in this section, have improved product characteristics compared to sludge (Tasca et al., 2019). Char is more resistant to microbial activity that would otherwise consume the biomass, resulting in slower decomposition and longer shelf-life (Wiedner et al., 2013). Additionally, it contains less moisture, which increases its energy content and reduces transportation costs. From a circular economy perspective, finding an application for a secondary stream is at the core of its principles, and char has many potential applications, which are detailed in section 2.9. This section provides an overview of the overall consistency of chars produced by biomass conversion technologies such as HTC and slow pyrolysis.

Char is composed of four fractions, in terms of proximate analysis:

1. FC
2. VM
3. Moisture
4. Ash

2.5.1. Fixed Carbon and Volatile Mater

The characteristics of FC and VM differ in their ignition point, structure, and chemical consistency, but they coexist in char. Research by Tasca et al. (2019) on varying reaction severity, a combination of retention time and temperature found that the ratio of FC and VM increases with increasing reaction severity, as shown in Figure 2.3. The impact of severity in combination with HTC and sludge on FC

and VM is discussed in detail in subsection 2.7.4. In this subsection, we distinguish VM and FC.

FC refers to the part of the char that remains as residue after VM, water, and ashes are removed (D. K. Sarkar, 2015). It consists mainly of carbon, with a small percentage of oxygen, nitrogen, hydrogen, and sulfur, which are not removed during char burning (D. K. Sarkar, 2015). In the HTC process, organic carbon reacts into stable carbon, increasing temperatures elevate the FC percentage (Ren et al., 2017). The percentage of FC in char is important when using it as a fuel, and the choice of combustion equipment is influenced by this factor (D. K. Sarkar, 2015). Char products with higher carbon percentages and lower moisture content are more solid. For example, bituminous (soft coal) and anthracite (hard coal) contain more carbon and less water than peat and lignite (D. K. Sarkar, 2015). These less solid fuels have a higher percentage of VM, which comprises more oxygen and nitrogen than FC (Liang et al., 2022). FC is more stable than VM, making char with higher FC percentage perform better for long-term carbon sequestration (Islam et al., 2021).

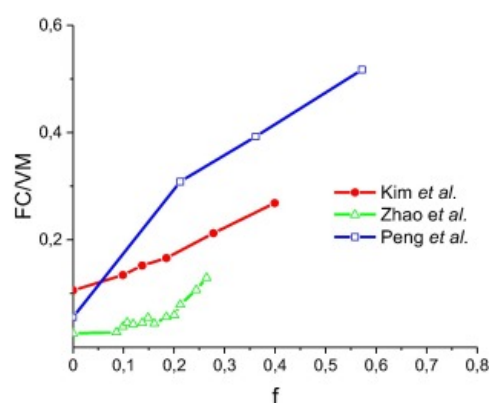


Figure 2.3: Literature study comparing FC/VM ratio of three studies with increasing reaction severity, which is a combination of temperature and time (Tasca et al., 2019).

VM influences the elemental composition of char and has a notable lowering effect on its peak temperature (Maaz et al., 2021). It is easily accessible and improves combustion-promoting performance (Su et al., 2022). However, a disadvantage of VM is that it has a lower energy density and releases less heat during combustion (Liang et al., 2022; Su et al., 2022). Volatile compounds are highly biodegradable, and VM has been linked to increased soil microbial activity, leading to increased mineralization (Abel et al., 2013; Breulmann et al., 2017; Cervera-Mata et al., 2022; Ren et al., 2017; Taskin et al., 2019). Furthermore, BC VM contains phenolic and aromatic compounds soluble in acetone, which were not found in BC with low VM (Maaz et al., 2021).

2.5.2. Ash

After biomass combustion, the remaining non-combustible residue is known as ash (Benavente & Fullana, 2021). Ash is composed of various elements, including Al, Ca, Cl, Fe, K, Mg, P, Na, S, Mn, Si, and Ti, if present in biomass (Vassilev et al., 2017). The incineration of ash-rich feedstocks, such as chicken litter, cow dung, and sewage sludge, can cause problems such as slagging, ash deposition, fouling, and bed agglomeration. Nonetheless, the residual ashes can contain valuable phosphorus and potassium contents useful as soil fertilizer ingredients (Maj et al., 2022; Ottosen et al., 2013).

Compared to lignocellulosic feedstocks, sludge has a higher ash content, which reduces its heating value (Leng, Yang, et al., 2021). However, the use of HTC is highly beneficial in separating ash from wet biomass. Water's subcritical characteristics dissolve ash and mineral components. Particularly alkali and alkaline metals dissolve into the aqueous phase and most phosphorus and HM are retained in the HC (R. Wang et al., 2019; Wray, 2022). This technique has been demonstrated on a pilot scale to be effective in removing ash from sludge and recovering valuable nutrients from the residual ash. Ash content in sludge can reach up to 20% on a dry basis, and for HC, it can be as high as 44.6% (Volpe et al., 2020; R. Wang et al., 2019).

2.5.3. Dewaterability: Bound and Free Water

Water in plants and biological tissues is composed of bound and free water (Zang et al., 2021). In Figure 2.4, a schematic view of free and bound water in bacterial floc structures is presented. Free water consists of interspace water, which can easily be separated through sludge settling (Mowla et al., 2013; D. Zhang et al., 2020). Floc water is trapped by the coagulated bacteria and can be separated by mechanical drying such as centrifuging or compression (Mowla et al., 2013; D. Zhang et al., 2020). Bound water, on the other hand, is more difficult to remove. Surface water is chemically bound or hydrated to surface particles of cells within a floc, while hydration and intracellular water are closed off by cell membranes (Mowla et al., 2013; D. Zhang et al., 2020). Methods other than mechanical dewatering are required to separate bound water.

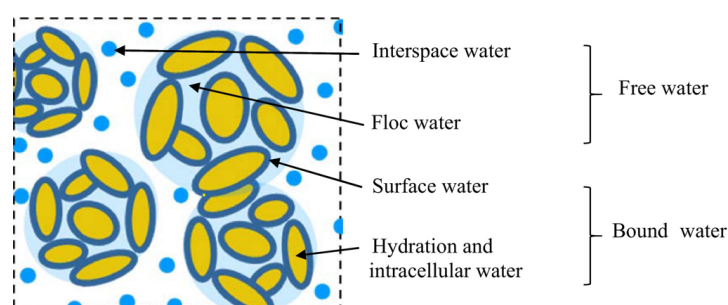


Figure 2.4: Free and bound for bacterial floc structures (D. Zhang et al., 2020)

Sludge's high moisture content poses a disadvantage for processing, as it increases disposal and transportation costs due to added weight (Mowla et al., 2013; Zhuang et al., 2018). Dewatering sludge is an energy-intensive process as thermal heating requires a significant amount of energy due to the latent heat needed for vaporization and mechanical techniques such as centrifuges, belt presses, and filter presses can only reduce moisture around 35% (Mowla et al., 2013; L. Wang et al., 2014). The mechanical techniques commonly used for dewatering are not effective at reducing bound water as hydrothermal techniques are (Mowla et al., 2013).

Using HTC, Zhuang et al. (2018) found that the bound water content of sludge could decrease from 80.8% to 50%, with the sharpest decline (15%) noted between 180°C and 210°C (Gao et al., 2019; Zhuang et al., 2018). The reduction in moisture content is primarily due to bound water becoming free water. However, deinking sludge from the paper industry does not behave similarly to sludge in terms of HC dewaterability, as its bound water slightly increases with temperature instead of decreasing (Gao et al., 2019; Zhuang et al., 2018). This result is because paper sludge is composed of lignocellulose, whereas sludge contains proteins and polysaccharides (Zhuang et al., 2018). Additionally, there is a relationship between particle size and moisture content, where smaller particles store less moisture (Zhuang et al., 2018).

The HTC reaction process has been found to enhance the dewaterability of sludge by breaking down the floc structure, which releases bound water and improves the separability of moisture (Zhuang et al., 2018). As a result, the bound water becomes free water, which increases the effectiveness of mechanical dewatering methods. Three mechanisms have been identified that contribute to this improvement: 1) reduction of hydrophilic functionality, 2) destruction of floc, and 3) shrinking of solids and release of volatiles, which helps to drive moisture out of the porous structure (Zhuang et al., 2022). Compared to thermal drying, HTC is a non-evaporative dehydration process that retains more latent heat, leading to significant energy savings (Zhuang et al., 2022).

Combining HTC and mechanical expression achieves up to 92% moist reduction (L. Wang, Chang, & Liu, 2019). In a study by Deng et al. (2019), the combination of HTC, mechanical, and thermal drying resulted in 25-40% less energy consumption and 17-30% lower operating cost compared to only thermal drying. Adding CaO in HTC was found to be effective for dewatering, with a higher influence factor than temperature and residence time (Deng et al., 2019). One explanation for its effectiveness

is that CaO causes extracellular polymer compounds to break down and sludge cells to release bound water (Deng et al., 2019). L. Wang et al. (2014) demonstrated that HTC coupled with mechanical compression is energetically superior to thermal drying, as mechanical drying cannot release bound water. This is illustrated in Figure 2.5B, it is shown that thermal and electro-dewatering consume more energy for the same desired moisture content.

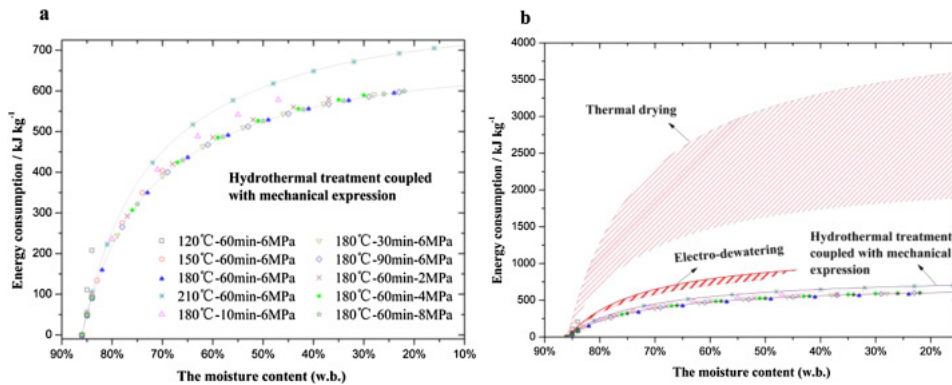


Figure 2.5: a) HTC experiments coupled with mechanical pressure and the total energy consumption b) same results but placed in the context of thermal drying and electro-dewatering (L. Wang et al., 2014).

2.5.4. Aqueous Phase

Inside the aqueous phase, proteins are dissolved which can form foams influenced by the length of the proteins as shown in Figure 2.6 (Germain & Aguilera, 2014). These proteins are substantially degraded into smaller components when temperatures increase to 240°C (Langone & Basso, 2020). Understanding the aqueous phase will lead to an increase in circularity and it is necessary that this stream may not have a worse environmental impact than the feedstock used.

The aqueous phase carbon content can contain up to 15% of the carbon feedstock, and COD between 10-80 g/L have been measured (Merzari et al., 2019; Reza et al., 2016). This carbon content is rich in aromatic organic compounds and short-chain fatty acids like acetic and formic acids, where acetic acid have been measured to take up to 6,2% of the Total Organic Carbon (TOC) (Langone & Basso, 2020). A list of compounds from anaerobically digested sewage sludge HTC aqueous phase and their main applications is shown in Table A.1. Even though it may contain toxic compounds like phenol, 5-HMF, and furfural, up to a few grams per litre it is necessary to use the aqueous phase to reduce waste and promote circularity (Gaur et al., 2020; Reza et al., 2016).

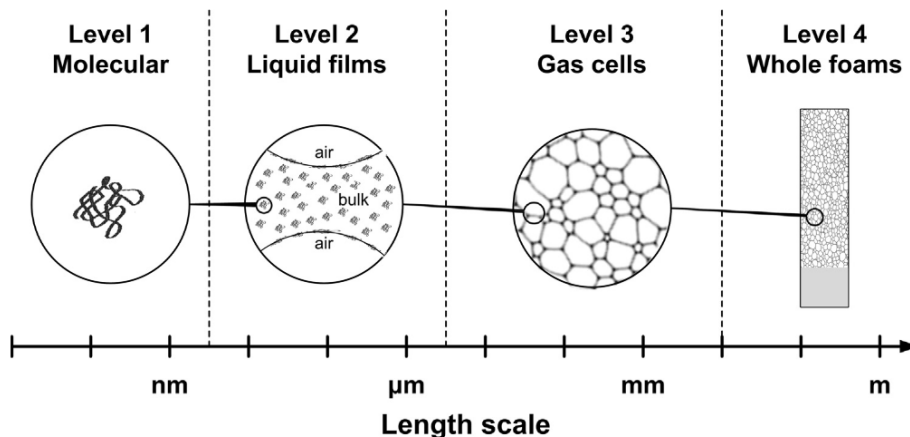


Figure 2.6: Four levels of foam; molecular, liquid film, gas cell, and continuous foam. Foam properties are influenced by the lengths of proteins (Germain & Aguilera, 2014).

2.5.5. Gas Phase

During the carbonization process, a small fraction (2%-5%) of the starting carbon is released into the gas phase, primarily as CO₂, resulting from decarboxylation (Heidari et al., 2019; Marzbali et al., 2021; Zhuang et al., 2022). At temperatures above 250°C, the formation of carbon monoxide and hydrogen can occur, which have been detected in low amounts from corn stover as a feedstock (Mohammed et al., 2020).

To maximize the circularity of the process, it is important to utilize the gas phase. One possible approach, investigated by González-Arias et al. (2022), is to use reverse gas-water shift to convert the CO₂ and hydrogen in the gas into syngas. However, this strategy may not be economically viable unless the price of syngas increases substantially (González-Arias et al., 2022; Kim et al., 2011). Alternatively, the CO₂ emissions from the gas phase can be offset through carbon capturing and storage or compensated for through carbon credits.

2.6. Hydrochar Compared to Biochar

With the growing interest in BC, HC has also received significant attention. However, these two types of chars differ in their physicochemical properties due to their distinct production processes (Masoumi et al., 2021). This section aims to distinguish between the two manufacturing processes and their char products to avoid confusion and ensure an understanding of the physicochemical characteristics that set them apart.

In general, BC has a higher proportion of FC and a lower proportion of VM compared to HC (Y. Zhang et al., 2021). Low temperature and short retention time pyrolysis can produce BC with a VM content of up to approximately 48%, which is higher than some HC (34.1%, 240 °C, 1 hour) (Tarelho et al., 2020; W. Wang et al., 2020). This difference in VM and FC has been linked with greater fungi activity in soils for HC, while BC is better suited for long-term carbon sequestration (Breulmann et al., 2017; Islam et al., 2021; Taskin et al., 2019).

The active sites on the surfaces of BC and HC differ, such as heteroatoms, oxygen-containing functional groups (OFGs), sp² carbon, defective sites, persistent free radical (PFR), and vacancies (J. Wang et al., 2022). The lower temperature of the HTC reaction in HC results in a char product with higher atomic H/C and O/C ratios than BC (Masoumi et al., 2021). This higher oxygen and hydrogen content leads to HC with more OFGs and more active sites (Gasim et al., 2022). The surface of BC is largely aromatic, while HC has more alkyl moieties on its surface chemistry (Gasim et al., 2022). BC has a higher quantity of PFR than HC (Gasim et al., 2022).

Studies have shown that there are differences in surface morphology between HC and BC. For instance, Gasim et al. (2022) reported that BC has a lower specific surface area (SSA) compared to HC. (Y. Zhang et al., 2021) found that the SSA of HC derived from sludge is 2-3 times larger than that of sludge-derived BC, mainly due to smaller pore radii. In contrast, (Abel et al., 2013) reported that BC had a significantly higher surface area (up to 60 times) than HC by comparing two studies. However, Y. Zhang et al. (2021) explained that the higher surface area of HC in sludge feedstocks is due to their inherently high surface area and the effective pore construction facilitated by HTC.

The pH value of BC can vary from acidic values around 5 to alkaline values up to 8, where HC shows more stable pH values around 5 (Jellali et al., 2022; Y. Zhang et al., 2021). The increase in pH can be explained by the higher ash content in BC and the polymerization/condensation reactions that increase the loss of carboxylic and hydroxyl groups during the pyrolysis process (Y. Zhang et al., 2021). The pH value of HC decreases with increasing severity, because of the dissolution of acidic groups (Jellali et al., 2022).

BC parameters are compared with HC in Table 2.5. The density of HC is not yet been written about in literature. The difference in pH can be seen where HC is more acidic and BC can be acidic but also alkaline, where its pH becomes more alkaline with increasing temperature. The yield of HC is a magnitude of two higher than that of pyrolysis BC, while BC is made under more energy-intensive

temperatures decreasing the GHG benefits (Akbari et al., 2021; Mohammadi et al., 2019; Reißmann et al., 2018).

Table 2.5: Comparison between sludge derived HC, and sludge derived BC.

	Hydrochar	Biochar	Temperature increase ↑	References
Density g/cm ³		0.08-1.7		(Abel et al., 2013)
Specific Surface area	3-17.30	340	BC↑HC↑	(J. H. Zhang et al., 2014)
Pore radius	18.20-20.27	64.59-90.32	BC↑HC↑	(Y. Zhang et al., 2021)
pH	4.4-5	5-8	BC↑HC↓	(Jellali et al., 2022; Y. Zhang et al., 2021)
Yield	~60%	~30%	BC↓HC↓	(Akbari et al., 2021; Mohammadi et al., 2019)
Morphology	Alkyl moieties	Aromatic		

2.7. Hydrothermal Carbonization Parameter Influences

The hydrothermal carbonization HTC process is influenced by several factors, including the feedstock, temperature, reactor, catalyst, pH, residence time, solid load, pressure, and hydrous conditions (bound/unbound water) (Masoumi et al., 2021). Among these, temperature plays a particularly significant role in driving various reaction mechanisms. During HTC and pyrolysis, a complex series of reactions occur, such as polymerization, dehydration, and degradation. The reaction factors and mechanisms are detailed in this section.

2.7.1. Reaction Mechanisms

Parameters such as temperature, catalyst or retention time have a significant effect on the underlying reaction mechanisms driving the chemical conversion. In Figure 2.7 a schematic view of the reaction mechanisms of non-lignocellulose biowaste is shown. The figure shows the different chemical pathways; hydrolysis, dehydration, depolymerisation, decarboxylation, deamination, Maillard reaction, rearrangement, cyclization, ring condensation and polymerization, where dehydration and decarboxylation are the main reactions occurring (Merzari et al., 2019).

Decarboxylation and dehydration reactions release carbon dioxide and water, respectively, resulting in deoxygenation. This deoxygenation reduces the polarity of the HC surface, which improves its dewaterability (Merzari et al., 2019). Both dehydration and decarboxylation have a negative heat of reaction, which makes the HTC process exothermic (L. Wang et al., 2014). The decarboxylation reaction is illustrated in Figure 2.8.

Non-lignocellulosic feedstocks, which comprise mostly proteins, undergo a different conversion compared to lignocellulosic feedstocks such as wood, due to two important pathways. The first pathway involves the self-arrangement of amino acids, while the second pathway involves the reaction between amino acids and sugars. At high temperatures, proteins break down into their amino acid building blocks, and some of these amino acids degrade further to form low molecular compounds such as CO₂, H₂, alkanes, alkenes, alcohols (up to C₅), aldehydes, amides, and carboxylic acids (Martins, 2003; Peterson et al., 2010).

Maillard reactions, also known for the dark brown colour and nutty smell of coffee, are an important factor in food quality (Martins, 2003; Peterson et al., 2010). Reduced sugars and amino acids can react through Maillard reactions, where an amine group from protein reacts with a carbonyl group in hydrocarbonates, as illustrated in Figure 2.9 (Peterson et al., 2010). The Maillard reaction is not a single pathway but a network of reactions (Martins, 2003). The final steps of the Maillard reaction produce Melanoidin products that are high molecular weight heterogeneous polymers (Martins, 2003). This reaction is able to produce both antioxidant molecules and toxic components (Martins, 2003). Higher sugar content increases HC nitrogen uptake through the Maillard reaction (Leng, Yang, et al., 2021). Maillard reactions dominate above 180°C, while processes at 160°C do not show any evidence of these reactions (T. Wang et al., 2018).

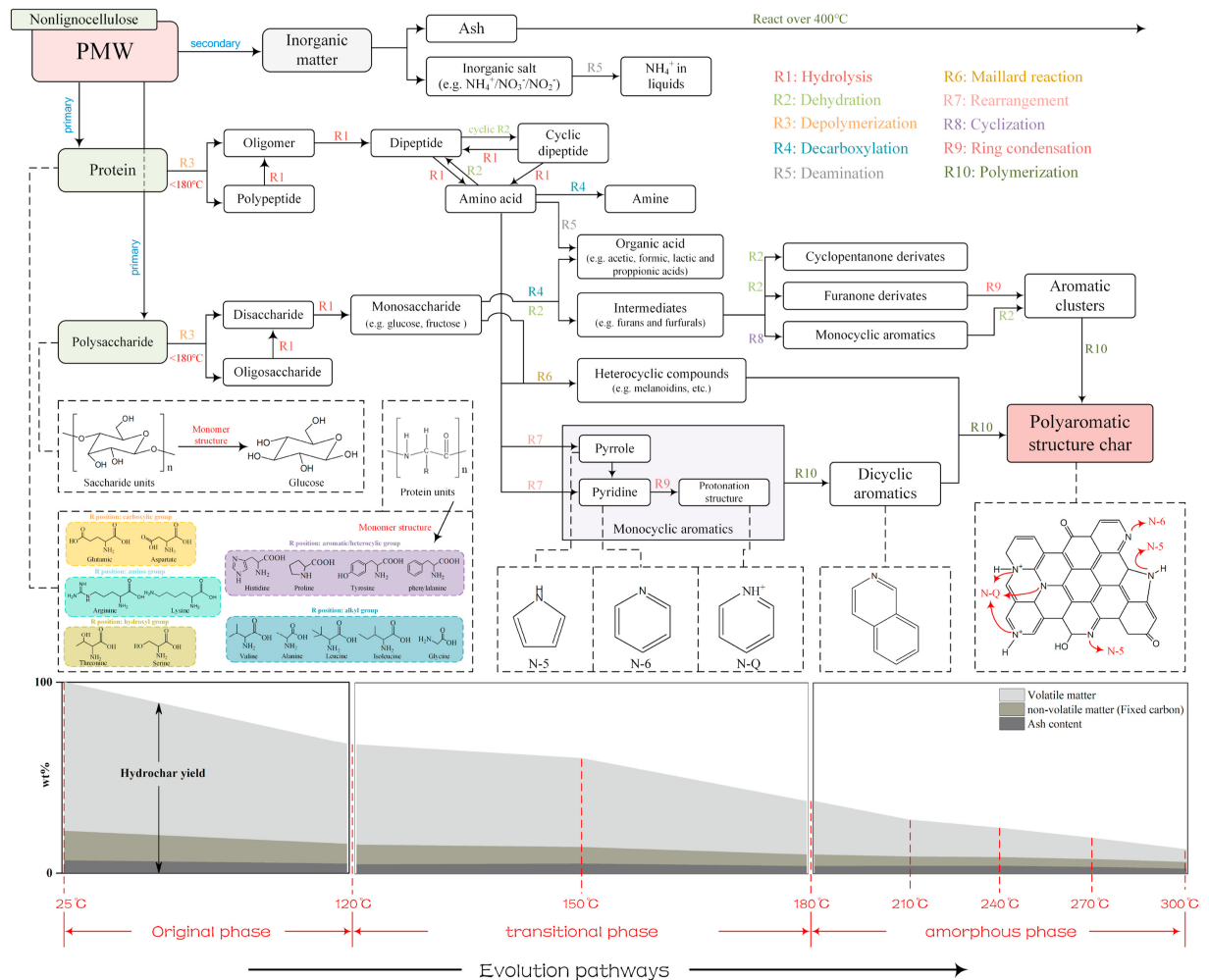


Figure 2.7: Reaction mechanisms of non-lignocellulose feedstock during HTC and separation between original phase, transitional phase and amorphous phase (Zhuang et al., 2022).

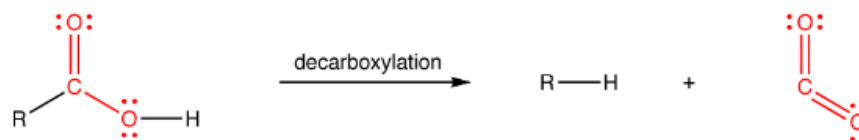


Figure 2.8: Decarboxylation where can be seen that CO₂ is formed, which deoxygenates the HC ("Decarboxylation | OChemPal", n.d.).

2.7.2. Temperature

Temperature is the most essential parameter for the HTC process as it has a significant impact on the yield of HC but can also affect the process in both positive and negative ways (F. Li et al., 2022; R. Sharma et al., 2020). Increasing temperature can lead to lower reaction time, and increased HC carbon levels, as well as improved dewaterability, it also has the downside of decreasing HC yield by releasing organic content into the aqueous phase (L. Wang, Chang, & Li, 2019).

At the start of the process, depolymerization has a stronger influence at lower temperatures, but as the temperature rises, polymerization of shorter chains becomes more active (L. Wang, Chang, & Li, 2019). Temperatures above 150°C improve biopolymer solubility, whereas above 180°C, polysaccharides and proteins start to decompose (L. Wang, Chang, & Li, 2019). Different types of organic molecules, such

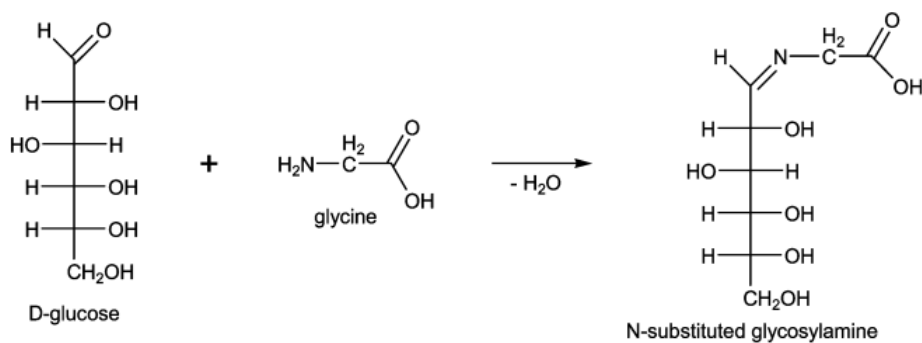


Figure 2.9: A Maillard reaction where D-glucose reacts with glycine.

as carbohydrates, lipids, and proteins, depolymerize at different temperatures, with proteins being easier to hydrolyze than polysaccharides, followed by lipids (L. Wang, Chang, & Li, 2019).

Increasing temperature also leads to increased carbonization and pore development, but pore blockage can occur at temperatures above 250°C, which is not beneficial for pore development (Khosravi et al., 2022). Additionally, high temperatures above 200°C produce low-density HC with smaller particle sizes, which can reduce water retention due to micropore blockage. However, increasing temperature can also lead to lower yield, a decline in certain HC characteristics (such as H/C, O/C, and volatile matter), and a decrease in the economy of the system (Deng et al., 2019).

Research has shown that there is a clear distinction between carbon-centred and oxygen-centred PFR in hydrochar cooked at different temperatures. For example, cooking at 260-280°C increases carbon-centred groups, which are more stable over the long term and HC made between 120-150°C obtained more oxygen-centred groups (Y. Zhu et al., 2019).

Pressure can also affect the HTC process indirectly through gas injection or directly through temperature control. According to Le Chatelier's principle, increasing pressure can have a positive effect on reaction speed by increasing the acidity and thermal conductivity of subcritical water (Zhuang et al., 2022).

2.7.3. Residence Time

From an industrial standpoint, short residence time is preferable because it reduces energy consumption and increases production, resulting in smaller equipment size and lower capital expenditure (CAPEX). However, longer residence time can increase the severity of the HTC process, as discussed in more detail in Section 2.7.4. It is important to note that there is currently a research gap in understanding the influence of process duration over a long enough period to observe a turning point. Thus, more research is needed to determine the optimal residence time for maximizing HC yield and quality while minimizing energy consumption and equipment size.

2.7.4. Severity

Severity is a key factor in the HTC process, as it represents the combination of time and temperature (Jeder et al., 2018). This relationship is described by Equation 2.1, where t stands for time and T for temperature. In a study on the HC product from organic sludge, a linear relationship was observed between the severity values of 4.13 to 5.90 and the VM, ash content, H/C ratio, and nitrogen content of the HC, indicating that the severity factor could serve as a useful indicator for analyzing hydrochar properties (W. Wang et al., 2020). Thus, understanding and controlling the severity of the HTC process is crucial for optimizing HC yield and quality.

$$R_0 = t \cdot \exp\left(\frac{T - 100}{14.75}\right) \quad (2.1)$$

2.7.5. Solid Loading

The solid loading of the feedstock is the ratio of solid compared to water and it can have a significant influence on the yield and carbon yield of the HC produced (Tasca et al., 2020). A lower amount of solid content used results in HC with lower higher heating value (HHV) (Tasca et al., 2020). This is because a higher solid content leads to a higher concentration of monomers in the liquid phase, which promotes faster polymerization, resulting in the formation of larger molecules and a higher carbon yield (Tasca et al., 2020). Furthermore, in the aqueous phase, the COD and ammoniacal nitrogen is increased with increased solid loading (Aragón-Briceño et al., 2020).

2.7.6. Catalyst

To improve yields or desired HC and aqueous phase characteristics catalysts such as salts, HM, or organics can be used (Djandja et al., 2023; L. Wang et al., 2023). Adding phloroglucinol to sludge as a cross-linking agent for HC decreased ash content (25.7%) and improved carbon content (15.4%), where the carbon content mainly improved the FC and the lower ash content comes from the increased yield from 68.9% to 88.4% (L. Wang et al., 2023). Citric acid and FeCl₃ have gained interest as they have shown potential catalytic improvements. As Fe can improve active sites of HC by transforming C-O into C-O-Fe groups (Djandja et al., 2023). Citric acids stimulate the hydrolysis of biopolymers, carbonization, and dehydration resulting in HC formation with increased carbon content (Djandja et al., 2023).

2.8. Heavy Metals and Fertilizer Elements

HM have been used for thousands of years, and overall improved society. However, some now dangerous metals, such as lead, were consumed in high amounts in wine by the ancient Romans (Järup, 2003). Trace metals ingested or coming in contact with humans, animals, or the environment can have devastating consequences. Far-fetched events like increased crime rates and the downfall of the Roman Empire have been designated to HM contaminants, raising awareness of the risks on a civilization level (Knapp, 2013; Lin-fu, 1982; Nriagu, 1983; Stilo, n.d.). Today, the health effects of HM are well known, but contamination is continuing, and in some areas, it is even increasing (Järup, 2003). The danger of HM for humans is mostly from chromium, lead, cadmium, mercury, and arsenic (Järup, 2003; Tchounwou et al., 2012). For example, if mercury comes in contact with people, it can lead to diminished reproductive function, low birth weight, functional deficit, DNA damage, and more. (Ha et al., 2017; Henriques et al., 2019; Tchounwou et al., 2012).

During the HTC reaction, metals and heteroatoms can function as catalysts or activators for the pyrogenic decomposition of biomass (D. C. Li & Jiang, 2017). Consequently, an increase in porous structure and defects can be beneficial for product characteristics, such as in areas like batteries, catalysis, soil amendment, and absorption (D. C. Li & Jiang, 2017). However, HM can inhibit HC application in soil, as they can inhibit microbial metabolism and consequently decrease the degradation efficiency of other toxic organic components (Y. Lin et al., 2019). In this section, we will discuss the impact of HM, the model that describes the toxicity of HM, and how different HM elements behave under HTC conditions.

Overall, it is important to consider a range of factors when evaluating the environmental impact of toxic substances, including their concentration, leachability, and distribution across different fractions of the material. The BCR (European Communities Bureau of Reference) three-step sequential extraction procedure is able to show the toxicity of HM across five different fractions (Rauret et al., 1999; Yue et al., 2017; Zhai et al., 2016). These fractions can be classified into five categories, namely exchangeable (F1), bound to carbonates (F2), bound to iron and manganese oxides (F3), bound to organic matter (F4), and residual (F5) (T. Liu et al., 2018; L. Wang, Chang, & Liu, 2019). Of these fractions, the F1, F2, and F3 categories are more bioavailable and pose greater risks to the environment than the more immobilized F4 and F5 fractions (L. Wang, Chang, & Liu, 2019). By taking a comprehensive approach to risk assessment, it is possible to develop effective strategies for mitigating the impact of HM on the environment and protecting the health of wildlife and humans.

2.8.1. Heavy Metals

According to L. Wang, Chang, and Liu (2019), most HM are immobilized within HC, except for arsenic. HMs such as Fe, Mn, Cu, and Zn show a linear increase with an increase in reaction severity in concentration within HC, while Cd, Pb, Hg, As, and Cr tend to increase in the aqueous phase (L. Wang, Chang, & Liu, 2019). However, the total amount of HMs that went to the effluent was less than 30% for Cr, 25% for Cd, Pb, Hg, As, Cu, and Zn, and 10% for Fe, Mn, and Ni, indicating that most HMs are assimilated into the HC (L. Wang, Chang, & Liu, 2019).

HM are better stabilized into HC when the feed water is more alkaline (Zhai et al., 2016). The accumulation of Cr, Cu, and Zn in HM is due to their low solubility, which causes them to dissolve and precipitate under subcritical conditions (Tasca et al., 2020; Zhai et al., 2016). Precipitation can be further increased by using a more alkaline solvent (Zhai et al., 2016).

(H. Li et al., 2021) studied the fate of copper from algae during a HTL process and found that between 82.1–92.7% of the copper is retained into the HC. The dominant form of copper was CuS, which accounted for 70.9% in the HC. HC created at lower temperatures had a higher capability of electron acceptance than electron donation, making it more effective in reducing CuS₂ to CuS.

2.8.2. Phosphorus

Phosphorus recovery has shown promising results in small-scale commercial plants, with recovery rates reaching up to 95% and the phosphorus content in the HC can go up to 3.6 wt% (Lucian et al., 2022; Wray, 2022). Increasing the temperature has been found to enhance phosphorus recovery and promote its immobilization (Huezo et al., 2021; Khosravi et al., 2022; L. Wang, Chang, & Liu, 2019). The predominant form of phosphorus in the HC is Fe chemisorbed to the surfaces of Fe- and Al-hydroxides, which may provide potential fertilizer value when applied to alkaline soils (Schneider & Haderlein, 2016).

2.8.3. Morphology

HM have a significant impact on the surface morphology of carbonaceous products (Sangjumras et al., 2018). The impact of various HM, such as Ag, Co, and Fe, have been researched in combination with starch and these HM can alter the morphology of HC resulting in fibre-like, flower-like, and spherical structures, respectively (Saadattalab et al., 2020). Furthermore, (Sangjumras et al., 2018) found that the addition of Cu, Cd, Fe, Ni, and Ba led to the formation of different nanoparticles on the surface of pineapple leaf and corn stalk HC after further carbonization at 700°C, as is shown in Figure 2.10.

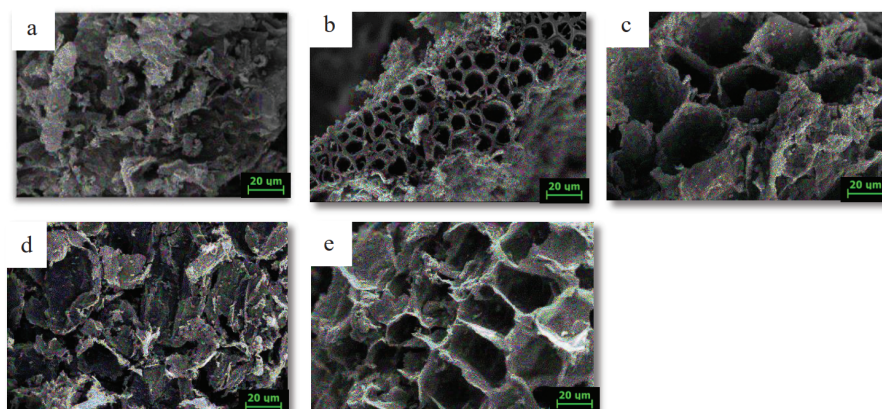


Figure 2.10: Corn stalk HC SEM images (500x) after carbonization process at 700 °C for 2 hours, where (a) copper nitrate (b) cadmium nitrate (c) iron nitrate (d) nickel nitrate (e) barium nitrate catalyst have been added.

2.9. Applications

HC could be implemented in many sectors, as a list of 55 different BC applications has been compiled and includes areas such as animal farming, soil conditioning, the building sector, decontamination, biogas production, wastewater treatment, metallurgy, cosmetics, energy, electronics, textile, medicine, wellness, and food conservation industries (Schmidt & Wilson, 2014). As Schmidt and Wilson (2014) suggest, BC is too valuable to be solely used as a soil amendment and should be utilized at least once for other beneficial purposes (Schmidt & Wilson, 2014). HC also has multiple applications, including its use as a solid renewable fuel, adsorbent, catalyst, supercapacitor, and as a soil amendment through the use of activated carbon precursors (Calderon et al., 2021; Gasim et al., 2022; D. Liu et al., 2020; Malool et al., 2022; Villamil et al., 2020). Using HC products before landfilling, incineration, or soil amendments can contribute to circularity and reduce waste.

2.9.1. Catalyst

In a study by S. Zhang et al. (2020), a lignocellulose HC impregnated with Al for improved catalytic activity was created for the isomerization of glucose to fructose, resulting in highly efficient catalytic performance (33%) and selectivity (93%). Similarly, L. Yang et al. (2022) investigated the isomerization of glucose to fructose and found that endogenous calcium-enriched HC water hyacinth demonstrated similar yields (31%) and selectivity (89%), with calcium being suggested as the catalytic component. Moreover, the use of sludge HC for the catalytic gasification of sludge has shown promising yields (Gai et al., 2017).

The research conducted by Gasim et al. (2022) demonstrated that hydrochar can serve as an activator for persulfate, including peroxymonosulfate or peroxydisulfate, with specific surface area, porosity, presence of oxygen functional groups, persistent free radicals, graphitization degree and aromaticity, defective sites, and heteroatoms such as N, S, O, or B, being crucial factors for achieving effective catalytic activity.

2.9.2. Soil Amendment

Land-use change, which encompasses activities such as biomass burning, deforestation, wetlands drainage, conversion of natural ecosystems to agricultural land, and soil cultivation, is the second most significant cause of anthropogenic GHG emissions, after the combustion of fossil fuels (Lal, 2004). Between 2007 and 2016, land-use change was responsible for 23% of global anthropogenic GHG emissions (Lam et al., 2021). This shift in land use, coupled with poor land management practices, has resulted in the loss of more than half of the original carbon content in once fertile carbon-rich lands (Lal, 2004). To sustain food production in a world where population growth is straining food supplies, it is critical to replenish carbon-depleted soil. Carbon-to-soil sequestration is a promising approach to both improve carbon-depleted soils and reduce emissions (Griscom et al., 2017).

In terms of CO₂ mitigation potential, BC has the most significant impact on agricultural lands and grasslands, as it can add more carbon to the soil, as shown in Figure 2.11 (Griscom et al., 2017). Revitalizing carbon-depleted soils can improve crop growth, purify surface and groundwater, retain more water in the soil, and stabilize ground temperatures (Lal, 2004). Adding, BC can help retain nutrients and agrochemicals in soil, which are essential for crop growth, and reduce runoff ("Biochar", n.d.). The use of BC as a soil amendment has received significant attention in recent years, following the discovery of productive soil named 'Terra-Preta' in the Amazon (Kambo & Dutta, 2015). Studies on biochar-rich dark earth in the Amazon have further demonstrated the positive influence of BC on soil characteristics and yields (Kambo & Dutta, 2015). Therefore, it is crucial to promote BC as a sustainable land-use practice and implement carbon sequestration measures to mitigate the impact of land-use change on climate change.

Water is a crucial component for plant life and carbonaceous structures, such as HC, can increase the WHC of soils, thereby mitigating the impact of climate change-induced heat stresses (Khosravi et al., 2022). The particle size and permeability of chars play a critical role in its ability to improve WHC, with studies showing that HC and BC can decrease bulk density and increase porosity, leading to better WHC (Abel et al., 2013; Khosravi et al., 2022). For example, a study by Abel et al. (2013) found that

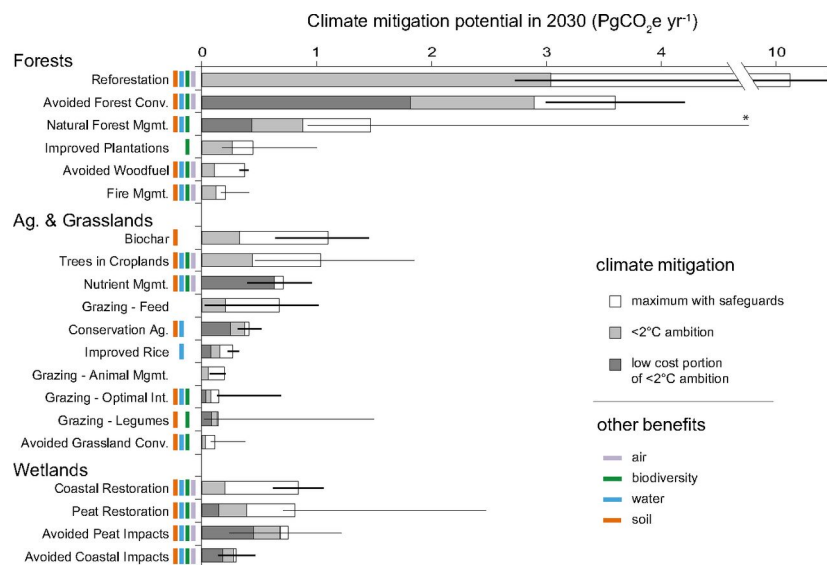


Figure 2.11: CO₂ mitigation potential of natural climate solutions on different land-use types (Griscom et al., 2017).

BC added to sandy soils increased WHC by up to 16.3% when 2.5wt.% BC was added. Moreover, HC amendment can increase the water-extractable carbon in soils, further enhancing soil health (Yue et al., 2017). Furthermore, adding chars alone may not decrease runoff and evaporation. Studies have shown that HC amendment does not necessarily improve wettability (Abel et al., 2013; Gupta et al., 2015).

The morphology of the HC surface can affect soil characteristics. Generally, HC is hydrophobic because of the low quantity of polar groups on the surface. After implementation into the soil, these groups become oxidized which leads to a more hydrophilic nature by creating carboxylic and phenolic functional groups. This effect leads to better characteristics such as cation exchange capacity, WHC, and nutrient retention capacity (Masoumi et al., 2021). Water-extractable carbon is higher in HC amendment soils (Yue et al., 2017).

Healthy soil needs fungi biotica in the hummus to survive. The increases in WHC, because of the hydrophobic character of HC, attributed to fungal colonisation (Abel et al., 2013). When this soil is dried the pores still contain water where microbes can survive and thus decrease mortality (Ren et al., 2017).

HM contamination in soil can disrupt the chemical cycle of soil microorganisms, which is a vital part of soil health (Y. Lin et al., 2019). It has been proven that Ni, Cd, Pb, Cu, As, Zn, Cr, and Hg HMs are toxic for soil microorganisms worldwide (Y. Lin et al., 2019). Unfortunately, these HMs accumulate into HC (L. Wang et al., 2014). The impact of different HM concentrations on soil microbiology and their combination is still not well known (Y. Lin et al., 2019). HC application to soil decreased oxidable and residual fractions were acid soluble and reducible fractions HM content increased (Yue et al., 2017). The change described to HM was released by HC decomposition. Comparing the bioavailability of HM of HC with sludge in soil, sludge has a higher bioavailability (Yue et al., 2017). Preventing leaching and disposing of HM is essential for society and the environment, and if not done correctly, it can end up harming all life, including us.

PAHs can harm the soil biota and have to be below the specified threshold to reduce harm to the environment (J. Wang et al., 2019). To decrease PAHs in HC, C. Wang et al., 2017 recommends firstly a feedstock with low or no PAHs to be used in the HTC process. Secondly, using low temperatures as this possibly creates lower toxic PAHs and fewer amounts of PAHs. However, char created with lower temperatures creates easier decomposed char because of its higher VM and thus PAHs are more accessible (C. Wang et al., 2017). The presence of Cu could suppress the formation of PAHs, while Zn

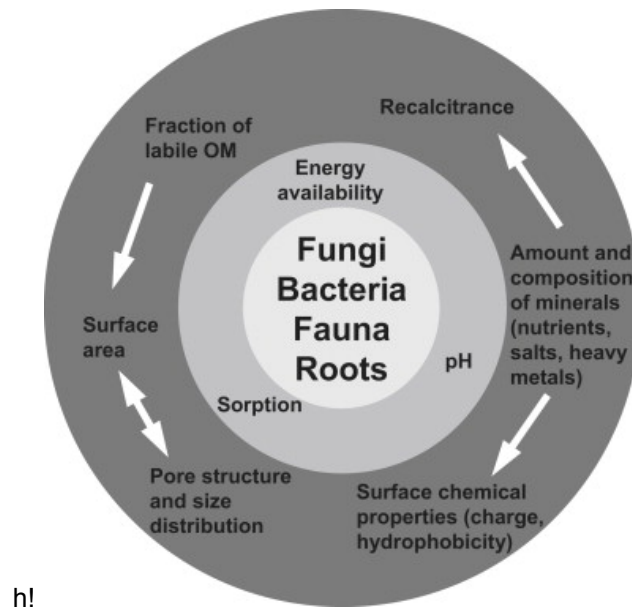


Figure 2.12: This schematic provides an overview of the connections between primary biochar properties (depicted in the outer circle), the soil processes they may affect (represented in the intermediate circle), and the soil biota (shown in the inner circle). The strength of the connections is qualitatively estimated by the distance between circles. White arrows indicate the influence of biochar properties on one another (Lehmann et al., 2011).

in contrast can increase the amount of PAHs in HC (Peng et al., 2017). Wiedner et al., 2013 showed that the environmental risk of PAHs in hydrochar is minimum, but temperature and feedstock affect PAHs significantly. Misuse combined with different legalisation can lead to PAHs into agrosystems as possible pollution.

In contrast, On the surface, carboxyl, hydroxyl, and phenolic groups are abundant and serve as excellent binding sites for heavy metals such as Cd (Ren et al., 2017). These surface groups absorb heavy metals that are present in the soil, reducing their phytoavailability (Ren et al., 2017). Cd can be accumulated by plants which cause the inhibition of plant growth and reduce the production of agricultural products (Ren et al., 2017). Phytoavailable, the availability of an element to plants from the soil, of Cd has been decreased with the implementation of HC (Ren et al., 2017). This has been linked to the high amount of OFGs HC posses (Ren et al., 2017). Furthermore, Ren et al. (2017) showed that Cd availability was decreased as Cd was increased from 22.85% to 50.36% in the oxidizable (F3), and residual (F4) fraction.

Yin et al. (2022) showed that HC can improve lettuce growth in acidic soil, but also showed that crop yield change depends on the feedstock as reed straw HC decreased lettuce yield in combination with acidic soil.

2.9.3. Absorbent

HC can be used as an absorbent for chemicals in sectors such as the printing, dye industries, and contaminated soil (Z. Lin et al., 2023; Maletić et al., 2022). Chemical interactions and acid–base, surface active sites, and redox equilibria between adsorbents and adsorbates can all influence absorption capabilities (Z. Lin et al., 2023). Research done by Z. Lin et al. (2023) showed that N-doped HC from sludge had increased (2 times) absorptive capabilities for congo red compared with the not doped HC control group. Also, they showed that the adsorption effectiveness depends on the pH of the congo red solution (Z. Lin et al., 2023). Still, the poor porosity and low surface area limit the adsorption capacities compared to BCs (Z. Lin et al., 2023). Creating HC on different temperatures (190, 220, and 250°C) and with and without KOH treatment, Ferrentino et al. (2020) showed that the KOH treatment combined with 250°C resulted in the highest absorption capacities. Wei et al. (2018) showed that the

surface area (45.3 m²/g) of HC from municipal sewage sludge was improved (9x) compared to its feedstock. Compared to high-performance porous biochar produced from catalytic pyrolysis of peanut shell the HC from Wei et al. (2018) had a 20 times lower surface area (979 g/m²) but its pore volume (0.382 cm³/g) is comparable (Wei et al., 2018; J. Yang et al., 2020). Furthermore,

2.9.4. Fuel

High concentrations of alkali and alkaline earth metals in biomass show undesirable behavior such as fouling, slagging, klinker formation, and corrosion during combustion in the energy sector (Kambo & Dutta, 2015). The amount of these metals is directly related to the fraction of ash from the char product. Besides heavy industries, the burning of biomass produces ashes that contain HM, these can be used in fertilizers but mostly are stored in landfills (Mierzwa-Hersztek et al., 2019).

Water containing biomass such as walnut shells, and coconut shell could be utilized as biofuels (Naderi & Vesali-Naseh, 2021). Naderi and Vesali-Naseh (2021) increased HHV from 18.85 to 27.95 when operating under optimal conditions found at 250 Celsius, 5 hour run time and 6:1 water solid ratio (85.7%). The Thorwash project of TNO is used in an EU project and showed that fuel from paper mill biosludge can increase fuel performance (Liang et al., 2022). sludge treated by HTC is advantageous for improving dewatering, storage, and feedstock logistics but the combustion properties are not significantly improved (Hansen et al., 2022). Furthermore, the HHV of fuel can be calculated with correlations using elemental composition or looking at FC and VM (Sheng & Azevedo, 2005).

Pollution of NO_x is an environmental hazard and must be limited. As biomass contains nitrogen and sludge has 5-10% nitrogen the potential danger of utilizing this feedstock as a fuel could lead to extensive NO_x emissions (Kulikova et al., 2022; T. Liu et al., 2017; Ozgen et al., 2021). This is in contrast with different qualities of coals that range from brown coal to bituminous coal which have 0.6–2.0% nitrogen content, dry ash free basis, respectively (Nelson et al., 1992; Shimizu & Toyono, 2007). Hansen et al. (2022) showed that HTC decreases nitrogen content in sludge by 10-20%, which could lower NO_x .

2.9.5. Battery

Qatarnah et al. (2021) and J. Wang et al. (2021), J. Wang et al. (2018) research hard carbon anodes from river driftwood, Phenolic resin, and reed straw-derived by HTC pre-treatment and pyrolysis to show the potential use of HTC for hard carbon anodes. Hard carbon (non-graphitizable carbons) materials, which have a good reversible capacity between 350-370 mAh/g, good coulombic efficiency and long cycle life, are used for low-cost anode material in batteries (Goriparti et al., 2014). Z. Xu et al. (2022) created two series of hard carbons from glucose where the first one was made by high-temperature carbonization (i.e. pyrolysis) and the second series by hydrothermal pre-treatment followed by high-temperature carbonization. The extra nanovoids and defects that arise from hydrothermal pre-treatment increased electrochemical performance in the second series. Also, the live cycle assessment (LCA) showed that the HTC pre-treatment process significantly increased sustainability impact, increase overall carbon yield improved carbon structure and morphology's (Y. Xu et al., 2020). A one-step synthesis method for HTC is unfavourable as is shown by Wan et al. (2020) who created an anode that has a 2.5 times higher discharge capacity than without the pyrolysis treatment.

2.9.6. Anaerobic Digestion

Anaerobic digestion can be used to enhance the overall energy yield of the HTC process by utilizing the aqueous phase. Nanou et al. (2020) demonstrated that the aqueous phase of HTC can be treated through anaerobic digestion to produce biomethane, with a potential of generating 11 m³CH₄/m³ effluent from a 2% dry matter sludge feedstock. Furthermore, production rates ranging from 166 to 237 ml CH₄ g/COD have been obtained (Cebi et al., 2022). HTC temperature influences the yield of effluent to biogas through anaerobic digestion, where an increase in HTC process temperature decreases biogas formation (Gaur et al., 2020; Merzari et al., 2019; Nanou et al., 2020). The increase in yield at lower temperatures can be ascribed to short-chain fatty acids like acetic and formic acid (Gaur et al., 2020). Higher reaction severity leads to more complex recalcitrant or inhibitory products that negatively influence the production of biogas. Some of these are; pyrroles, pyridine, ketone, alcohol, and pyrazine (Gaur et al., 2020; Merzari et al., 2019).

HC additives to anaerobic digestion have shown improved hydrogenotrophic methanogenesis promoting the reduction of CO₂ to CH₄ by a higher amount of H⁺ intermediates as HC has the ability to facilitate electron transfer (DIET: direct interspecies electron transfer) (Rodriguez et al., 2021). Adding HC show improvements in biogas creation by increasing alkalinity, increasing intermediates (acetic acid and hydrogen), supplying nutrients, purifying the biogas by retaining part of the CO₂, decreasing the lag phase, providing microbial support and reducing the inhibition of high ammonium concentration (Rodriguez et al., 2021). As an additive for anaerobic digestion the specific methane production rates when adding HC (49.8%) outperforms BC (34.3%) (Shi et al., 2021).

2.10. Conclusion

With HTC, emissions can be decreased because it consumes less energy, has a higher yield than dry thermal conversion methods, and does not require harsh reactor conditions. It is more justifiable to use HTC than any other thermochemical process to convert high moisture content biomass to useful products (Heidari et al., 2019). Hydrothermal treatment of high moisture biomass does, however, still have certain limitations because the technology is not yet ready for industrial use.

There is no agreement in the literature regarding how the sludge is produced or where it comes from, except for the occasional distinction between primary and secondary sludge. It is challenging to compare HC through the elemental (CHNO) composition of sludge to another due to the wide variations in their composition. Cultural differences may contribute to this difference; for instance, using toilet paper may increase the lignocellulosic content of the sludge.

Every nation has different laws, some stricter than others. The regulations for BC, which is similar to HC, are often given forth by two institutions, IBI and EBC. When a market for this material develops, these laws will likely apply to HC as well as the char implication into soil. There are various grades available with the EBC depending on the application field. Given that there are stricter rules for the application in organic farming and as an addition to cow food, using EBC-Agro will be adequate for soil implication and thus be used to benchmark results. Measuring the pH of the produced HC is necessary to understand its possible impact as a soil amendment, as pH is one of the critical factors affecting soil biota and vegetation (Lehmann et al., 2011). The EBC made a pH value mention obligatory (Schmidt et al., 2022).

Reaction severity can be calculated by combining data like temperature and retention time. This combination can be used to evaluate how different feedstocks were treated. Less yield, more HM accumulation, and a higher FC/VM ratio result from higher temperature and retention time, which also raises the HHV. Additionally, more FC enhances the carbon stability, making less mass accessible to bacteria but increasing the potential for carbon sequestration. A temperature of 180°C is the minimum temperature for the decomposition of proteins and polysaccharides and the most notable decline in moisture content happens at this temperature. At least 180°C is necessary for dewatering the biosludge and starting of important Maillard reaction. Where temperatures above 250°C could potentially block pore structure. Also, the region of HTL would be reached, creating an oil phase, subsequently increasing the number of phases and, thus, the process complexity.

3

Materials and Methods

Seven steps can be used to organize the planning, carrying out, and analyzing of an experimental campaign (Montgomery, 2013). The first step is to (1) recognize and state the problem; (2) a selection of factors, levels, and ranges is needed to determine the boundaries and incorporate research time constraints; (3) response variables selection is done to add to the boundaries and research time constraints. Multiple experiment designs are possible. Depending on the results of the experiments, (4) a fitting experimental design is more time and resource-efficient; (5) carrying out the experiments and how are essential. A (6) statistical analysis is required to determine how the input variables affect the outcome. Finally, (7) conclusions and recommendations must be provided to interpret the data and advise on possible future experiments (Montgomery, 2013). This chapter describes points 2 to 4, where chapter 4 shows steps 5 and 6. The analyses performed are explained in this chapter for repeatability.

3.1. Experimental Design

The experimental design considered time and temperature as factors in a central composite surface response design. Each independent factor consists of three levels. For temperature, these levels are set to 180, 210 and 240°C. The retention time was set to 2, 4, and 6h. On each temperature-retention time point, HTC process is performed at least in duplicate and some points have been made in triplicate. The analyses for characterizing HC, the aqueous phases, and the gas phase are shown in Table 3.1.

Table 3.1: Analysis performed on the produced phases and their units.

	Analyses	Units		Analyses	Units
Yields	Hydrochar	%	Hydrochar	ICP-OES	mg/kg
	Aqueous phase	%		Ultimate analysis	%
	Gas + residue	%		Proximate analysis	%
	Dry solid	%		BET	m ² /g
Aqueous phase	ICP-OES	mg/kg	Leaching	mg/L	
	Ammoniacal nitrogen	mg/l	total organic carbon	mg/L	
	Chemical oxygen demand	g/l	Leaching ICP-OES	mg/kg	
	pH	-log([H ⁺])	XRF	%	
			XRD	Intensity	
Gas	HPLC	%	pH	-log([H ⁺])	
			Bomb Calorimetry	MJ/kg	

3.2. Material

From a GTL energy site, approximately 25 kg of centrifuged and sun-dried biosludge were sampled and transported to the Red lab of civil Engineering TU Delft. The biosludge was refrigerated at 4°C. The received sludge had a 43.4% humidity percentage. A 4838 Parr Reactor Controller in combination

with a 1.5-litre stainless steel vessel non-stirred pressure vessel was used for HTC, from Parr USA. It has no steering capacities.

3.3. Experiment Procedure for HTC

Three phases are produced by the HTC process: gas, HC, and an aqueous phase shown in Figure 3.1. Understanding the challenges and potential random and systematic uncertainties in producing these phases was crucial before analyzing them. This section will outline the HTC process in eight steps, illustrated in Figure 3.2. Also, this section, has provided greater detail on potential errors to provide a better understanding of the yield data.

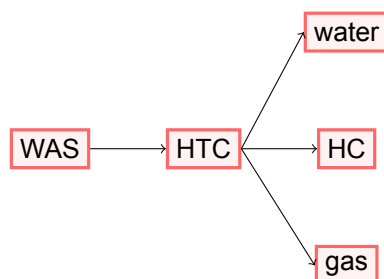


Figure 3.1: Simple process diagram of the process, input, and products

First, the vessel was filled with the provided biosludge and demi water. The demi water was added after loading the sludge into the vessel. A 20% solid/water mixture was created by mixing 353,4g of sludge (43,4% moisture) with 646,6g of demi-water. The mass load of the vessel weights approximated 1000g.

The next step was preparing the vessel. To prevent gas from escaping and further oxidising the reactor vessel was flushed with N₂ and sealed with a lid. Pressure builds up when the gas relief valve was closed during nitrogen venting. Nitrogen gas pressure build-up was expected not to affect the response variables significantly.

Before the retention time begins, the vessel was preheated at an increment of 5°C per minute. When the proper temperature was reached, a timer was set. Once the run was completed, the vessel was cooled overnight outside the reactor jacket.

Collecting the phases and cleaning the vessel were the next steps. The HC and aqueous phase were vacuum filtered using a 2-litre vacuum vial and a porcelain Buchner filter with Macherey-Nagel 85/70 (0,6µm) 150mm filter paper, from Germany. The vial and the Bucher filter are weighted, including the parafilm and filter paper. The HM and aqueous phase mixture inside the large vessel was carefully emptied into the Bucher filter under vacuum. The first mass to leave was mostly liquid. The vessel was further scraped out to retrieve most of the sample. Some substance was lost because it was attached to the vessel walls and scrapping spoon, lost by splattering, and process handling. This amount was recorded as residue. The residual amount attached to the walls was calculated using the vessel's weight. The aqueous and HC yields are then measured by weighting, the Bucher filter, and the vial. To identify the gas composition, a sample of gas from the vessel was taken before releasing the gas by detaching the vessel cap. The vessel was weighed to determine how much mass was being released as a gas.

Finally, the wet HC was dried at 105 °C overnight, the aqueous phase was stored, and the vessel was cleaned. The process was repeated by the above-described experiment schedule, which was summarized in Figure 3.2.

3.4. Analyses Methods

This section presents the methods used for analysing HC, aqueous and gas phase response variables.

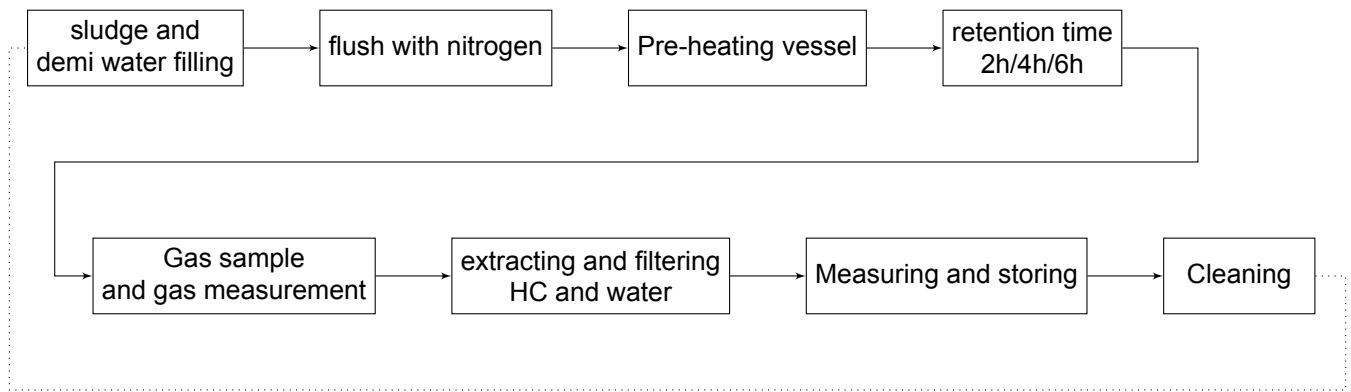


Figure 3.2: Flow diagram of the steps necessary to create HC, aqueous and gas phases. These steps, possible errors, and difficulties are described in section 3.3

3.4.1. Mass Yields

The mass yield, liquid, and gas yield have been analysed using eqs. (3.1) to (3.3). The residue was also denoted during the process and calculated by Equation 3.4. The residue consists of residual product inside the vessel, vessel cap, and spatula used to scrape the product, evaporated moisture during vacuum filtration, and effluent splashes during the pouring of the product into the vacuum filtration setup. Equation 3.5 calculates the total dry masses added into the vessel and how much of this was recovered into the HC. The procedure to obtain the data used in eqs. (3.1) to (3.5) was described in section 3.3. The data was shown in Figure 4.1.

$$Y_{gas} = \frac{Mass_{before HTC} - Mass_{after HTC}}{Mass_{total}} \quad (3.1)$$

$$Y_{liquid} = \frac{Mass_{liquid after filtration} + Y_{solid} \cdot \%_{moist solid}}{Mass_{total}} \quad (3.2)$$

$$Y_{solid} = \frac{Mass_{solid after filtration} \cdot (100 - \%_{moist solid})}{Mass_{total}} \quad (3.3)$$

$$Y_{losses} = 100 - Y_{solid} - Y_{liquid} - Y_{gas} \quad (3.4)$$

$$Y_{dry solid} = \frac{S_{in}}{S_{out}} \quad (3.5)$$

3.4.2. Hydrochar and Aqueous Phase pH

The pH of the aqueous phase and HC was determined with a WTW™ inoLab™ Multi 9430 IDS™ Digital Benchtop Multiparameter equipped with a SenTix® 94x electrode, from Xylem Analytics Germany.

Aqueous phase

For the aqueous phase characterization, each phase was stirred well before the measurement. This was because the test runs showed that long-standing aqueous phase led to COD deviation at different sample heights. The pH data was shown in Figure 4.15c. With respect to hydrochar pH, we used the method described in Singh et al. (2017). A 5,0g dry HC sample was milled (4188 Maschrenweite 0,63mm) into a bucket. The sample was poured into a bottle, filled with 50mL of demineralised water (5 times 10ml pipet), and it was shaken thoroughly. These bottles were stirred for 1 hour at 25°C. A 30-minute period of rest for the suspension took place. Then the pH was measured, and the pH sensor was cleaned (Singh et al., 2017). The results of this analysis are shown in Figure 4.5.

3.4.3. Ammonia and COD Hach Kits

Ammonia

The concentration of ammoniacal nitrogen in the aqueous phase was determined using a LCK 303 Ammonium kit from Hach. Ammoniacal nitrogen refers to the nitrogen in water that is in the form of ammonia (NH₃) or ammonium (NH₄⁺). The samples were shaken before measurements took place. The kit was used according to instructions supplied by Hach. Each aqueous sample was measured in triplicate, where the average was used as the data point. The ammoniacal nitrogen data is shown in Figure 4.15b.

COD

COD of the aqueous phase was measured using a test kit. The kit used was the TNTplus®824 kit from Hach, with a range between 5-60g/l COD. Each aqueous phase was shaken before being measured because test samples showed better accuracy. The test kit was tested according to method 10212 supplied by Hach. Every sample was measured in triplicate, with the average serving as the data point. The COD data is shown in Figure 4.15a.

3.4.4. Inductively Coupled Plasma - Optical Emission Spectrometry

To obtain HM concentrations and elemental concentrations in the aqueous and HC phases, inductively coupled plasma atomic emission spectroscopy (ICP-OES) was used. The acid mixture to make the HM accessible can be found underneath. The vials' lids are opened to let out any accumulating gas. Otherwise, excessive pressure will cause the vial caps to pop off. Each aqueous and HC sample was analysed in triplicate. The aqueous phase and HC ICP-OES data are shown in detail Figure A.1 and Figure A.2, respectively. Where bar plots are shown in section 4.6.

Aqueous Phase

In a vial with two times 4.5ml of demi water, 1ml of 30% Aqua regia, and 0.1ml sample are added.

HC

For the HC samples, at least 0.1g was added to a vial, and 10ml of Aqua regia was added.

3.4.5. Ultimate Analysis

The carbon, nitrogen, and hydrogen part of the ultimate analysis was performed by an external company, Bureau Veritas, by ASTM D5291C standard. All samples are pre-dried for 24 hours at 105°C before being analyzed. Because of budget constraints, only one sample of a time-temperature point has been measured. The results obtained from Bureau Veritas are the averages of duplicate measurements. The oxygen content was calculated by difference, as is shown in Equation 3.6 where the data of Figure A.2r was used for sulfur.

$$\text{Percentage of Oxygen} = 100 - \text{percentage of (C + H + S + N + Ash)} \quad (3.6)$$

3.4.6. Proximate Analysis

Moisture content of HC wet cake was available but not shown in this thesis because the values are inaccurate because of vacuum filtration. Therefore, moisture was not used as each sample was measured after drying at 105°C. The data obtained for proximate analysis was shown in section 4.3. FC was calculated by Equation 3.7, where ash (A) percentage analysis was described underneath, M stands for the moisture percentage, and VM stands for the volatile percentage. Furthermore, the VM was determined with thermogravimetric analysis (TGA) as described below.

$$FC = 100 - M(\%) - A(\%dry) - VM(\%dry) \quad (3.7)$$

TGA

To determine the VM, a TGA was used. This analysis was conducted on a TGA SDT Q600, from TA instruments in Belgium. For sample preparation, an alumina crucible was filled with 17–20 mg of sample. The program starts with nitrogen gas, heated at 10°C per minute to 110°C. The temperature was held at 110°C for 10 minutes. Ramping up the temperature continues, from 10°C to 600°C. Here, the temperature was held for 10 minutes. The gas was switched from nitrogen to oxygen. Finally, the sample was burned isothermally at 600°C for 15 minutes. The data obtained was shown in section 4.3.

Ashes

At 105°C, the dried HC was dried for another 24 hours. Ash analysis was performed with a Nabertherm muffle furnace LV 15/11/P330, Germany, and according to the NREL/TP-510-42622 method. The samples are heated at 550°C for 1 hour. The ash analysis was done in triplicate in each experiment. The ashes were stored for XRD analysis, as described in subsection 3.4.8.

3.4.7. Bomb Calorimetry

The nine HC samples that were also analysed by ultimate analysis were measured regarding their heating value using a bomb calorimeter. For each measurement, a 1g sample was pelletized under 25 bars. Bomb calorimetry analysis was performed according to method supplied by Parr. The results can be found in section 4.5.

3.4.8. XRD and XRF

Ruud Hendrixx of the TU Delft's X-RAY Facilities Group performed the X-ray diffraction (XRD) and X-ray fluorescence (XRF) analyses of the HC. The results are shown in section 4.9.

XRF

The XRF analyses are performed on the HC samples used for ultimate analysis and on the ashes of 9 other samples than those used in the ultimate analysis. This was because trial and error showed that a high percentage of carbon was still in the ashes. Therefore, the samples are heated in a Nabertherm muffle furnace L 15/12/B180 at 815°C for 2 hours before XRF analysis (Xing et al., 2016). The XRF analyses are performed with a Panalytical Axios Max WD-XRF machine. The data obtained was processed by SuperQ5.0i/Omnian software.

XRD

For XRD, a Bruker D8 Advance diffractometer Bragg-Brentano geometry and Lynxeye position sensitive detector was used. The Bruker uses Cu K α radiation, a divergence slit V12, a scatter screen height of 5 mm, and at 45 kV 40 mA. The sample spinning was on. Detector settings LL 0.19 W 0.06 where the analysis was performed from Coupled θ - 2θ scan 5° - 110°, with step size 0.041 ° 2 θ , counting time per step 2 s. The data was evaluated with Bruker software DiffracSuite.EVA vs 6.1.

3.4.9. Surface Area

Brunauer–Emmett–Teller theory (BET) determines the surface area and porosity. One sample per temperature at 180, 210, and 240°C was analysed. These three samples all have a 4 hours retention time. Each point was measured in duplicate. The machine used for this analysis was a Quantachrome Instruments Autosorb IQ-XR-AG. Where 0,1 g was added into a 9mm glass rod. It was first desorbed at 150°C for 120 minutes under a vacuum. Hold for 30 minutes with a vacuum. A filled liquid nitrogen dewer controls the temperature when measuring absorption. Where helium was used to perform the analysis.

3.4.10. Leaching of Heavy Metals and Total Organic Carbon

The leaching experiments are performed on one sample at 180-4, 210-4, and 240-4. The samples have been prepared in duplicate. 1g of HC was grounded and put into a vial with 200ml of demi water. This vial was agitated at 200 rpm. and 37°C. A 17ml sample was taken at 1, 2, 4, 6, 20, and 24 hours. This was according to Yi et al. (2015). At each point, the total organic carbon was measured. This data was shown in section 4.7. ICP-OES was used to determine the leaching of HM in the samples.

3.4.11. Gas Chromatography - Mass Spectrometry Biogas

From each run, a gas sample was taken. This was analysed with an Agilent Technologies 7890A Gas chromatography Mass Spectroscopy (GC-MC) system. The results are shown in section 4.11.

Experimental Results and Discussion

In this chapter, the data obtained by the experiments described in chapter 3 are shown, explained, and discussed. The data points obtained from the different analyses with the data regressions model planes for the central composite designs are shown in this chapter. Underneath the figures, the statistical p-values of the overall model, the temperature (factor A) and time (factor B) are stated. $P(B)$ shows quantitatively how temperature is affecting the response variables, $p(A^2)$ shows quantitatively that temperature exerts a quadratic effect on the response variable, and $P(AB)$ shows that there is an interaction between temperature and time with respect to the response variable. The data regression model equations and ANOVA tables of the provided figures in this chapter can be found in Appendix A.

4.1. HTC Product Distribution

Figure 4.1 displays the mass yields of the HC, aqueous phase, and gas and losses phase as a function of time and temperature. Figure 4.1a illustrates the mass yield of the HC obtained after the vacuum filtration step. The HC yield decreases as temperature and residence time increase. Specifically, the highest HC yield of 28.6 wt.% is attained at 180°C for 2h, while the lowest yield of 12.2 wt.% is obtained at 240°C for 6h. The decrease in yield is primarily attributed to the thermal degradation of the biosludge during carbonization. During HTC, the bound water in biosludge is transferred to free water, and the solid HC becomes more hydrophobic, which decreases the amount of moisture and thus weight (Figure 4.1a). Furthermore, results indicate that residence time has little impact on HC yield, with a decrease of 1,3 wt.% between 180°C 2h and 6h. At 240°C for 6h and 180°C for 4h, a relatively large standard deviation (SD) is observed due to experimental inaccuracy caused by the extended vacuum filtration time (over 4h) compared to the typical 5-15 minutes for other samples.

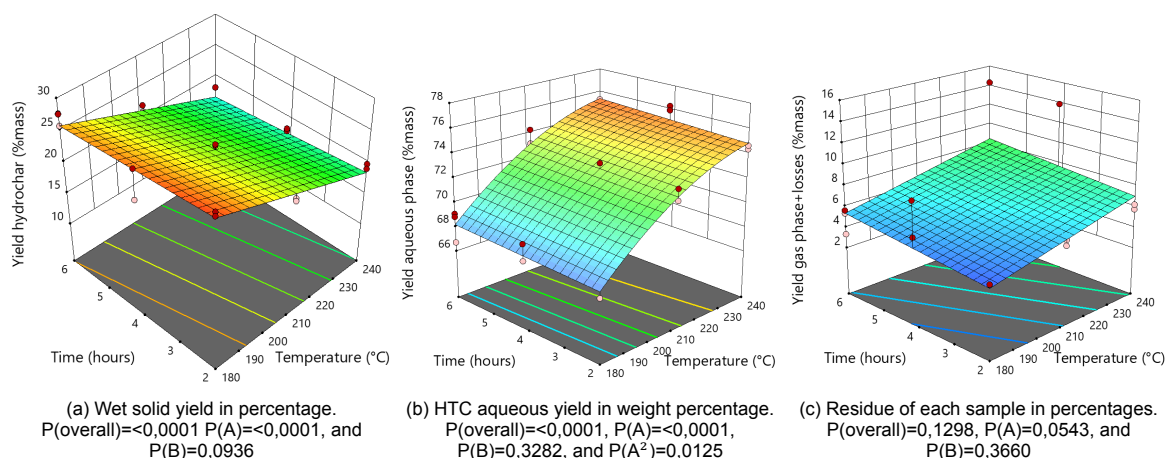


Figure 4.1: Mass yields of the (a) HC, (b) aqueous phase, and the (c) gas plus losses with all p-values. Factor A represents temperature and factor B represents time.

The aqueous phase is the most abundant product obtained during HTC, as shown in Figure 4.1b. The yield of the aqueous phase increases with increasing temperature, showing a statistically significant linear and quadratic relationship. The aqueous phase yield mostly increases between 180°C and 210°C, with the highest yield of 76.3 wt.% obtained at 240°C and the lowest yield of 66.7 wt.% obtained at 180°C. This is due to HTC being a non-evaporative dehydration process, where higher temperatures intensify the removal of moisture, which results in higher fractions of process water. (Zhuang et al., 2022). The steep increase in aqueous phase yield between 180°C and 210°C can be attributed to the conversion of bound water to free water, releasing more aqueous fraction from the HC than at higher temperatures between 210°C and 240°C. With respect to the gaseous phase, results indicate that as temperature increases, the HC is thermally decomposed into gaseous compounds (Figure 4.1c).

The dry solid HC yield, from now on biochar (BC) yield, with respect to the dry input, is presented in Figure 4.2. Between 50 wt.% and 60 wt.% of BC can be recovered for every gram of dry biosludge. The results show a similar trend to that observed in Figure 4.1a, with the temperature being the primary operational variable influencing the BC yield. The largest decrease in BC yield occurs from 180°C to 210°C between 8%-4% wt.%, while the BC yield between 210°C and 240°C decreases only by 1-2 wt.%.

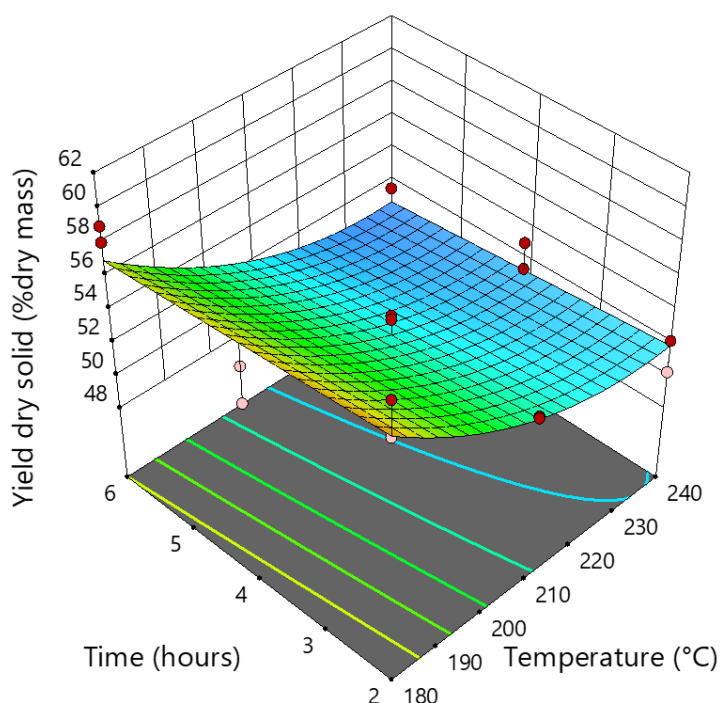


Figure 4.2: BC yield per dry input. $P(\text{overall}) < 0,0001$, $P(A) < 0,0001$, $P(B) = 0,1698$, and $P(A^2) = 0,0202$

4.2. Ultimate Analysis

The ultimate analysis of the raw biosludge is presented in Table 4.1, which shows the percentages of carbon, hydrogen, oxygen, and nitrogen. As can be seen from Table 4.1, the biosludge contains a high amount of N (6.77 wt.%).

Table 4.1: Ultimate analysis of the raw biosludge (wt.% d.b.)

	C	H	N	O
Raw biosludge	45,67	6,41	6,77	41,15

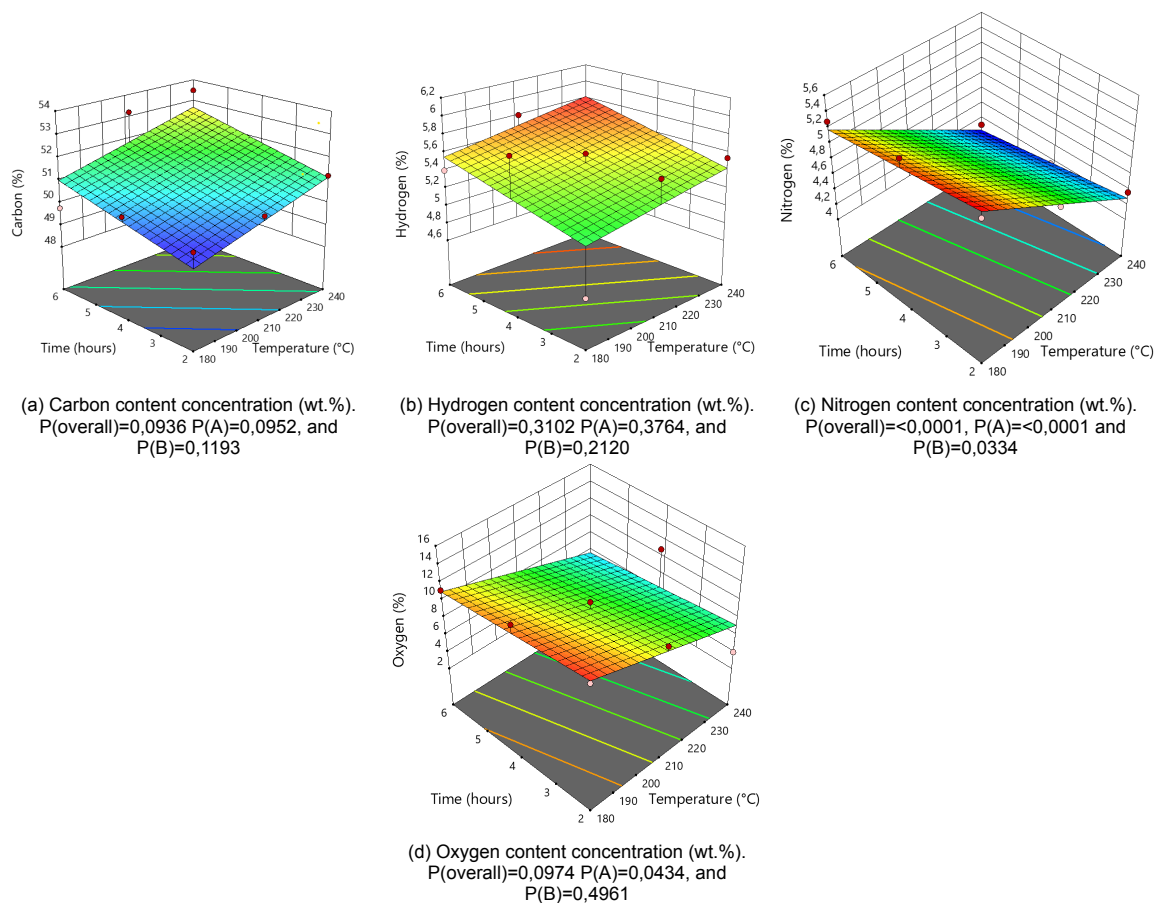


Figure 4.3: Percentage of carbon, hydrogen, nitrogen, and oxygen content (wt.% d.a.f.). Factor A represents temperature and factor B is the influences of time

The BC ultimate analysis is presented in Figure 4.3. The carbon content is shown in Figure 4.3a where with increasing temperature and residence time, the HC becomes more carbonized and its carbon content is observed to increase. The carbon content varies between 49,8 wt.% and 53,5 wt.%, which is an improvement of at least 4,29 wt.% from the raw biosludge. BCs above 50 wt.% carbon content meet the requirements of the EBC to be considered as BC.

With respect to hydrogen (Figure 4.3b), the overall data regression model shows that an increase in temperature and residence time increases the hydrogen content. The hydrogen content of BC at 180°C and 2h declined to 4,6 wt.% (180°C and 2h) from 6,4 wt.% in the raw biosludge after HTC. But, as the temperature increased, the hydrogen content raised up to 5,8 wt.% for 240°C and 6h. Where the data regression model shows content varying between 5,2 wt.% (180°C and 2h) - 5,8 wt.% (240°C and 6h).

After HTC processing, the nitrogen concentration decreased to 5.4 wt.% at 180°C and 2h from 6.8 wt.% in the raw biosludge. With increasing temperature and time the nitrogen content was further reduced to 4.1 wt.% at 240°C and 6h. Processing with HTC reduced nitrogen content between 22 wt.% (180°C and 2h)-40wt.% (240°C and 6h), double the average amount of 10-20% nitrogen reduction reported in literature for primary sludges (Hansen et al., 2022). This could differ because the nitrogen content of the raw biosludge (secondary sludge) has over double the amount of nitrogen content compared to primary sludge (Hansen et al., 2022; Kulikova et al., 2022). Furthermore, comparing BC with conventional coal, the amount of nitrogen is at least more than double that of bituminous coal (<2,0%) and compared to brown coal (>0.6%) at the minimum seven times higher (Nelson et al., 1992). When used as a fuel, this could lead to more NO_x emissions, which must be considered to weigh the environmental impact in the context of fossil fuel alternatives.

Figure 4.3d shows that oxygen content in BCs decreases with temperature and residence time. The oxygen content of the starting material includes ashes, where the oxygen contents shown in Figure 4.3d, have been calculated by distracting ash content. Because of this, the oxygen contents can not yet be compared. The figure indicates that the oxygen content of BCs linearly decreases from around 12 wt.% at 180°C to approximately 10% at 210°C and 7% at 240°C. Out of the nine BC samples, six samples are in agreement with the regression model, while three points at 210°C 6h, 240°C 4h, and 240°C 6h could be considered outliers.

4.3. Proximate Analysis

Figure 4.4 shows the proximate analysis including VM, FC, and ash data from the BC samples in figs. 4.4a to 4.4c. The moisture contents of the BCs are not shown because of the thermal drying.

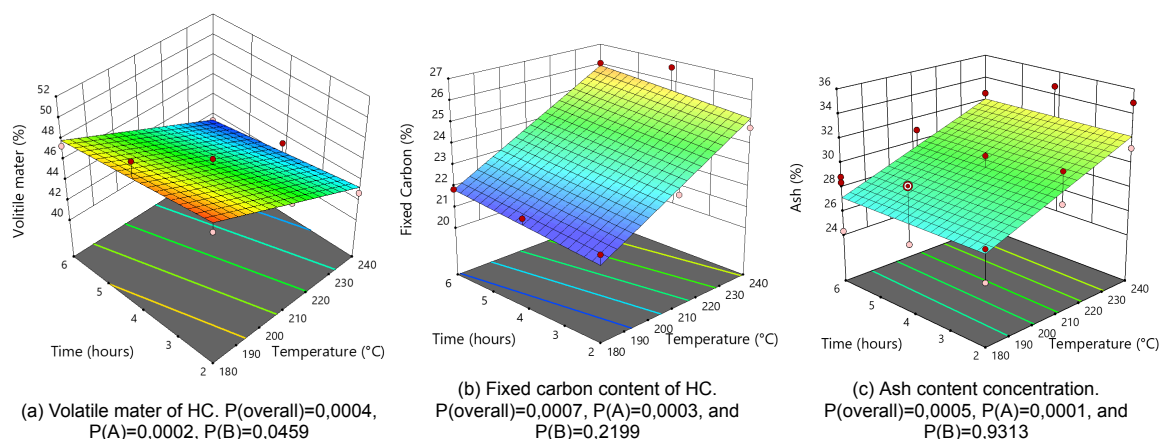


Figure 4.4: Proximate analysis showing volatile matter, fixed carbon, and ashes of the BC samples.

As observed in Figure 4.4a, temperature and residence time have a significant impact on the VM content of BCs. The VM content of BCs lies between 50-41 wt.%, where the highest VM content is observed at 180°C 4h (50,53 wt.%) This measurement is statistically the greatest outlier by DFFITS and cook's distance. The opposite trend is observed for FC content, where an increase in temperature and residence time rises FC content. Figure 4.4b shows that the average FC content ranges between 21.1-25.9 wt.%.

Figure 4.4c shows that the ash content increases with temperature. On the other hand, it is observed that the residence time does not impact ash concentration. The 6h BC samples at 180°C had 27.2 wt.% ash, at 210°C 29.7 wt.% and at 240°C 32.1 wt.%, which is an increase compared to dry biosludge (17,0 wt.%). literature reported ash content in dry-based biosludge can have 21 wt.% and BC ash percentage of up to 40 wt.% have been measured (Paiboonudomkarn et al., 2023; Volpe et al., 2020; R. Wang et al., 2019). in a study by Vassilev and Vassileva (2009), 37 coals from various locations around the world were analyzed and categorized based on their type and ash content. The results showed that the average ash content among these coals was 19.8 wt% (Vassilev & Vassileva, 2009). The ash analysed showed an average of 30 wt.% ash content which in coal terms would be categorized as an high-ash containing coal (Vassilev & Vassileva, 2009). with The three oxygen content measurements that did not correspond with the regression model are all BCs with a higher amount of ash content which could explain the variance in Figure 4.3d.

4.4. Hydrochar pH

In Figure 4.5 the pH of the BC is presented as a function of the HTC residence time and temperature. According to Lehmann et al. (2011), the mineral ash content in BC is positively correlated with its pH, such that biochars with higher ash content tend to be more alkaline. As shown in Figure 4.4c, the mass percentage of ash in the BC increases with HTC temperature, which can result in a more alkaline

pH (Figure 4.5). However, the surface chemistry of BC is more complex. For example, Zhuang et al. (2018) reported that the hydrochar contains more acid groups, such as COOH and OH, with increasing temperature, and it becomes more hydrophobic. Nevertheless, the decarboxylation of the COOH carboxylic acid groups can lead to a less acidic hydrochar (Roslan et al., 2023). Jellali et al. (2022) showed that increasing the time from 0.5 h to 1 h at 250°C can decrease the pH of BC, with a decrease in pH from 6.0 to 5.5.

The presence of the residence time-temperature interaction term results in a decreasing pH along the 180°C 2-4-6h line and an increasing pH at the 2-4-6h line at 240°C. It is still inconclusive how the AB factor causes this behavior.

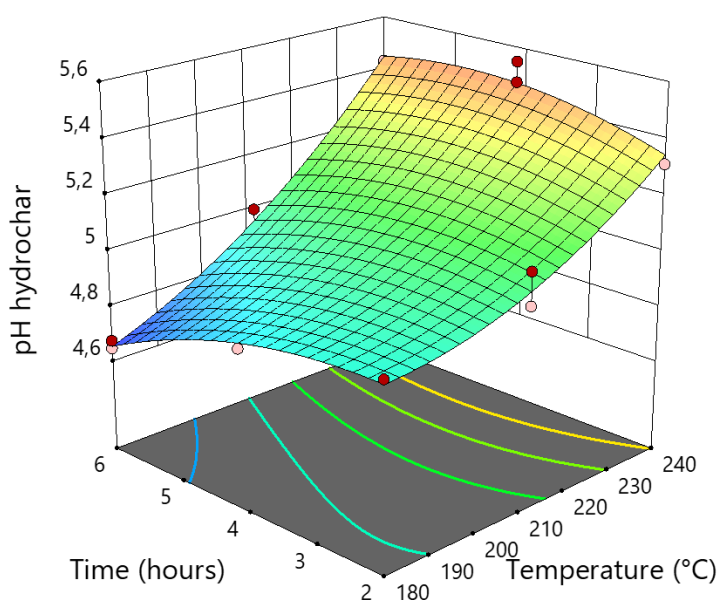


Figure 4.5: Hydrochar pH. $P(\text{overall}) < 0,0001$, $P(A) < 0,0001$, $P(B) = 0,0593$, $P(AB) = 0,0027$, $P(A^2) = 0,0178$, $P(B^2) = 0,0496$

The results presented in Figure 4.5 confirm literature findings of Lehmann et al. (2011). Where at 240°C, the BC with the highest amount of ash (Figure 4.4c) reports a more alkaline pH than samples at 180°C. The sample with the lowest ash content has the most acidic pH at 180°C and 6h. The pH of the BCs made at 180°C and 2, 4, and 6h corresponds to the pKa of short-chain fatty acids produced by HTC, like acetate (4.76), propionate (4.9), and n-butyrate (4.82) (K. Zhu et al., 2021).

4.5. Bomb Calorimetry

The analysis conducted on the heating value HHV of BCs is presented in Figure 4.6a. The results indicate that the average HHV range for BCs falls between 21.9-23.5 MJ/kg, which is comparable to the higher end of the HHV for sub-bituminous coal (IEA, n.d.). It is worth noting that an increase in temperature and residence time leads to an increase in the HHV of BCs, as demonstrated by the trend observed in Figure 4.6a. These results are also in agreement with the increase in C content at the expense of O reported in figs. 4.3a and 4.3d. Furthermore, the average HHV of BCs is 14% higher than that of raw biosludge (19.8 MJ/kg).

The energy content graph resembles the inverse of the oxygen content (Figure 4.3d), which is most evident on the 240°C axis. The decreasing oxygen content increases the HHV, as does the increase of carbon content (Sheng & Azevedo, 2005).

Figure 4.6b presents the HHV per dry input. As can be observed, the HHV per dry input is outweighed by the low amount of BC yield produced at higher temperatures and residence time. The most interesting finding in Figure 4.6b is that low temperature and low residence time BCs might be more attractive

when used as fuels than BCs with higher C content produced at higher temperatures. However, it is important to note that these findings were based on a HHV perspective, assuming that all moisture was evaporated. A lower heating value perspective and energy balance analysis would provide a more accurate assessment of the dewatering potential of the HTC process, as compared to thermal drying. Such an analysis might even contradict the aforementioned conclusion. In addition, the dry BC yield that is lost ends up mostly in the aqueous phase from which energy can be utilized through anaerobic digestion improving energy recovery.

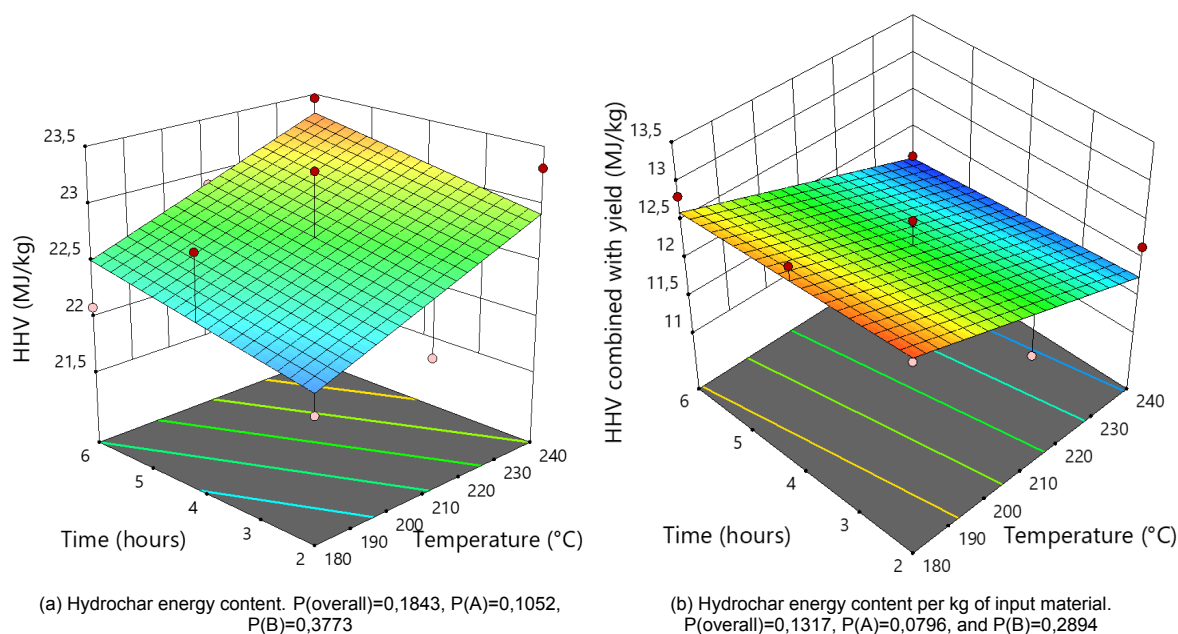


Figure 4.6: (a) HHV of HC samples and (b) the HHV multiplied with the dry solid yield.

4.6. ICP-OES Analysis

The elements detected by ICP-OES have mostly ended up in the BC. Al, B, Ba, Ca, Cl, Co, Cr, Cu, Fe, K, Mg, Mn, Na, Ni, Sr, Zn, P, S, Si, and Mo were detected in the aqueous and HC phases. In this section, the HM regulations have been coupled to the data and subsection 4.6.1 shows the ICP-OES data in detail, as does subsection 4.6.2 for the ICP-OES data of HC. The surface response models of each elemental varying with time and temperature factors can be found in Appendix A.

Eight HM species are under regulation by the EBC namely; Pb, Cd, Cu, Ni, Hg, Zn, Cr, and As, where Cu, Ni, Cr and Zn have been found in the biosludge, the aqueous phase, and HC (Schmidt et al., 2022). The IBI also takes Mo into account ("Biochar", n.d.). Table 4.2 shows that Co concentration is between 4 and 5 times higher than the highest allowing regulations, from IBI. Cr concentration is 2-3 times higher than EBC regulation thresholds for customer products and Cu is 7-8 times higher. Ni concentration for some samples is within regulations. The amount of Zn is a factor between 22-29 higher than regulations.

4.6.1. Aqueous Phase

The elements detected by ICP-OES in the aqueous phases are shown in Figure 4.7, where Figure 4.7a shows the elements Ca, Fe, K, Mg, Na, Cl, S, and Si that range between 35-3500 mg/kg and Figure 4.7b shows the elements ranging between 0.2-200 mg/kg, which are Al, B, Co, Cr, Mn, Ni, Sr, Zn, P, and Mo. Overall it can be seen that HM concentration is significantly reduced compared to the original biosludge and that with increasing time and temperature, the concentrations are declining further. Only the alkali metals K and Na are showing an increase with time and temperature for the aqueous phase. Cl is detected because of the aqua regia used to dissolve the HMs.

Table 4.2: Original sample HM profile obtained by ICP-OES, the average concentration of all HC per elemental, the highest and lowest elemental concentrations measured, at which temperature and time these were measured, and the thresholds of regulations stated in section 2.4, where DEC stands for declaration.

Elements (mg/kg)	Al	B	Ba	Ca	Co	Cr	Cu	Fe	K	Mg	Mn	Na	Ni	Sr	Zn	P	S	Si	Mo
Biosludge	710	139	51	19893	363	122	378	99029	711	3047	1800	2786	259	215	3484	16995	25014	126	373
Average content in all BCs	1120	92	73	24470	399	160	511	139349	339	3941	2624	820	128	312	5055	27472	18012	90	415
Highest content in all BCs	1407	113	81	29035	479	185	563	162969	530	18317	3108	1287	256	361	5842	31714	19762	174	451
Sample label with highest content	240-4	210-6	240-4	240-6	240-4	240-6	240-4	240-4	180-2	210-6	240-4	180-2	180-2	240-4	240-4	240-4	180-2	210-2	180-6
Lowest content in all BCs	980	80	66	20576	346	141	473	115854	70	2272	2173	386	12	268	4536	23420	16263	4	382
Sample label with lowest content	180-4	240-4	180-2	180-4	180-4	180-6	180-2	180-4	240-2	180-4	180-4	240-4	240-2	180-4	180-4	180-4	210-6	240-2	180-4
Higher threshold - regulations				DEC	100	1200	6000	DEC	DEC	DEC	DEC	DEC	100	DEC	700	DEC	DEC	DEC	75
Lower threshold - regulations				DEC	34	70	70	DEC	DEC	DEC	DEC	DEC	25	DEC	200	DEC	DEC	DEC	5

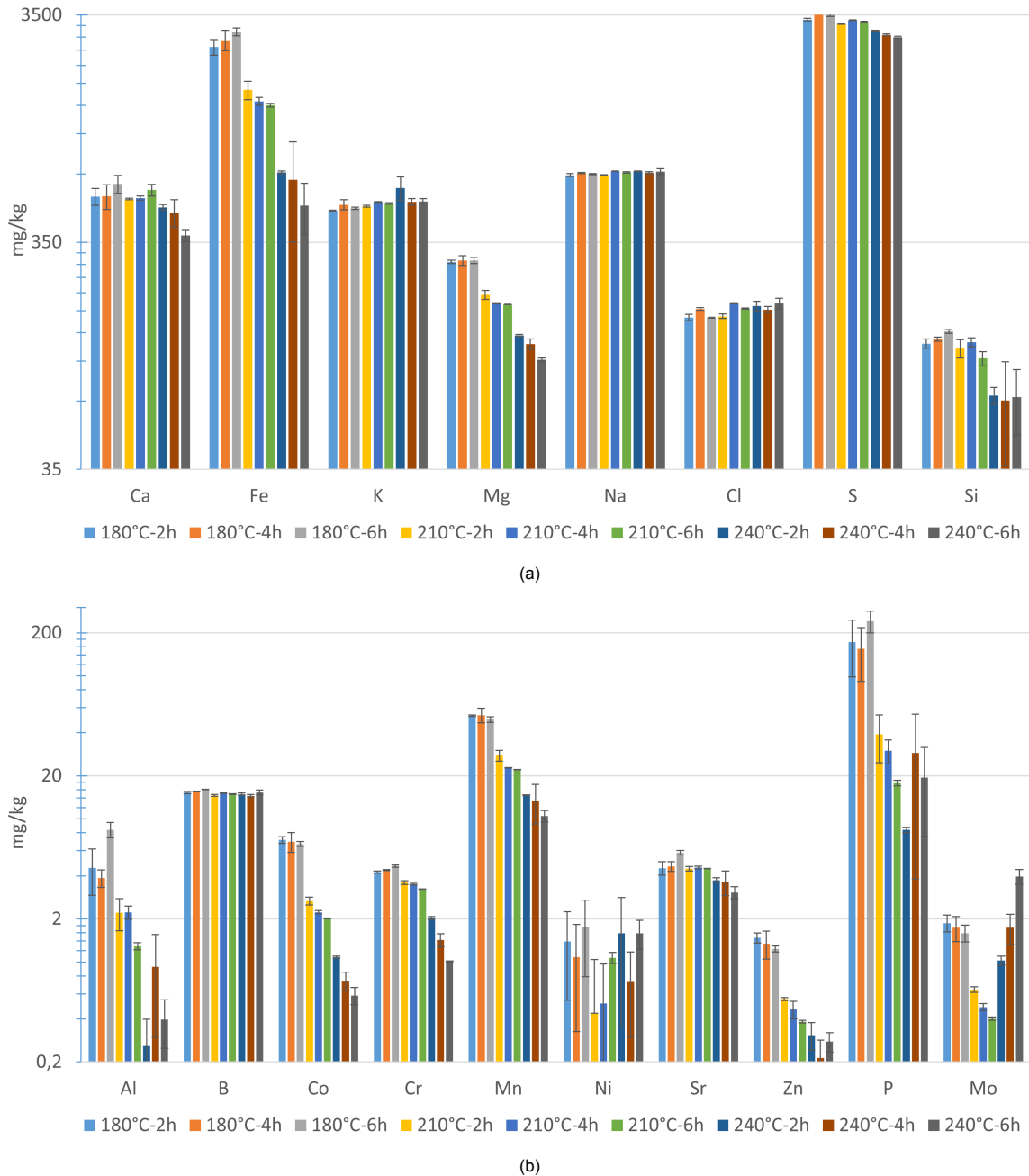
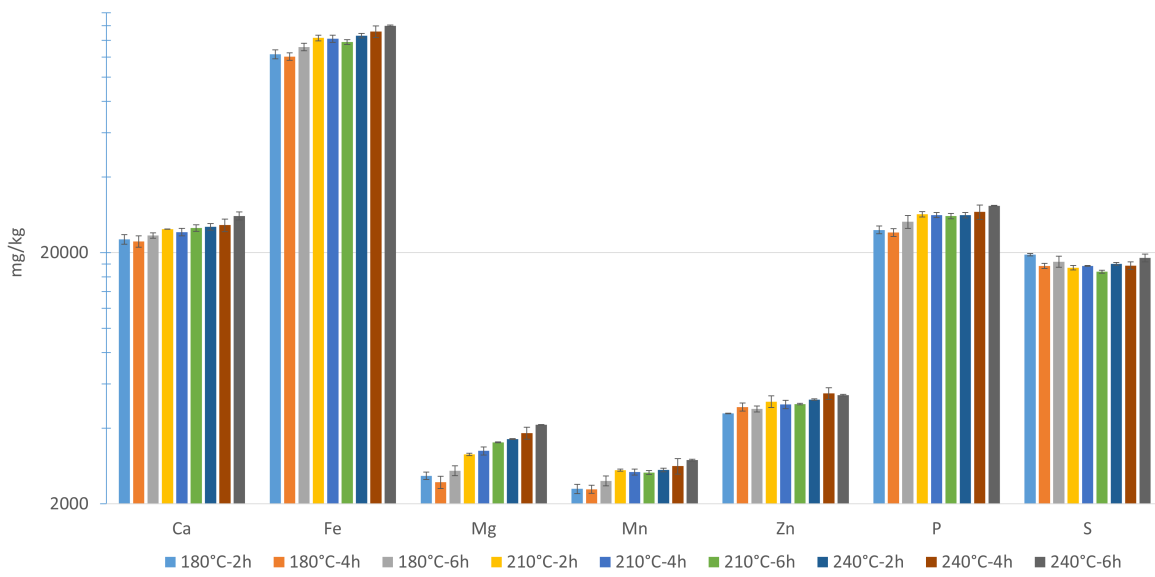


Figure 4.7: Logarithmic plots of aqueous phase elemental concentration where (a) are the elements Ca, Fe, K, Mg, Na, Cl, S, and Si obtained within the range of 35-3500mg/kg and (b) are the elements Al, B, Co, Cr, Mn, Ni, Sr, Zn, P, and Mo in the range of 0.2mg-200mg/kg. The results are received by ICP-OES and from left, to right the samples 180°C-2h, 180°C-4h, 180°C-6h, 210°C-2h, 210°C-4h, 210°C-6h, 240°C-2h, 240°C-4h, 240°C-6h are shown for each element.

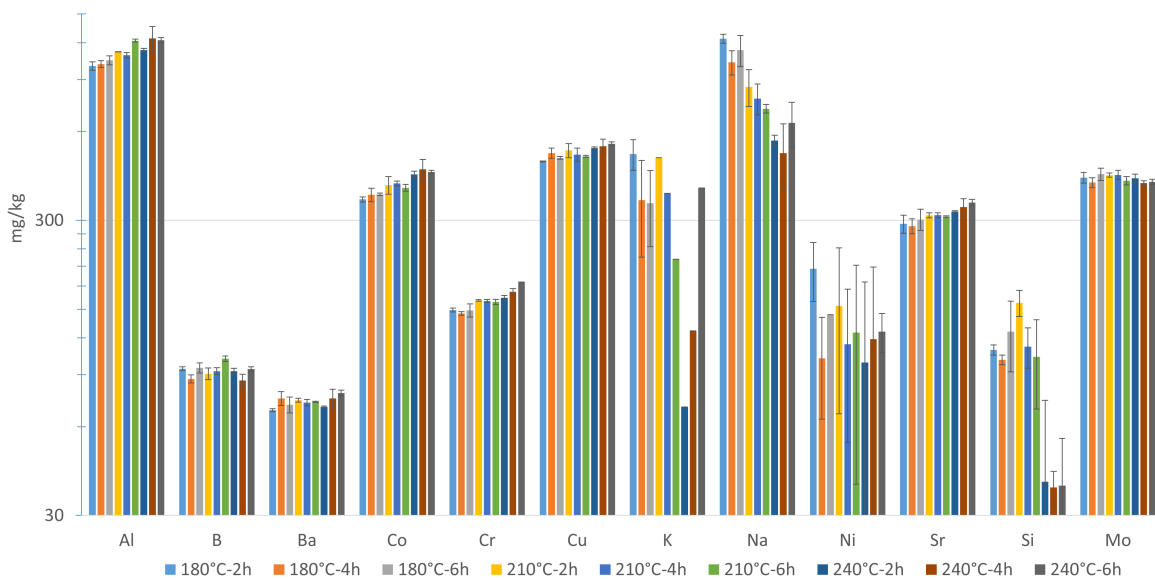
4.6.2. Biochar

The high amount of ash shown in Figure 4.4c consists of different elements, where Fe, Ca, Mg, Mn, Zn, P, and S takes up most of the ashes as shown in Figure 4.8a. The elements below 1300mg/g shown in Figure 4.8b are Al, B, Ba, Co, Cr, Cu, K, Na, Ni, Sr, Si, and Mo. Figure 4.8 shows that all elements are influenced by temperature except for Ba, B, S, and Ni, which shows no trend at all, where more detailed figures with statistical values are provided in Figure A.2. Time is only significant for Mg, as can be seen in Figure A.2i. Furthermore, Si concentration is clearly decreased at the 240°C samples. For the aqueous phase, similar decrease is noted, which goes against the law of conservation of mass. Ash analysis has not shown such behaviour, as is further elaborated on in section 4.9. The element

Ba and Cu are only detected in the HC, which shows that these HM are completely transferred to the HC phase.



(a)



(b)

Figure 4.8: Logarithmic plots of BC elemental concentration where (a) are the element concentrations of Ca, Fe, Mg, Mn, Zn, P, and S within the range 2000-16000mg/kg and (b) are the element concentrations of Al, B, Ba, Co, Cr, Cu, K, Na, Ni, Sr, Si, and Mo in the range of 30mg-1800mg/kg. The results are received by ICP-OES and from left to right the samples 180°C-2h, 180°C-4h, 180°C-6h, 210°C-2h, 210°C-4h, 210°C-6h, 240°C-2h, 240°C-4h, 240°C-6h are shown for each element.

4.7. Leaching of Heavy metals and Total Organic Carbon

Figure 4.9 shows the TOC leaching from 180°C, 210°C, and 240°C HC, each with a residence time of 4h. The three samples analysed all exhibit the same leaching profile with increasing time. The 180°C sample leaches around 80 mg/L more than the 210°C sample and around 180 g/L more than the 240°C sample. Showing that higher temperatures create more stable HC because of the further carbonized structure. The leaching results also indicate that higher temperatures lead to less leaching of organic content which could be a reason for the lower pH at lower temperatures as shown in Figure 4.5. Furthermore, there appears to be no further leaching of TOC between 20 and 24 hours, which could implicate that after 24h more leaching will not occur.

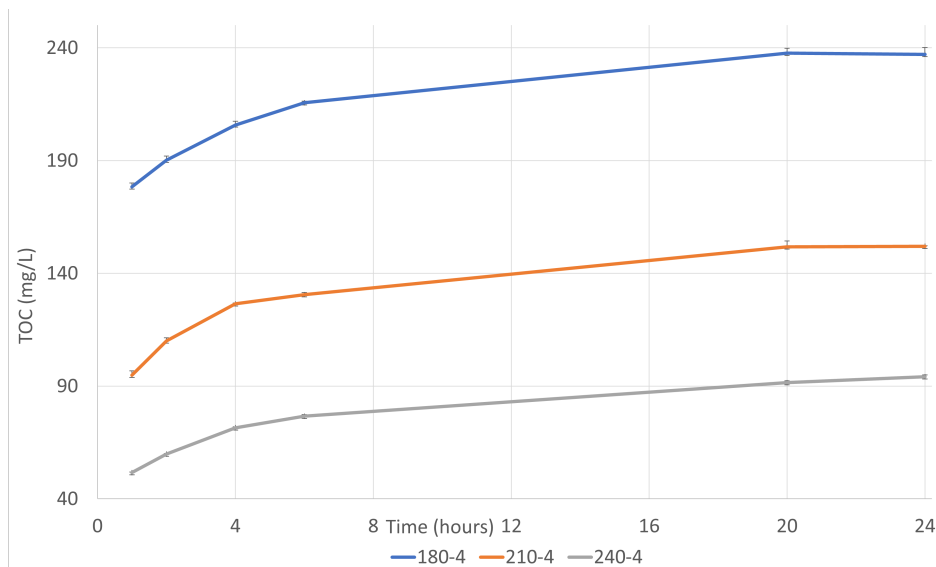


Figure 4.9: Leaching of TOC for three samples made on 180°C, 210°C, and 240°C in combination with 4h residence time.

While the VM of the 180°C HC sample is higher (17%) than that of the 240°C HC sample, it is not enough to account for the increase in TOC leaching from 51 mg/L to 177mg/L. This may be attributed to the fact that the hydrophobicity of HC increases with temperature, resulting in less soluble carbon and reduced TOC leaching levels in combination with samples created at higher temperatures. Additionally, the hydrophobic nature of HC may lead to lower moisture content through mechanical drying, resulting in energy savings.

A TOC of around 50 mg/L is in the range (0.1-59.4 m/L) of 400 groundwater samples from 8 European Union countries but is higher than the median of 2.7 (Gooddy & Hinsby, 2008). Also, the quality of the organic carbon that has leached is not determined, which could be a hazard. Filtering water with a faster flow rate could result in lower TOC concentrations. Furthermore, the leaching of TOC could be decreased by washing as precipitated short-chain fatty acids are the most abundant leached TOC.

Elements that have leached from the HC in the water have been detected by ICP-OES as the total amount of elements is shown in Figure 4.10. Corresponding with TOC higher amounts of elements are detected at the 180°C sample but after 4h the 240°C samples show similar leaching, whereas the 210°C sample was around 10 mg/kg lower after 24h compared to the 180°C and 240°C samples. One should expect that comparable ranking with TOC would occur but the 240°C sample leaches more than the 210°C sample and shows similar leaching with 180°C. The total leaching per hour (mg/h) decreased in all samples over time and stabilization occurs at the 210°C and 240°C samples but the 180°C total leaching between 20 and 24h is 0,82 compared to 0.95 between 6 and 20h.increases with The ICP-OES data, shown in Table A.3, shows that the HM content consist of around 60% SO₄ and circa 30% is contributed by Ca for the three samples at 240°C. The last 10% can be contributed to Al, B, Co, Cr, Cu, Fe, K, Mg, Mn, Na, Sr, Zn, PO₄, SO₄, Si, and Mo.

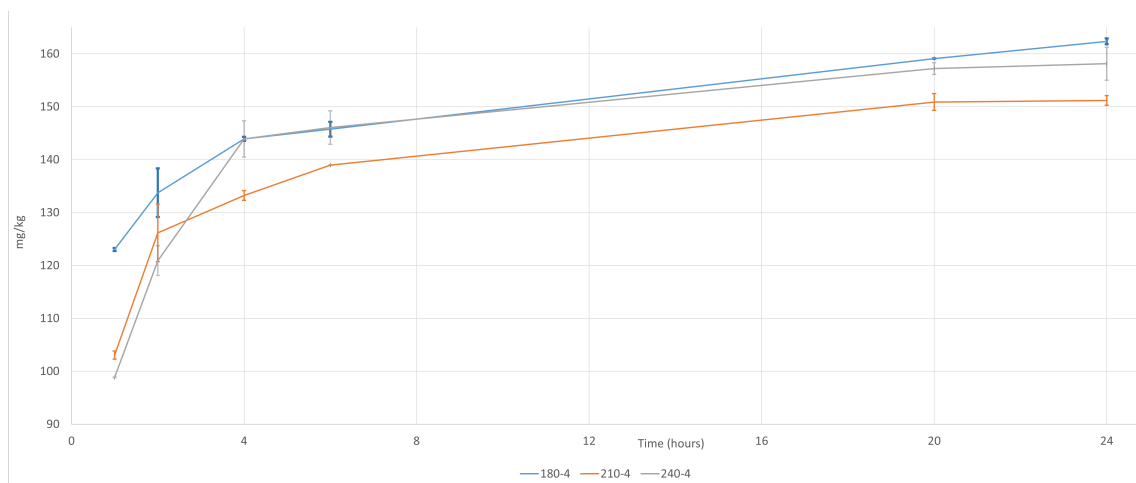


Figure 4.10: Leaching of elements, detected by ICP-OES, for three samples made on 180°C, 210°C, and 240°C in combination with 4h residence time.

4.8. Absorption

BET analysis was conducted on three BC samples produced at 180, 210, and 240°C with a residence time of 4 hours. As shown in Figure 4.11, the surface area of the biochar ranged from 7-3.5 m²/g, with higher temperatures resulting in lower surface area. This trend can be attributed to pore collapse caused by the higher pressure in the HTC process, which is consistent with the BET analyses of J. H. Zhang et al. (2014) findings; 8,7 m²/g at 190°C 6h and 5.4 m²/g at 260°C 6h.

Freshwater sludge derived BCs has shown higher porosity with a surface area of around 100 m²/g, which had high ash (>60 wt.%) content (Y. Zhang et al., 2021). Literature describes that high ash content leads to lower porosity and higher carbon content increases porosity (Leng, Xiong, et al., 2021). Pyrochar from lignocellulosic feedstocks can have even higher BET values, reaching up to 500 m²/g, while pyrochars from sludge feedstocks typically have values up to 100 m²/g (Leng, Xiong, et al., 2021). The high ash percentage is clogging the micropore structure leading to lower surface areas. The median surface area across multiple studies summarized by Leng, Xiong, et al. (2021) is approximately 25 m²/g.

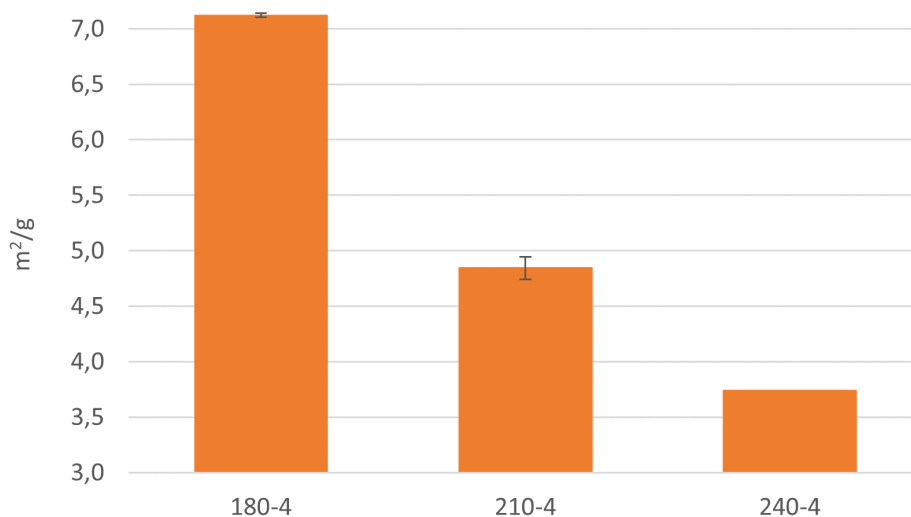


Figure 4.11: BET surface area analysis of a 180, 210, and 240°C sample all with a residence time of 4h.

4.9. XRD of Biochars and XRF of Biochar Ashes

XRD analyses of the samples are shown in Figure 4.12. The sample created on 180 and 2h shows no significant peaks, where from 180 and 4h and all samples with more severe reaction conditions show clear peaks. This could indicate that the biosludge at 180 degrees 2h is not carbonized. The XRD analysis revealed the presence of three crystal structures: anhydrite, graphite H2, and hydrogen calcium phosphate in BC, which are shown in Figure 4.13.

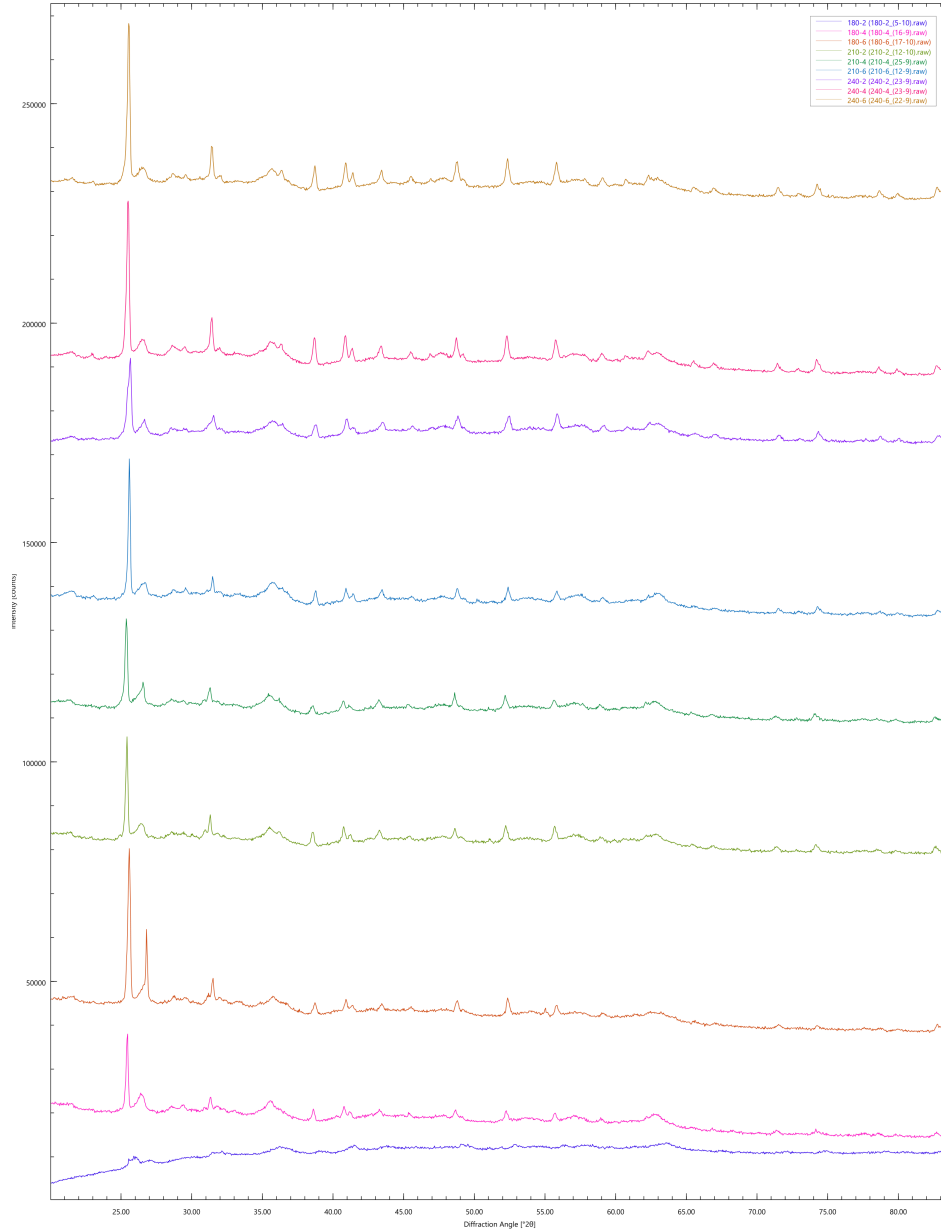


Figure 4.12: XRD data with from low to top; 180-2, 180-4, 180-6, 210-2, 210-4, 210-6, 240-2, 240-4, and 240-6 samples.

Figure 4.14 shows the XRF analyses of the BC ashes as weight percentage. Here it can be seen that Fe_2O_3 , ZnO , P_2O_5 , and CaO take up around 90% of the ashes. Fe_2O_3 is the most abundant substance found in the ashes, accounting for around 64% of the ashes. P_2O_5 is a common fertilizer component and with around 15% ash content it could be recycled from the ashes. Cl is detected twice in nine samples which account for lower than <0.3% of the ash content. The SiO_2 content in the ashes does not show the sharp decline obtained from the ICP-OES data analysed in subsection 4.6.2.

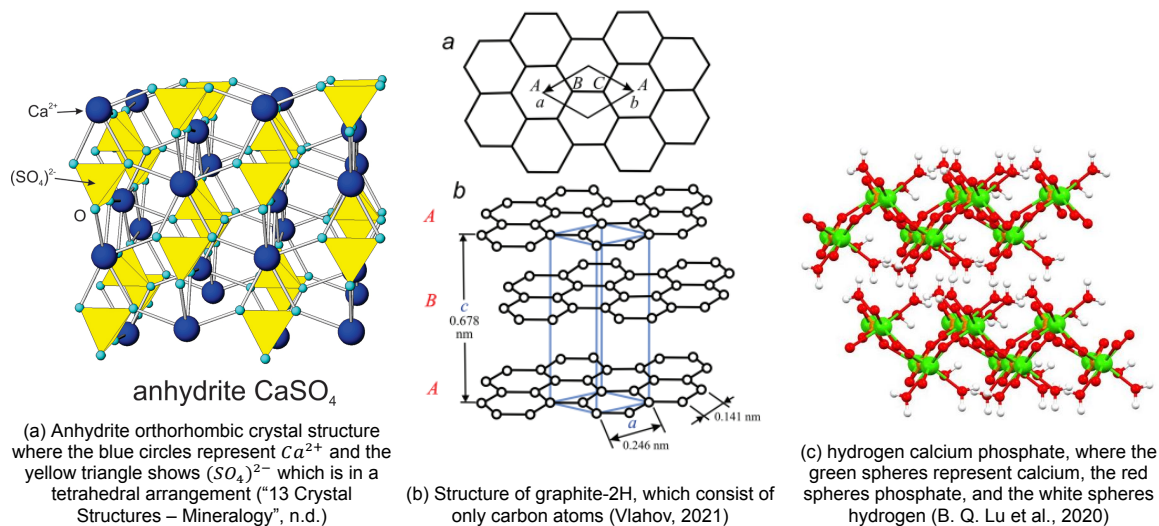


Figure 4.13: Crystal structures revealed by XRD; anhydrite, graphite-2H, and hydrogen calcium phosphate

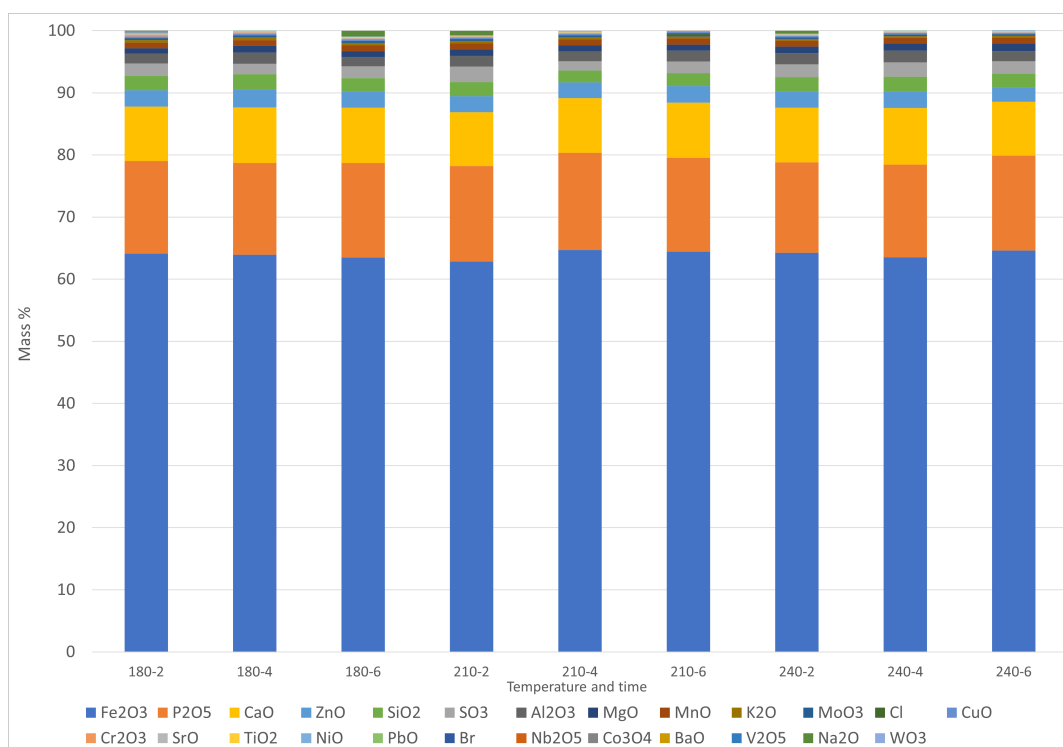


Figure 4.14: Ash content of the HC determined by XRF.

4.10. Aqueous Phase Analysis

To assess the potential usability of the aqueous phase for anaerobic digestion, qualitative characterization by measuring three key parameters: COD, pH, and ammoniacal nitrogen have been conducted. The results of these analyses are presented in Figure 4.15. The results indicate a decrease in COD with increasing temperature, while the ammoniacal nitrogen concentration increases. The pH of the aqueous phase also increases from acidic to alkaline regions. The high COD value shows potential for utilization by anaerobic digestion, but high ammonia concentration could inhibit biogas production (Cebi et al., 2022; Krakat et al., 2017).

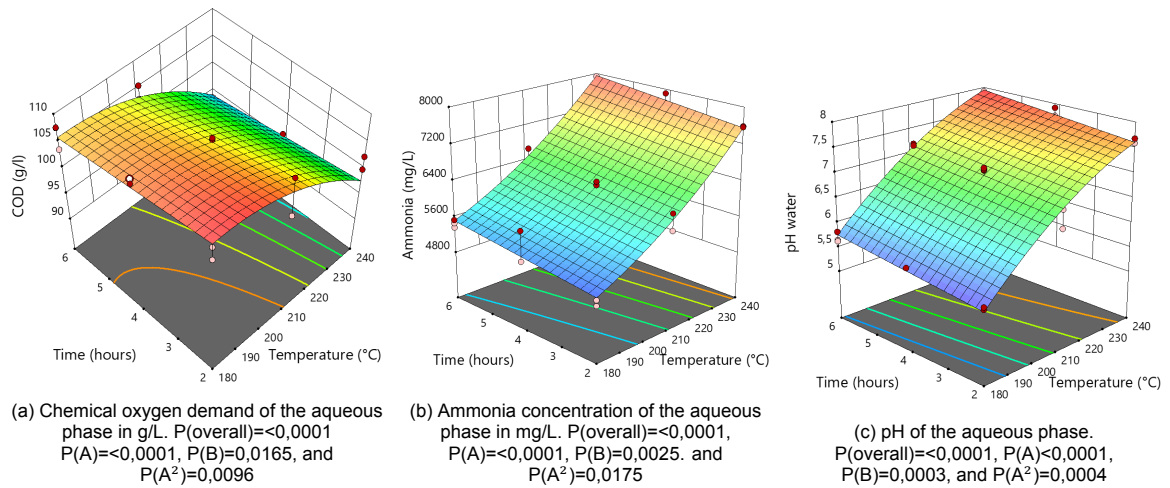


Figure 4.15: Chemical oxygen demand, ammoniacal nitrogen concentration, and pH of the aqueous phase

Foam formation was observed in the aqueous phase, particularly at lower temperatures (180°C and 210°C). This could be due to the presence of proteins and fatty acids in the aqueous phase (Atrafi & Pawlik, 2017; Germain & Aguilera, 2014). At 240°C 2h a small amount of foam and at 4h and 6h no foam could be seen. At longer residence time proteins have longer be exposed to sub-critical water, which hydrolyses the proteins in shorter molecules. Further investigation is needed to determine the molecules causing the foam formation.

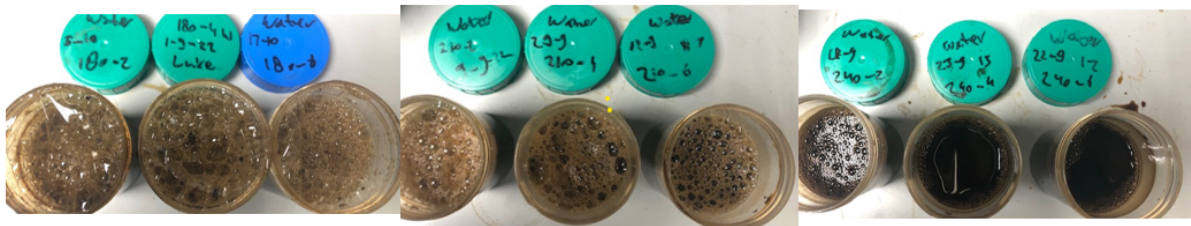


Figure 4.16: Foam development of stored aqueous samples after shaking. Thick foam can be seen on the left, created at 180°C. When moving to the right, 210°C and 240°C samples are shown. These have less foam.

The COD amounts observed in the experiments (ranging from 90 to 110 g/L) are higher than those reported in the literature, but consistent with high solid load experiments (Merzari et al., 2020). The high COD concentration in the effluent may be beneficial for biogas production, as it provides a rich substrate for anaerobic microorganisms.

The increase in ammoniacal nitrogen concentration observed in Figure 4.15b can be attributed to the decrease in HC nitrogen concentration observed in the ultimate analysis (see section 4.2). Other HTC research have shown ammoniacal nitrogen content ranges between 0.4-1.0g/l, but high solid loading (15.0%) experiments have shown values between 2.70-6.9g/L (Merzari et al., 2020). The increase in pH at higher temperatures may have shifted the ammonium/ammonia equilibrium towards ammonia, leading to an increase in ammoniacal nitrogen concentration. However, 90% and 99% of the ammonia will be ionized at pH 8.25 and 7.25 (25°C, 1 ATM), respectively (Lang et al., 1998). No decrease in ammoniacal nitrogen is seen so no significant amount of volatile ammonia gas escaped from the aqueous phase.

The pH increase observed in the aqueous phase may be due to the extraction of HM into the BC. There is a strong relation between pH and iron ions, where iron is oxidized to become ferric hydroxide, also known as rust, which causes the pH to become more alkaline (Saadattalab et al., 2020). Figure 4.5 and Figure 4.15c are showing similar pH values (around 5) at 180°C, which is because of the

short chain fatty acid for example; acetate (4.76), propionate (4.9), and n-butyrate (4.82) (K. Zhu et al., 2021). The pH increase to alkaline regions let HM favour the HC as acidic water improves the solubility of HM (Metzger, 2005).

4.11. Gas Phase Analysis

Qualitative measurements of the gas phase are presented in Figure 4.17. The gas samples were found to contain only N₂ and CO₂, despite the gas chromatography being able to measure CH₄, O₂, and H₂. The first sample analysed did show traces of CH₄, but as no other samples contained any amount of CH₄, this is likely a measurement error. The SD observed is high, which may be due to singular measurements, and deviation would likely shrink if gas samples were measured in duplicate or triplicate. section 4.11 showed a higher concentration of CO₂ in the gaseous phase at longer and higher residence times and temperatures, which could indicate that the fatty acids have been decarboxylated. A strong odour was detected when the vessel was vented, suggesting the presence of volatile molecules in the gas sample. The high amount of ammonia detected, shown in section 4.10, could also contribute to the strong odour, as ammonia is well-known for its pungent smell.

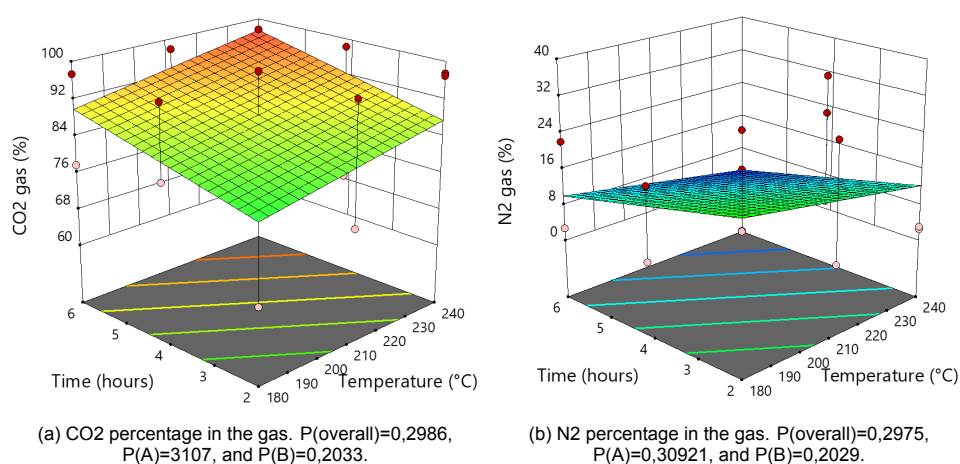


Figure 4.17: Qualitative gas analysis

4.12. Optimization

To ensure the accuracy of the models created by the central composite design, an optimization process was carried out, and the two samples produced were analyzed for their elemental composition by ICP-OES, their yields, and CHNO compositions. The optimization aimed to maximize the dry solid yield, C/N ratio, and HHV, while minimizing O/C and H/C ratios, as well as the content of Ni and Zn. The optimized conditions were at 240°C and 6 hours, and duplicate samples were produced according to the same method as previous samples.

The response variables were then analyzed, and the results are presented in Table 4.3. The aqueous and solid BC yield met the expected values, and the ICP-OES data for Ni, Sr, S, and Mo were also within the 95% predicted interval. Whereas Ni and Mo have no model as their corresponding trends are straight planes along the axis of time and temperature, leading to values inside of the 95% prediction interval. K and S are showing higher values than the previous data. Most other elements are slightly below the lower end of the 95% predicted interval, which could be because of precision error. The CHNO responses fall inside of the 95% prediction intervals.

It is worth noting that the ICP-OES results are at least 10% lower, which will not lead to any concentrations passing regulatory thresholds. Furthermore, in Figure 4.4c the deviation for ash could also be up to 5 wt.%. A combination of uncontrollable factors and a lower ash content could lead to falling outside of the 95% prediction interval. Determining the ash could lead to a better understanding of the accuracy of these ICP-OES responses. The CHNO trends are based on only nine points where the

p-values showed that there was a large uncertainty. Nonetheless, the CHNO values fall within the 95% prediction interval showing that the data can be used to model desired CHNO values.

Table 4.3: Model confirmation where the yields, CHNO, and HC ICP-OES are shown. The bold numbers are the numbers not in range of their 95% prediction interval.

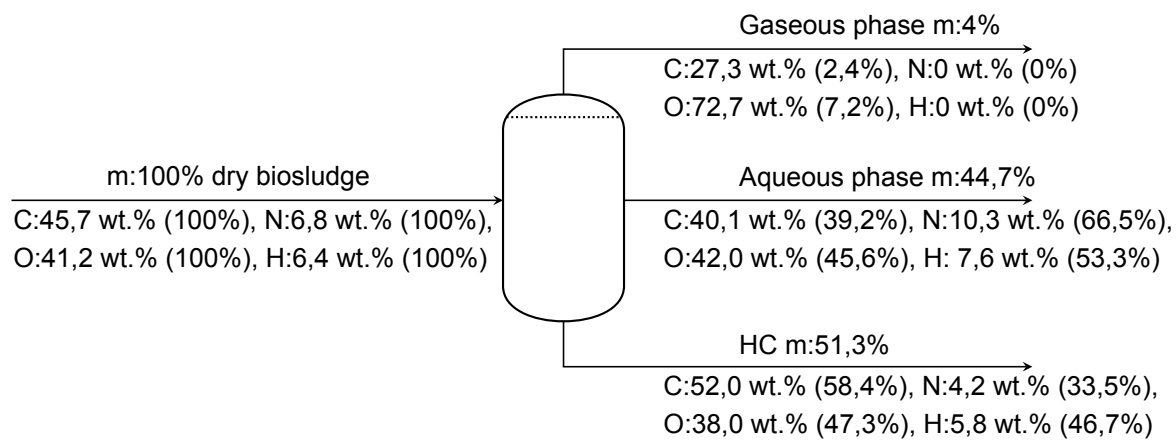
Response variables	Predicted mean ± deviation	Data mean ± deviation	Calculated error (%)
Aqueous phase	75,4 ± 1,0	74,1 ± 0,2	-1,8
Hydrochar	16,7 ± 1,9	21,2 ± 0,3	27,1
Gas+losses	9,7 ± 4,5	4,7 ± 0,1	-51,1
Biochar yield	50,7 ± 1,5	51,6 ± 0,8	1,9
C	52,7 ± 1,1	50,8 ± 0,2	-3,6
H	5,8 ± 0,3	5,4 ± 0,04	-7,9
N	4,0 ± 0,1	4,1 ± 0,03	3,0
O	37,5 ± 1,1	39,7 ± 0,1	6,0
Al	1246,8 ± 69,4	894,0 ± 4,0	-28,3
B	95,9 ± 6,1	56,5 ± 1,5	-41,1
Ba	75,7 ± 4,4	66,0 ± 1,0	-12,9
Ca	26712,3 ± 1247,0	23364,0 ± 265,0	-12,5
Co	437,9 ± 21,2	346,5 ± 28,5	-20,9
Cr	181,8 ± 5,2	163,5 ± 2,5	-10,0
Cu	534,2 ± 24,2	446,0 ± 33,0	-16,5
Fe	155228,0 ± 7314,1	111389,0 ± 2008,0	-28,2
K	309,1 ± 125,5	1870,0 ± 151,0	505,0
Mg	4132,4 ± 156,2	3154,5 ± 134,5	-23,7
Mn	2919,3 ± 146,7	2468,5 ± 101,5	-15,4
Na	518,9 ± 140,5	887,5 ± 46,5	71,0
Ni	123,1 ± 76,6	56,0 ± 10,0	-54,5
Sr	335,2 ± 16,2	332,5 ± 0,5	-0,8
Zn	5418,3 ± 222,7	4461,5 ± 199,5	-17,7
P	30142,0 ± 1561,8	25224,4 ± 1770,5	-16,3
S	18636,8 ± 741,9	17467,2 ± 4310,5	-6,3
Si	30,7 ± 25,0	176,5 ± 7,5	474,3
Mo	414,8 ± 18,1	413,5 ± 1,5	-0,3

4.13. Mass Balance

In Figure A.3, a dry-based mass balance on the organic CHNO content is presented. The CHNO analysis data from the 240°C 6h samples in section 4.2 were combined with a gas phase set at 4 wt.% with only CO₂ as its composition. N₂ gas is assumed to balance out as it can be assumed the detected N₂ was the N₂ used for flushing the vessel. The data for the aqueous phase is calculated by subtracting the BC and gas phase from the feedstock. In Figure A.3 a mass balance on the organic CHNO content is shown which incorporates moisture content.

For the C content around 58 wt.% is contained in the BC and 39,5 wt.% went into the aqueous phase. During the process, CO₂ is created through decarboxylation, which accounts for only 2.5 wt.% of the total carbon balance, but 7.2 wt.% of oxygen. The decrease of BC nitrogen content and the amounts of aqueous phase ammoniacal nitrogen in Figure 4.3c and Figure 4.15b are further addressed by Figure 4.18 where 2/3 of the total nitrogen went to the aqueous phase, while only 1/3 remained in the BC. The separation of H is even, with the aqueous phase having a slightly higher amount (5,6 wt.%) than the BC.

Figure 4.18: Mass balance of the HTC process at 240°C and 6h on a dry basis. The wt.% are normalized between brackets.



5

Conclusions

During the HTC process, three fractions are produced: HC, an aqueous phase, and a gas+losses phase. The yields obtained for the BC and aqueous phases were statistically significant, providing useful information about the process streams. However, the method used to quantify the yield of the gas phase was found to be inaccurate, and a gas bag would be required for more precise measurements. Additionally, while N₂ and CO₂ were measured during degassing, the presence of a distinct odor suggests that other volatile compounds may also escape from the vessel. However, the gaseous phase would be considering a small amount of the mass streams (<5%). Despite these limitations, the response variables have provided valuable insights into the different phases produced during the HTC process and have helped to answer the main research question:

Can hydrochar be made from industrial Fischer-Tropsch biosludge that complies with regulations and generates socioeconomic benefits?

The ICP-OES analyses of the aqueous and BC phases show that HTC effectively concentrated HMs into the BC, making the aqueous phase a relatively clean stream. However, the BCs derived from Fischer-Tropsch biosludge contains amounts of Cr, Cu, Ni, Zn, and Mo, which exceed the thresholds for most BC applications. Because of this only EBC-BasicMaterials BC products can be made under regulations, leading to disallowing on consumer applications such as BC soil amendment. EBC-BasicMaterials are materials used in a controlled environment where they cannot harm the environment or end-user, such as building materials, road construction asphalt, electronics, sewage drains, and composite materials like skis, boats, cars, rockets (Schmidt et al., 2022).

The HTC process results in a more carbonized product which makes it suitable for long-term carbon sequestration by landfilling or adding it to construction materials. However, there are other potential applications that could extend the lifespan of the material. For example, BC can be used as an absorbent for removing contaminants from water or as a catalyst for chemical reactions. After usage in these kinds of fields, carbon sequestration or incineration for green energy could be applicable, further extending the utility of the material.

The surface area of BC by HTC is significantly lower compared to alternative feedstocks combined with pyrolysis and pre- and post-processing would be necessary to create a suitable material. This is due to the high ash content and the HTC high-pressure withholding pore development. Catalyst and absorbent materials will be a difficult field of application without pre- or post-processing.

the aqueous phase produced during the HTC process has a high amount of COD combined with a low amount of HMs, which presents potential for biogas creation through anaerobic digestion. However, the high amount of ammoniacal nitrogen present in the aqueous phase could inhibit anaerobic digestion. This can be overcome by reducing the solid loading and using a suitable bacteria family.

The HHV of BC, corresponds to the HHV of sub-bituminous coal, indicating that BC could be utilized as a carbon-neutral biofuel. The higher N content compared to fossil-fuel sub-bituminous coal could

lead to more NxOx emissions, and this needs to be taken into account to get a correct comparison of the co₂-equivalent emissions. Furthermore, after using BC for heat generation, the high ash content will not be beneficial for the processing of the BC biofuel.

To conclude, the applications of BC as an absorbent or soil amendment without pre- or post-processing could not be adding social-economic benefit thus an extra step would be necessary before a useful product can be created. The aqueous stream is showing potential to be further utilized decreasing the dry solid biosludge by almost half (average 46,5%). The FC content of BC enhances its shelf-life and makes it suitable for carbon sequestration in building materials or storage. A stockpile of BC can be created for use in the near future as a more specific application for this kind of BC is identified through further research.

The effects of temperature on the characteristics of the phases produced through the HTC process have been investigated, and the results are summarized in Table 5.1. Increasing the residence time from 2h to 4h or 6h has only a minor effect on the response variables, indicating that longer residence time may not have any significant benefits from a processing perspective.

Table 5.1: Trend of the response variables by increasing the temperature factor, where + stands for an increase and - for a decrease in the corresponding response variable.

	Analyses	Change		Analyses	Change
Yields	Hydrochar	-	Biochar	HM	+
	Aqueous phase	+		Alkali metals	-
	Gas+ Residue	+		C	+
	Dry solid	-		H	+
Aqueous phase	HM	-		N	-
	Alkali metals	+		O	-
	Ammoniacal nitrogen	+		FC	+
	COD	-		VM	-
	pH	+		Ash	+
Gas	N ₂	+		BET	-
	CO ₂	+		TOC	-
Biochar	HHV	+		pH	+

6

Recommendations

For each use case, this chapter provides recommendations for further experiments and analyses that can be conducted to improve the confidence of product application, the economics and environmental impact.

According to the ICP-OES analysis, the application of a soil amendment for Fischer-Tropsch biosludge is not feasible due to high concentrations of Cr, Cu, Ni, Zn, and Mo exceeding regulatory thresholds. However, potential solutions such as pre- or post-treatment, modifying the Fischer-Tropsch process, or changes in regulations may result in HM concentrations that comply with regulatory limits. To achieve a more circular system, upgrading the BC to a material with excellent absorption properties for filtering HM could lead to a soil amendment BC that surpasses regulations. Figure 6.1 illustrates this possibility, where the BC is separated into a filter and fertilizer product stream. The filter helps reduce the concentration of HM in the sludge. After use, the filter is incinerated to produce heat for upgrading the BC into a filter. This process results in a minimal ash stream, which can potentially be recycled in the effluent treatment process.

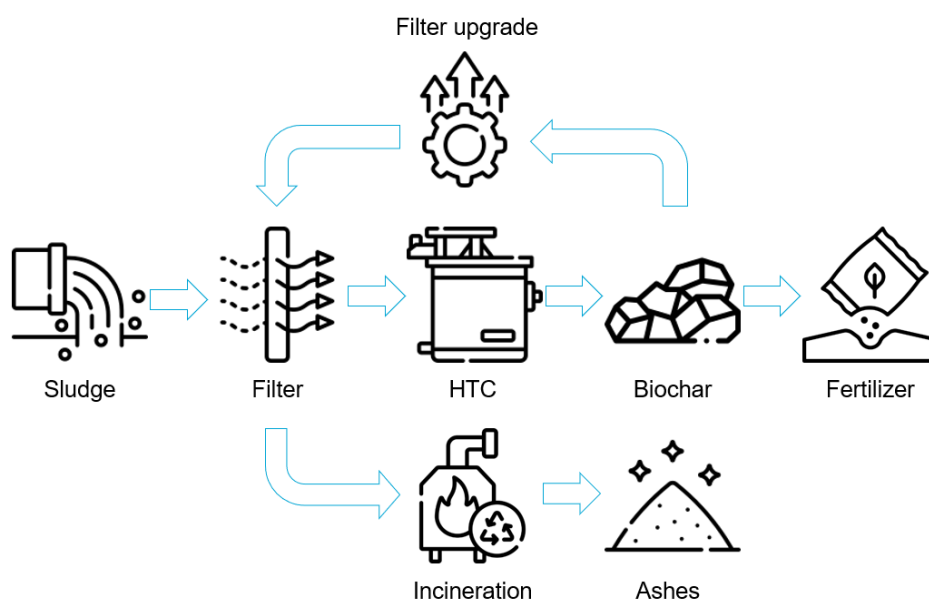


Figure 6.1: A systematic view of the implication of BC as a soil amendment coupled with an absorbent made from the same BC product.

A literature study about possible pre and post-treatments coupled with lab work and ICP-OES anal-

ysis of the BC samples will show a trade-off between different treatments to reduce the HM. Following positive results, the development of a Fischer-Tropsch biosludge soil amendment could be undertaken. Caution has to be addressed as pre- and post-treatments, such as filtering, alter the sludge and thus affect the BC product. Nonetheless, when passing regulation, it will not provide a guarantee for effectiveness as a soil amendment. Another option is to perform a BCR three-step sequential extraction procedure determining the accessibility of HM and to test leachability in soils to show and convince regulation institutes that no harm could possibly be inflicted. Finally, changes in the Fischer-Tropsch production process could decrease HM content of Cr, Cu, Ni, Zn, and Mo. The following are recommendations for use as a soil amendment:

1. Perform a BCR three-step sequential extraction.
2. Perform literature research on pre- and post-treatment processes to create an allowable BC.
3. Look into the combination of soil, BC, and plants with long-term studies.

To understand the absorption pathway, different upgrading technologies have to be researched together with BET, IR-spectroscopy, and SEM analyses to obtain knowledge about surface morphology, how porous the structure is, and what kind of characteristic surface groups are available. Moreover, a use-case test comparing Fischer-Tropsch biosludge BC to off-the-shelf alternatives shows if this can be a promising product application or not. Recommendations for the end user as an absorbent are stated below:

1. Perform BET, IR-spectroscopy, and SEM analyses on upgraded BC.
2. Compare absorption capabilities in test cases with off-the-self alternatives.
3. Perform economic analysis on absorbent products.

Studies have reported promising results for anaerobic digestion of the aqueous phase by HTC. The lab work in this thesis has shown that the HTC process produces a low HM aqueous phase with most of the HM contained in the BC. In this thesis, the BC phase was considered the primary stream and the aqueous stream as secondary. However, by interchanging the two, the HTC process can be viewed as a HM decreasing anaerobic digestion pre-treatment removal technology. Moreover, BC can be utilized to enhance biogas production by promoting hydrogenotrophic methanogenesis and increasing the specific methane production rates, thereby reducing the residence time and potential the CAPEX of an anaerobic digestion system (Shi et al., 2021). A systematic view of this process is presented in Figure 6.2.

To perform a comprehensive economic analysis of anaerobic digestion coupled with the HTC, it is essential to obtain accurate and reliable data on the potential biogas yield from the aqueous phase. Additionally, further characterization of the aqueous phase can enhance our understanding of the chemical composition and molecular structures available for biogas production. Based on a rough estimate, a biogas yield of around 4 million m³ per year can be achieved from 55,000 dry tons of aqueous phase with a COD of 100g/L and a solid loading of 20%, assuming a yield of 200 ml/g COD (Cebi et al., 2022). However, it is crucial to note that the actual biogas yield may vary depending on various factors, such as operating conditions, feedstock characteristics, and digester design. To better understand anaerobic digestion coupled with the HTC process, four recommendations are made:

1. Anaerobic digestion tests to determine possible biogas yield.
2. Perform GC-MC to determine how the composition of the aqueous phase is altered by temperature and time.
3. Perform an economic and environmental analysis to determine if a HTC anaerobic digestion is a possible pathway.
4. Add BC to anaerobic digestion to understand the benefits and downsides of this additive.

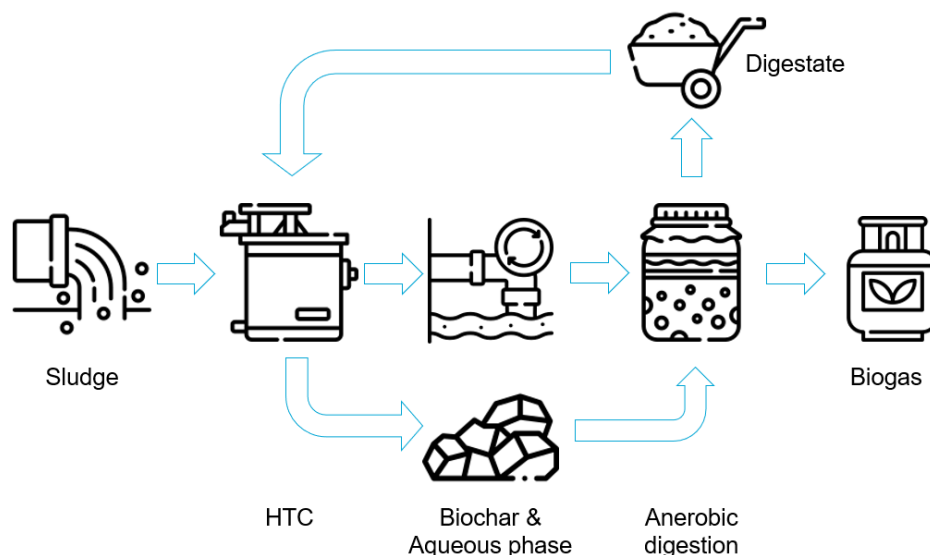


Figure 6.2: Systematic view of HTC process where the primary stream is the aqueous phase used in anaerobic digestion to produce biogas and BC is added to enhance biogas production. The digestate secondary stream of the anaerobic digestion is recirculated through the HTC process.

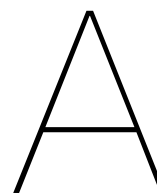
If BC can be used as a product to extend its use-life, it will eventually reach its end-of-life, which requires disposal. There are three ways to dispose of it: landfilling, which is the current method for biosludge, incineration for energy generation and recycling valuable elements from the ashes and recycling the end-of-life product through HTC. The most circular option allows for a closed system by recycling the used product. The second option utilizes the BC for its energy and reuses the ashes, and the landfilling option is, from a circular perspective, the least desirable as it would contaminate soil and slowly degrade, emitting GHG.

For incineration, the analysis has indicated that BC corresponds with the higher range of sub-bituminous coal. Since the ash compositions have been identified, it is possible to recover important components to increase circularity. Disadvantages of BC biofuel (high N and ash content) have to be assessed to understand its operational and environmental impact. The energetic benefits of the HTC process would be determined from a lower heating value perspective combined with a filter press and energy consumption study. To better understand BC as a fuel three recommendations are made:

1. Perform burning tests to understand fuel performance and slagging, and fouling.
2. Compare these results with alternatives and include exhaust gas analysis to determine their CO₂ equivalence impact.
3. Research on ash recirculation and separation to obtain critical raw elements.

With advancements in technology readiness and increasing research in recent years, HTC has become a viable option for converting biosludge into useful products, which can promote the circularity of Fischer-Tropsch industries. By utilizing HTC to create products from biosludge generated by Fischer-Tropsch industries, there is potential for significant environmental benefits. However, it is important to conduct social-economic and life-cycle analyses to evaluate the economics and impact of HTC products. Therefore, comprehensive economic studies on the data generated in this thesis are required to determine the potential business case for the product applications, their environmental benefits, and possible profits.

Appendices



Raw Data, Statistics, and Model Equations

In this appendix data from analytic equipment, raw material and samples can be found in this appendix.

A.1. Aqueous Phase Literature

Table A.1: Molecules identified from anaerobically digested sewage sludge HTC process water and their main possible application (Langone & Basso, 2020).

Compound	Application
1-Methyl-4-nitromethyl-4-piperidinol	Production of antitumor agents and products involved in the treatment of cardiovascular diseases
1-Methyldodecylamine	Preparation of N,N,N,N,N-trimethyldodecylammonium bromide
1-Phenethyl-piperidin-4-ol	-
1-Propanol, 2-amino-	Organic syntheses (e.g. Schiff base ligands)
2,5-Pyrrolidinedione, 1-ethyl-	Organic syntheses
2,5-Pyrrolidinedione, 1-methyl-	Organic syntheses, as well as in some industrial silver-plating processes
2-Butanamine, (S)	Production of some pesticides
2-Cyclopenten-1-one, 2,3-dimethyl-	-
2-Cyclopenten-1-one, 2-methyl-	-
2-Heptanamine, 5-methyl-	-
2-Propanamine	Production of some herbicides and pesticides including atrazine, bentazon, glyphosate; agent for plastics; intermediate in organic synthesis of coating materials, pesticides, plastics, rubber chemicals, pharmaceuticals and others; additive in the petroleum industry
3-Aminopyridine	Synthesis of organic ligand 3-pyridylnicotinamide.
3-Buten-2-one, 3-methyl-, dimethylhydrazone	-
3-Cyclohexene-1-carboxaldehyde, 4-methyl-	-
4-Fluorohistamine	Organic syntheses
Acetic acid	Production of cellulose acetate for photographic film, polyvinyl acetate for wood glue, and synthetic fibers and fabrics; descaling agent, used in the food industry, in biochemistry
Benzoic acid, 2,4-dihydroxy-, (3-diethylamino-1-methyl)propyl ester	-
Dimethylamine	Dehairing agent in tanning, in dyes, in rubber accelerators, in soaps and cleaning compounds; agricultural fungicide
dl-Alanine	Food and pharmaceutical industry; plating chemicals and animal feed
Formic acid phenyl ester	Used for palladium-catalyzed carbonylation of aryl, alkenyl and allyl halides; used as a reagent for the formulation of amines
Hydrogen chloride	Used in cleaning, pickling, electroplating metals, tanning leather, and refining and as an agent for producing a wide variety of products
Methylpent-4-enylamine	-
Phenethylamine, p-methoxy-alpha.-methyl-, (+/-)-	-
Phenol	Precursor to many materials and useful compounds; used to synthesize plastics and related materials; production of polycarbonates, epoxies, Bakelite, nylon, detergents, herbicides such as phenoxy herbicides, and numerous pharmaceutical drugs.
Phenol, 4-methyl-	Production of antioxidants, e.g., butylated hydroxytoluene
Pyrazole, 1-methyl-4-nitro-	-
Tetrahydro-4H-pyran-4-ol	-

A.2. Model Equations

The equations of each model shown in this work are shown in Table A.2.

Table A.2: Model equations expressed as factors, where A represents temperature and B represents time.

Element	Figure	A	B	AB	A ²	B ²
Phosphorus	Figure A.2m	+27449,13	+2212,52	+480,34		
Sulfur	Figure A.2r	+17369,14	-183,86	-185,14	+614,95	+1021,72
Silicon	Figure A.2n	+122,86	-36,87	-7,12		-48,13
Molybdenum	Figure A.1q	+414,76				
Zinc	Figure A.2q	+5052,69	+321,11	+44,49		
Strontium	Figure A.2p	+312,16	+20,34	+2,71		
Nickel	Figure A.2k	+123,10				
Sodium	Figure A.2o	+820,63	-280,45	-21,24		
Manganese	Figure A.2j	+2622,06	+254,41	+42,80		
Magnesium	Figure A.2i	+3227,89	+647,73	+139,96	+116,79	
Potassium	Figure A.2l	+316,13	-99,86	-2,63	+95,44	
Iron	Figure A.2h	+1,393E+05	+14041,87	+1929,22		
Copper	Figure A.2g	+510,78	+21,82	+1,54		
Chromium	Figure A.2e	+160,33	+12,87	+2,87	+5,70	
Cobalt	Figure A.2f	+398,87	+38,20	+0,7948		
Calcium	Figure A.2d	+24469,55	+1846,65	+396,05		
Barium	Figure A.2b	+72,93	+1,32	+1,49		
Boron	Figure A.2c	+88,39	-0,1001	+1,74		+5,86
Alluminium	Figure A.2a	+1118,03	+95,38	+33,33		

A.3. ICP-OES

A.3.1. Aqueous Phase

Figure A.1 shows the concentrations of the HM found in the aqueous phase samples. Where Figures A.1a to A.1l, A.1n and A.1q have a significant overall model and Figures A.1o and A.1p do not have a significant model. On the data of nickel no possible model could be determined by the software, because data is random. For the influence of time, only Cr, Mn, and S are significantly altered by time and S contains an exponential time factor, as is shown in Figures A.1e, A.1h and A.1m. HM concentration increases with temperature for the alkali metals; K and Na shown in Figures A.1j and A.1o.

At Al, Co the limitations of ICP-OES can be noted as higher temperature and time can lead to concentrations under the detection limit of 1 mg/kg, as shown in Figures A.1k and A.1q. Co and P decreasing exponential with temperature to around the detection limit. At Figure A.1q, strange behaviour can be seen as the concentration of Mo decreases with the temperature from 180°C to 210°C. The concentration starts to increase with the temperature from 210°C to 240°C. Overall a decrease in HM concentration with increasing temperature can be seen. Where N does not show any influence with change in temperature or time.

A.3.2. Hydrochar

The high amount of ash showed in subsection 3.4.6 consist of different HM. Where Fe, Ca, Mg, Mn Zn, P, S takes up most parts and Al, B, Ba, Co, Cr, Cu, K, Na, Ni, Sr, Si, and Mo contributed <0.1% to the ash matrix. In Figure A.2 can be seen that all elements are influenced significantly by temperature except for Ba, B, S, and Ni, which shows no model at all. Time has significant influences only for Mn, as can be seen in Figure A.2i.

In the starting material, the concentration of Fe is below 10% and this is increased to around 12.5% at 180°C and further increases to above 16% at 240°C. Fe makes up a high mass percentage of the HC, as is shown in Figure A.2h. The second element is P which contributes 2-3%.

A.3.3. Leaching

Table A.3: ICP-OES data from the leaching experiment in mg/kg.

Temp-Time	Hours	Al	B	Ca	Co	Cr	Cu	Fe	K	Mg	Mn	Na	Sr	Zn	PO4	SO4	Si	Mo
180-4	1	0,015	0,125	33,445	0,18	0,01	0,04	1,44	2,055	2,66	1,285	2,25	0,305	0,71	0,435	77,765	0,22	0,08
180-4	2	0,015	0,13	37,42	0,205	0,01	0,03	1,58	2,17	2,77	1,465	2,385	0,34	0,83	0,485	83,57	0,25	0,095
180-4	4	0,03	0,145	40,425	0,26	0,015	0,045	2,155	2,38	2,99	1,71	2,545	0,36	1,135	0,93	88,375	0,31	0,12
180-4	6	0,03	0,145	41,505	0,285	0,02	0,04	1,435	2,365	3,11	1,84	2,59	0,365	1,385	0,745	89,405	0,35	0,13
180-4	20	0,06	0,17	45,05	0,43	0,02	0,075	2,49	2,73	3,68	2,245	2,96	0,385	2,53	1,44	94,13	0,51	0,175
180-4	24	0,045	0,175	47,245	0,435	0,02	0,075	1,155	2,695	3,765	2,225	3,185	0,395	2,57	1,175	96,475	0,54	0,185
210-4	1	0,005	0,08	32,4	0,085	0	0,01	0,255	1,435	1,875	0,805	1,755	0,29	0,32	0,235	63,27	0,195	0,045
210-4	2	0	0,095	39,83	0,12	0,01	0,005	0,21	1,715	2,17	1,04	2,045	0,365	0,41	0,39	77,46	0,245	0,06
210-4	4	0,005	0,105	42,495	0,155	0,01	0	0,395	1,82	2,31	1,2	2,15	0,38	0,585	0,31	80,935	0,305	0,075
210-4	6	0	0,11	44,31	0,185	0,01	0	0,4	1,93	2,425	1,275	2,205	0,395	0,7	0,915	83,655	0,345	0,09
210-4	20	0,01	0,135	47,865	0,31	0,01	0,02	0,4	2,14	2,935	1,615	2,48	0,42	1,455	0,83	89,66	0,48	0,135
210-4	24	0,01	0,135	47,945	0,325	0,01	0,02	0,31	2,16	2,945	1,605	2,5	0,415	1,525	0,77	89,86	0,495	0,145
240-4	1	0	0,04	33,5	0,02	0	0	0,06	1,19	1,06	0,445	1,21	0,33	0,115	0,585	60,15	0,12	0,04
240-4	2	0	0,05	41,11	0,03	0	0	0,055	1,33	1,235	0,56	1,34	0,405	0,125	0,875	73,59	0,145	0,06
240-4	4	0,005	0,065	49,14	0,04	0	0	0,09	1,46	1,5	0,72	1,635	0,48	0,16	1,195	87,145	0,195	0,085
240-4	6	0	0,07	49,925	0,06	0	0	0,11	1,535	1,615	0,785	1,695	0,48	0,215	1,41	87,835	0,23	0,1
240-4	20	0,005	0,09	53,57	0,12	0	0	0,095	1,725	2,05	1,005	1,975	0,495	0,465	1,205	93,95	0,315	0,15
240-4	24	0,005	0,095	53,845	0,135	0	0	0,09	1,685	2,095	1,03	2,095	0,5	0,5	0,475	95,095	0,33	0,16

A.4. Dry Sludge

Table A.4: Elemental analysis supplied by Shell of the sludge

Metal	mg/kg	Metal	mg/kg	Metal	mg/kg	Metal	mg/kg
Aluminium	508.6	Copper	252.9	Potassium	2358	Zinc	1766 mg/kg
Barium	49.74	Iron	59110	Calcium	10360	Phosphorous	17210 mg/kg
Boron	68.67	Lead	32.5	Magnesium	1410	Arsenic	<20 µg/kg
Cadmium	<0.5	Manganese	976.4	Sodium	2701	Selenium	<20 µg/kg
Chromium	76.63	Molybdenum	206.4	Strontium	160.2		
Cobalt	142.2	Nickel	26.11	Vanadium	<0.5		

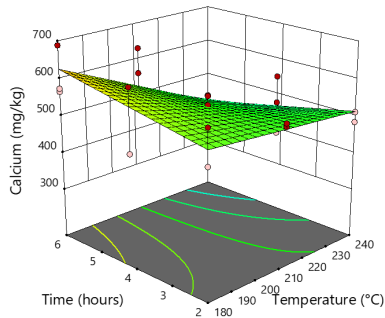
Sample date	Temperature-time	Al	B	Ba	Ca	Co	Cr	Cu	Fe	K	Mg	Mn	Na	Ni	Sr	Zn	P	S	Si	Mo
29-jul	240-4	1130	80	68	25078	479	169	563	144759	3642	2636	386	53	307	5842	27296	18604	30	402	
1-sep	180-4	980	90	71	20576	346	143	495	115854	375	2433	2173	1135	153	268	4718	23509	17252	97	382
6-sep	210-6	1289	113	67		397	151	504	128422		18317	2500	559	199	302	5059	26289	16263	108	385
9-sep	210-2	1118	86	75	24847	422	160	546	139432	488	3114	2695	972	66	306	5378	27720	17789	174	420
12-sep	210-6	1149	91	78	25046	376	167	484	147304	222	3515	2829	875	51	315	4919	29592	17324	99	432
15-sep	180-4	1044	87	73	22521	360	148	491	125985	494	2612	2369	1050	60	309	4743	25258	17642	106	417
16-sep	180-4	1022	84	80	23362	392	144	535	119918	186	2272	2318	901	93	284	5120	23420	18268	100	409
19-sep	240-2	1120	95	70	24563	440	167	532	148957		3633	2774	535	12	320	5232	28876	18276	74	430
20-sep	210-4	1110	91	70	23443	407	157	538	137148	370	3112	2638	905	33	304	5248	27463	17593	118	407
21-sep	210-4	1056	91	72	23687	403	160	488	140473		3238	2611	727	127	316	4840	28137	17787	89	431
22-sep	240-6	1250	96	80	29035	431	185	553	160827	386	4132	3010	754	107	336	5450	30829	19743	55	397
23-sep	240-4	1407	89	81	27787	397	178	494	162969	127	4112	3108	687	245	361	5121	31714	17434	41	410
28-sep	240-2	1148	90	70	26112	420	161	524	142936	70	3603	2680	583	186	323	5165	27510	17831	4	403
29-sep	210-4	1097	96	75	25292	390	162	479	148465		3404	2781	696	182	317	4847	29071	17752	130	444
3-okt	240-6	1197	92	76	26947	443	185	537	159000		4117	2961	530	145	353	5381	30660	18352	21	414
4-okt	180-2	997	94	66	22207	351	150	473	120873	476	2608	2244	1287	256	288	4536	24358	19762	103	423
5-okt	180-2	1003	95	70	22951	356	149	477	125671	530	2567	2346	1188	156	296	4622	24896	19473	116	415
6-okt	4-240	1188	89	75	24341	464	169	549	147037		3722	2741	447	58	331	5548	28126	17209	40	394
12-okt	210-2	1115	95	73	24807	368	162	489	146770		3181	2751	729	242	318	4833	29113	17076	142	434
13-okt	180-6	1010	91	67	22818	364	141	494	127303	244	2592	2359	996	144	277	4902	25006	17474	92	410
17-okt	180-6	1082	99	76	23971	371	156	483	136224	443	2832	2582	1270		327	4647	28069	19352	160	451
Original	Original	327	64	23	9151	167	56	174	45554	327	1402	828	1282	119	99	1603	7818	11507	58	171

A.5. Mass Balance

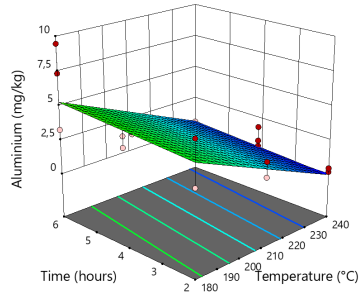
During the HTC process molecules will be dehydrated to form water, which is not incorporated as this is boiled-off by the thermal drying step. Without the drying step the HC will still contain water. In Figure A.3 a mass balance on the organic CHNO content is shown which incorporates moisture content and the data of the samples at 210°C and 4h is used and nitrogen in the gas phase is not neglected. The mass balance simulates biosludge at a 20% solid loading, where the CHNO data of biosludge (Table 2.2) is added with 80% water and the resulted HC fraction is derived by adding 50% moisture to the data obtained from the ultimate analyses (Figure 4.3). In Figure A.3 it can be seen that the HC has a higher O and H content because of the water.

Sample date	Temperature-time	Al	B	Ca	Co	Cr	Fe	K	Mg	Mn	Na	Ni	Sr	Zn	Cl	P	S	Si	Mo
29-jul	240-4	0	15	390	1	1	275	553	116	8	719	1	3	0	184	5	2848	29	2
1-sep	180-4	3	15	566	8	4	2813	491	303	57	709	0	4	2	176	148	3620	128	2
6-sep	210-6	1	15	560	2	3	1430	523	186	22	714	1	5	0	180	19	3280	116	0
9-sep	210-2	2	15	546	3	3	1486	509	196	25	693	0	4	1	169	25	3203	108	1
12-sep	210-6	1	15	630	2	3	1378	514	187	22	705	1	4	0	178	17	3249	100	0
15-sep	180-4	4	16	468	5	4	2332	550	272	44	710	1	4	1	181	81	3533	134	1
16-sep	180-4	5	16	637	8	4	3007	495	298	58	700	2	5	1	177	235	3569	131	2
19-sep	240-2	0	15	485	1	2	719	536	135	15	715	0	4	0	193	9	2998	68	1
20-sep	210-4	2	15	531	2	4	1503	527	187	23	720	1	5	1	190	37	3320	126	0
21-sep	210-4	2	15	555	2	3	1382	525	190	23	718		4	0	188	23	3346	120	0
22-sep	240-6	1	16	398	1	1	637	545	108	11	737	1	3	0	198	31	2823	96	4
23-sep	240-4	2	15	551	1	2	1030	519	132	18	703	0	5	0	176	63	2895	112	2
28-sep	240-2	0	15	512	1	2	701	678	137	15	721	3	4	0	174	8	2975	80	1
29-sep	210-4	2	15	557	2	3	1495	527	188	23	716	0	5	0	187	30	3311	135	1
3-okt	240-6	0	15	353	1	1	378	515	105	9	697	2	3	0	178	8	2760	50	3
4-okt	180-2	6	15	602	7	4	2732	484	282	53	680	2	5	2	158	246	3296	120	2
5-okt	180-2	3	16	509	7	4	2330	480	292	52	701	1	4	1	168	98	3381	131	2
6-okt	210-4	1	14	477	1	1	674	509	126	14	699	0	3	0	171	18	2841	70	1
12-okt	210-2	3	14	538	3	4	1788	498	215	30	686	1	5	1	162	53	3190	130	1
13-okt	180-6	7	16	574	6	5	2838	489	282	47	694	1	6	1	162	199	3455	139	1
17-okt	180-06	9	16	688	7	5	3070	500	300	52	701	3	6	1	164	282	3565	144	2
	Original	327	64	9151	167	56	45554	327	1402	828	1282	119	99	1603		7818	11507	58	171

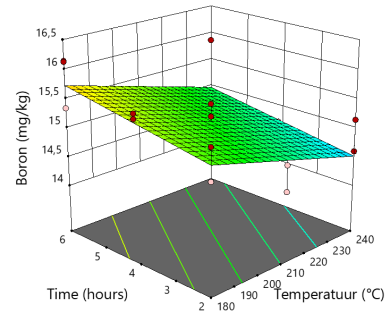
[HTML]FFFFFFDate	[HTML]FFFFFFTemperature-time	N2	Co2	O2	Ch4
29-jul	240-4	22,68362	77,1961	0,044603	0,075682
1-sep	180-6	22,15822	77,84178	0	0
6-sep	210-6	2,283361	97,71664	0	0
9-sep	210-2	2,336733	97,66327	0	0
12-sep	210-6	2,313034	97,68697	0	0
15-sep	180-4	2,957139	97,04286	0	0
16-sep	180-4	19,24774	80,75226	0	0
19-sep	240-2	2,53043	97,46957	0	0
20-sep	210-4				
21-sep	210-4	1,96322	98,03678	0	0
22-sep	240-6	2,699483	97,30052	0	0
23-sep	240-4	1,768653	98,23135	0	0
28-sep	240-2	3,057982	96,94202	0	0
29-sep	210-4	2,144301	97,8557	0	0
3-okt	240-6	2,458176	97,54182	0	0
4-okt	180-2	36,85574	63,14426	0	0
5-okt	180-2				
6-okt	240-4	31,19183	68,80817	0	0
12-okt	210-2	28,87996	71,12004	0	0
13-okt	180-6	2,68634	97,31366	0	0
17-okt	180-6	42,79265	57,20735	0	0



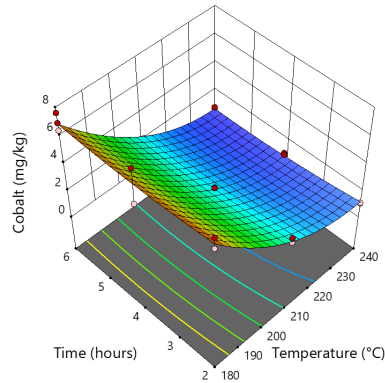
(a) Calcium liquid concentration.
 $P(\text{model})=0,0049$ $P(A)=0,0022$ and
 $P(B)=0,8157$



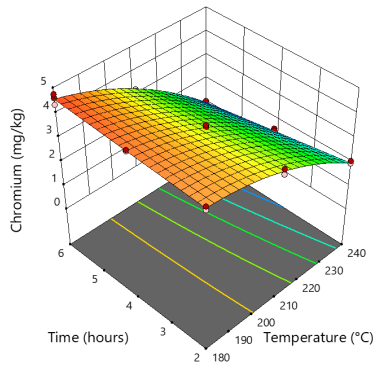
(b) Aluminium liquid concentration.
 $P(\text{overall})<0,0001$ $P(A)<0,0001$ and
 $P(B)=0,5760$



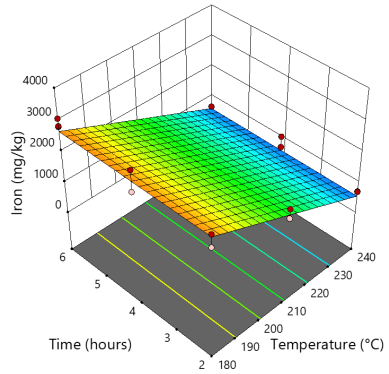
(c) Boron liquid concentration.
 $P(\text{overall})=0,0349$ $P(A)=0,0255$ and
 $P(B)=0,2106$



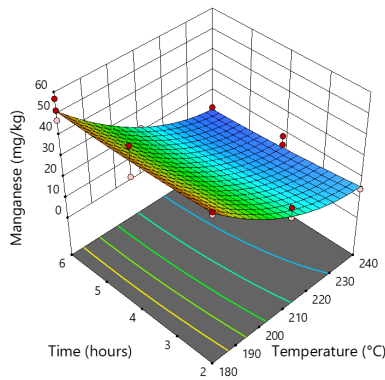
(d) Cobalt liquid concentration.
 $P(\text{overall})<0,0001$ $P(A)<0,0001$,
 $P(B)=0,4611$, $P(A^2)<0,0001$



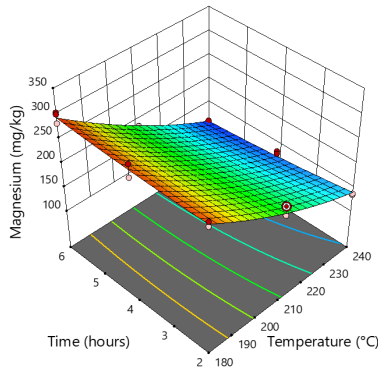
(e) Chromium liquid concentration.
 $P(\text{overall})<0,0001$, $P(A)<0,0001$,
 $P(B)=0,3030$, and $P(AB)=0,0175$



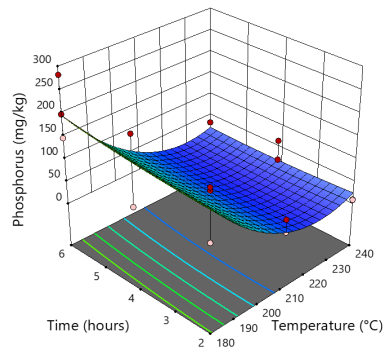
(f) Iron liquid concentration.
 $P(\text{overall})<0,0001$ $P(A)<0,0001$, and
 $P(B)=0,8985$



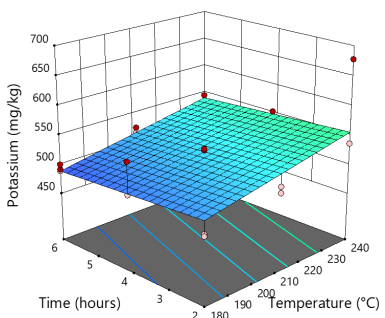
(g) Manganese liquid concentration.
 $P(\text{overall})<0,0001$, $P(A)<0,0001$,
 $P(B)=0,1235$, and $P(A^2)=0,0001$



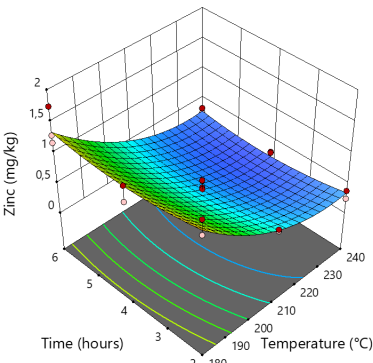
(h) Magnesium liquid concentration.
 $P(\text{overall})<0,0001$, $P(A)<0,0001$,
 $P(B)=0,0154$, $P(AB)=0,0043$, and
 $P(A^2)=0,042$



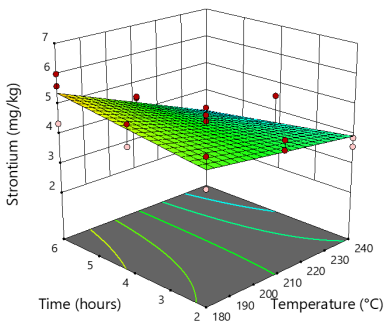
(i) Phosphorus liquid concentration.
 $P(\text{overall})=0,003$ $P(A)<0,0001$, $P(B)=0,6421$,
and $P(A^2)=0,0043$



(j) Potassium liquid concentration.
 $P(\text{overall})=0,0389$, $P(A)=0,0176$, and
 $P(B)=0,4370$



(k) Zinc liquid concentration.
 $P(\text{overall})<0,0001$ $P(A)<0,0001$, and
 $P(B)=0,1466$



(l) Strontium liquid concentration.
 $P(\text{overall})<0,0215$ $P(A)<0,0064$, and
 $P(B)=0,9933$

Figure A.1: HM concentration in aqueous phase samples measured by ICP-OES

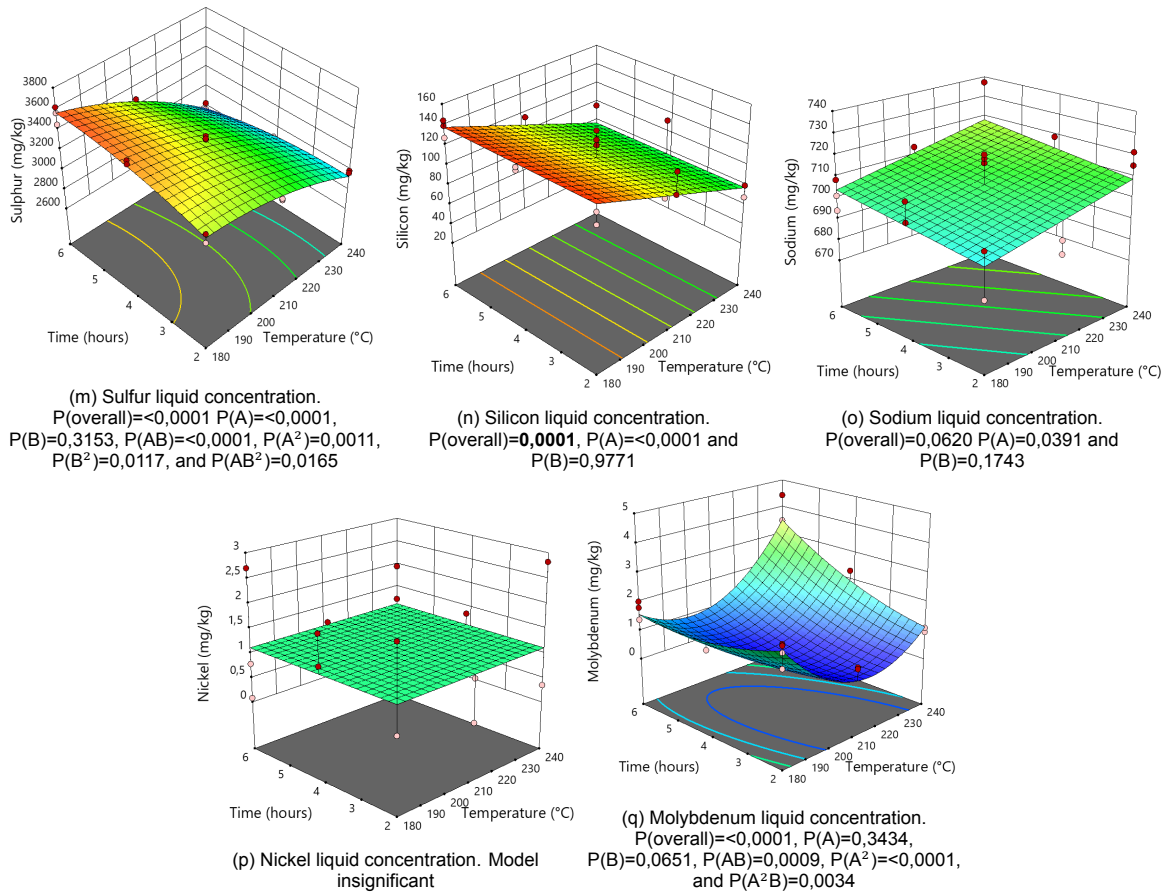


Figure A.1: Heavy metal concentration in water samples measured by ICP-OES

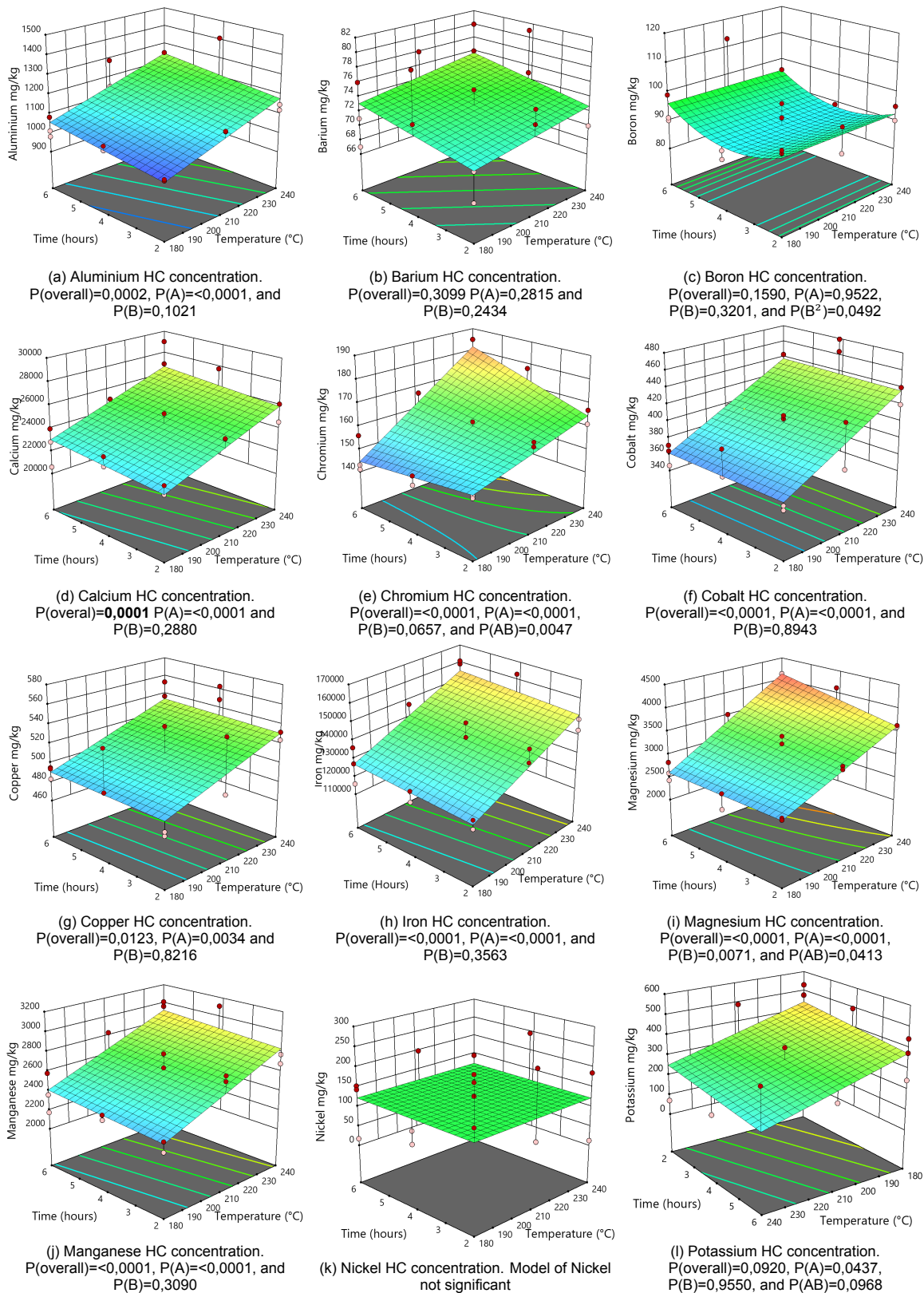


Figure A.2: Heavy metal concentration in HC samples measured by ICP-OES

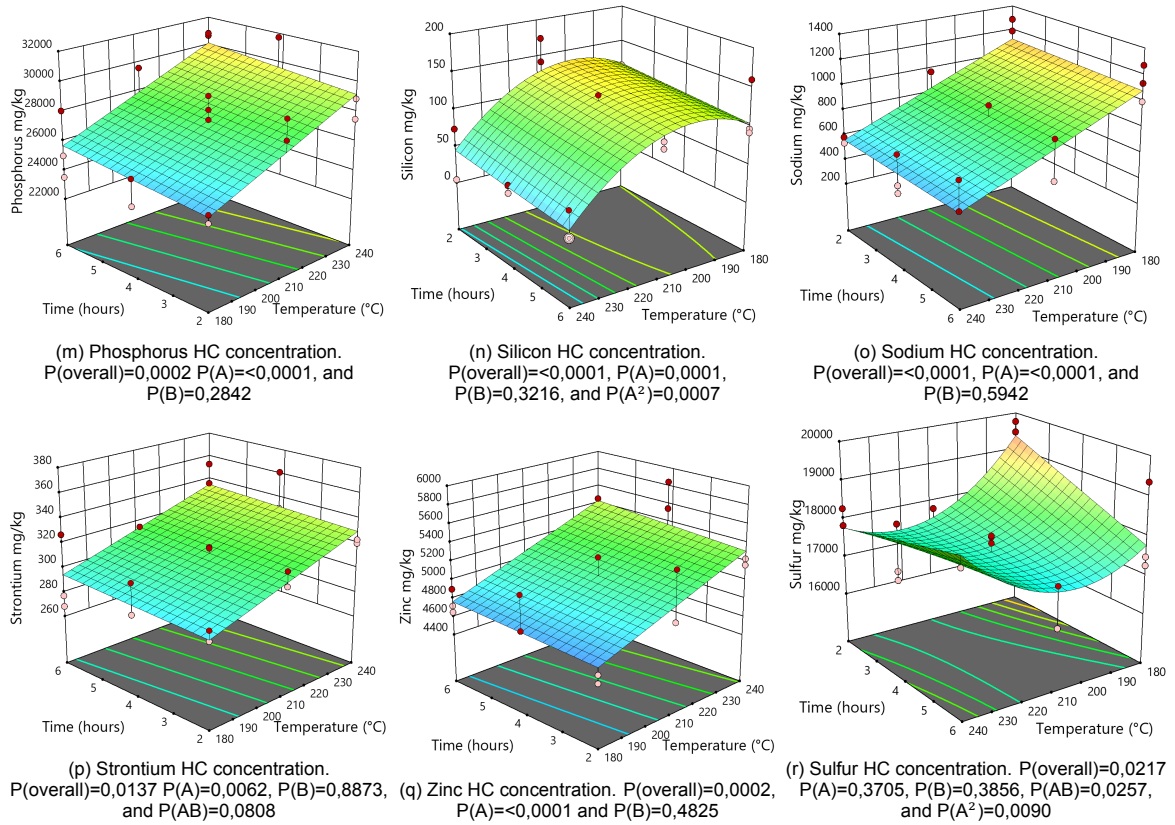
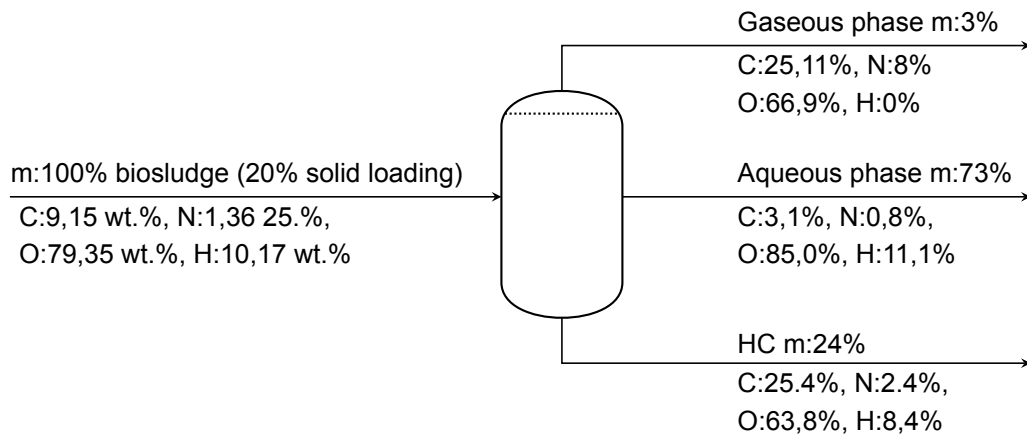


Figure A.2: Heavy metal concentration in HC samples measured by ICP-OES

Figure A.3: Mass balance of the HTC process at 210°C and 4h with moisture.



Bibliography

- 13 Crystal Structures – Mineralogy. (n.d.). <https://opengeology.org/Mineralogy/13-crystal-structures/>
- Abel, S., Peters, A., Trinks, S., Schonsky, H., Facklam, M., & Wessolek, G. (2013). Impact of biochar and hydrochar addition on water retention and water repellency of sandy soil. *Geoderma*, 202–203, 183–191. <https://doi.org/10.1016/J.GEODERMA.2013.03.003>
- Akbari, M., Oyedun, A. O., Gemechu, E., & Kumar, A. (2021). Comparative life cycle energy and greenhouse gas footprints of dry and wet torrefaction processes of various biomass feedstocks. *Journal of Environmental Chemical Engineering*, 9(4). <https://doi.org/10.1016/j.jece.2021.105415>
- Appels, L., Baeyens, J., Degrève, J., & Dewil, R. (2008). Principles and potential of the anaerobic digestion of waste-activated sludge. <https://doi.org/10.1016/j.pecs.2008.06.002>
- Aragón-Briceño, C. I., Grasham, O., Ross, A. B., Dupont, V., & Camargo-Valero, M. A. (2020). Hydrothermal carbonization of sewage digestate at wastewater treatment works: Influence of solid loading on characteristics of hydrochar, process water and plant energetics. *Renewable Energy*, 157. <https://doi.org/10.1016/j.renene.2020.05.021>
- Atrafi, A., & Pawlik, M. (2017). Foamability of fatty acid solutions and surfactant transfer between foam and solution phases. *Minerals Engineering*, 100. <https://doi.org/10.1016/j.mineng.2016.10.012>
- Benavente, V., & Fullana, A. (2021). Low-cost additives to improve the fusion behaviour of hydrochar ash. *Fuel*, 285. <https://doi.org/10.1016/j.fuel.2020.119009>
- Biochar. (n.d.). Retrieved April 12, 2022, from <https://biochar-international.org/biochar/>
- Breulmann, M., van Afferden, M., Müller, R. A., Schulz, E., & Fühner, C. (2017). Process conditions of pyrolysis and hydrothermal carbonization affect the potential of sewage sludge for soil carbon sequestration and amelioration. *Journal of Analytical and Applied Pyrolysis*, 124, 256–265. <https://doi.org/10.1016/J.JAAP.2017.01.026>
- Buta, M., Hubeny, J., Zieliński, W., Harnisz, M., & Korzeniewska, E. (2021). Sewage sludge in agriculture – the effects of selected chemical pollutants and emerging genetic resistance determinants on the quality of soil and crops – a review. *Ecotoxicology and Environmental Safety*, 214, 112070. <https://doi.org/10.1016/J.ECOENV.2021.112070>
- Calderon, A. G., Duan, H., Seo, K. Y., Macintosh, C., Astals, S., Li, K., Wan, J., Li, H., Maulani, N., Lim, Z. K., Yuan, Z., & Hu, S. (2021). The origin of waste activated sludge affects the enhancement of anaerobic digestion by free nitrous acid pre-treatment. *Science of the Total Environment*, 795. <https://doi.org/10.1016/j.scitotenv.2021.148831>
- Cebi, D., Celiktas, M. S., & Sarptas, H. (2022). A Review on Sewage Sludge Valorization via Hydrothermal Carbonization and Applications for Circular Economy. *Circular Economy and Sustainability*. <https://doi.org/10.1007/s43615-022-00148-y>
- Cervera-Mata, A., Delgado, G., Fernández-Arteaga, A., Fornasier, F., & Mondini, C. (2022). Spent coffee grounds by-products and their influence on soil C–N dynamics. *Journal of Environmental Management*, 302, 114075. <https://doi.org/10.1016/J.JENVMAN.2021.114075>
- Chen, Y.-C., & Kuo, J. (2016). Potential of greenhouse gas emissions from sewage sludge management: a case study of Taiwan. *Journal of Cleaner Production*, 129, 196–201. <https://doi.org/10.1016/j.jclepro.2016.04.084>
- Chen, Z., Wang, D., Dao, G., Shi, Q., Yu, T., Guo, F., & Wu, G. (2021). Environmental impact of the effluents discharging from full-scale wastewater treatment plants evaluated by a hybrid fuzzy approach. *Science of The Total Environment*, 790, 148212. <https://doi.org/10.1016/J.SCITOTENV.2021.148212>
- Chung, C. S., Choi, K. Y., Kim, C. J., Jung, J. M., & Chang, Y. S. (2020). Overview of the policies for phasing out ocean dumping of sewage sludge in the Republic of Korea. <https://doi.org/10.3390/su12114553>
- Decarboxylation | OChemPal. (n.d.). <http://www.ochempal.org/index.php/alphabetical/c-d/decarboxylation/>
- Deng, W., Ma, J., Xiao, J., Wang, L., & Su, Y. (2019). Orthogonal experimental study on hydrothermal treatment of municipal sewage sludge for mechanical dewatering followed by thermal drying. *Journal of Cleaner Production*, 209. <https://doi.org/10.1016/j.jclepro.2018.10.261>

- Djandja, O. S., Liew, R. K., Liu, C., Liang, J., Yuan, H., He, W., Feng, Y., Lougou, B. G., Duan, P.-G., Lu, X., & Kang, S. (2023). Catalytic hydrothermal carbonization of wet organic solid waste: A review. *Science of The Total Environment*, 873, 162119. <https://doi.org/https://doi.org/10.1016/j.scitotenv.2023.162119>
- Ekanthalu, V. S., Narra, S., Sprafke, J., & Nelles, M. (2021). Influence of acids and alkali as additives on hydrothermally treating sewage sludge: Influence on phosphorus recovery, yield, and energy value of hydrochar. *Processes*, 9(4). <https://doi.org/10.3390/pr9040618>
- Escala, M., Zumbühl, T., Koller, C., Junge, R., & Krebs, R. (2013). Hydrothermal carbonization as an energy-efficient alternative to established drying technologies for sewage sludge: A feasibility study on a laboratory scale. *Energy and Fuels*, 27(1). <https://doi.org/10.1021/ef3015266>
- EurEau. (2021). *Europe's Water in Figures An overview of the European drinking water and waste water sectors* (tech. rep.). The European Federation of National Associations of Water Services.
- Fang, J., Zhan, L., Ok, Y. S., & Gao, B. (2018). Minireview of potential applications of hydrochar derived from hydrothermal carbonization of biomass. *Journal of Industrial and Engineering Chemistry*, 57, 15–21. <https://doi.org/10.1016/j.jiec.2017.08.026>
- Ferrentino, R., Ceccato, R., Marchetti, V., Andreottola, G., & Fiori, L. (2020). Sewage sludge hydrochar: An option for removal of methylene blue from wastewater. *Applied Sciences (Switzerland)*, 10(10). <https://doi.org/10.3390/app10103445>
- Fijalkowski, K., Rorat, A., Grobelak, A., & Kacprzak, M. J. (2017). The presence of contaminations in sewage sludge – The current situation. *Journal of Environmental Management*, 203. <https://doi.org/10.1016/j.jenvman.2017.05.068>
- Funke, A., Tomasi Morgano, M., Dahmen, N., & Leibold, H. (2017). Experimental comparison of two bench scale units for fast and intermediate pyrolysis. *Journal of Analytical and Applied Pyrolysis*, 124, 504–514. <https://doi.org/10.1016/J.JAAP.2016.12.033>
- Fyttili, D., & Zabaniotou, A. (2008). Utilization of sewage sludge in EU application of old and new methods-A review. <https://doi.org/10.1016/j.rser.2006.05.014>
- Gai, C., Zhang, F., Guo, Y., Peng, N., Liu, T., Lang, Q., Xia, Y., & Liu, Z. (2017). Hydrochar-Supported, in Situ-Generated Nickel Nanoparticles for Sorption-Enhanced Catalytic Gasification of Sewage Sludge. *ACS Sustainable Chemistry and Engineering*, 5(9). <https://doi.org/10.1021/acssuschemeng.7b00924>
- Gao, N., Kamran, K., Quan, C., & Williams, P. T. (2020). Thermochemical conversion of sewage sludge: A critical review. *Progress in Energy and Combustion Science*, 79, 100843. <https://doi.org/10.1016/j.pecs.2020.100843>
- Gao, N., Li, Z., Quan, C., Miskolczi, N., & Egedy, A. (2019). A new method combining hydrothermal carbonization and mechanical compression in-situ for sewage sludge dewatering: Bench-scale verification. *Journal of Analytical and Applied Pyrolysis*, 139. <https://doi.org/10.1016/j.jaap.2019.02.003>
- Garg, N. K. (2009). Multicriteria Assessment of Alternative Sludge Disposal Methods Neeraj Kumar Garg. *Environment*.
- Gasim, M. F., Lim, J. W., Low, S. C., Lin, K. Y. A., & Oh, W. D. (2022). Can biochar and hydrochar be used as sustainable catalyst for persulfate activation? <https://doi.org/10.1016/j.chemosphere.2021.132458>
- Gaur, R. Z., Houry, O., Zohar, M., Poverenov, E., Darzi, R., Laor, Y., & Posmanik, R. (2020). Hydrothermal carbonization of sewage sludge coupled with anaerobic digestion: Integrated approach for sludge management and energy recycling. *Energy Conversion and Management*, 224. <https://doi.org/10.1016/j.enconman.2020.113353>
- Geissdoerfer, M., Savaget, P., Bocken, N. M., & Hultink, E. J. (2017). The Circular Economy – A new sustainability paradigm? <https://doi.org/10.1016/j.jclepro.2016.12.048>
- Germain, J. C., & Aguilera, J. M. (2014). Multi-scale properties of protein-stabilized foams. <https://doi.org/10.1016/j.foostr.2014.01.001>
- González-Arias, J., Baena-Moreno, F. M., González-Castaño, M., & Arellano-García, H. (2022). Economic approach for CO₂ valorization from hydrothermal carbonization gaseous streams via reverse water-gas shift reaction. *Fuel*, 313, 123055. <https://doi.org/10.1016/J.FUEL.2021.123055>

- Goody, D. C., & Hinsby, K. (2008). Organic Quality of Groundwaters. *Natural groundwater quality* (pp. 59–70). John Wiley & Sons, Ltd. <https://doi.org/https://doi.org/10.1002/9781444300345.ch3>
- Goriparti, S., Miele, E., De Angelis, F., Di Fabrizio, E., Proietti Zaccaria, R., & Capiglia, C. (2014). Review on recent progress of nanostructured anode materials for Li-ion batteries. <https://doi.org/10.1016/j.jpowsour.2013.11.103>
- Griscom, B. W., Adams, J., Ellis, P. W., Houghton, R. A., Lomax, G., Miteva, D. A., Schlesinger, W. H., Shoch, D., Siikamäki, J. V., Smith, P., Woodbury, P., Zganjar, C., Blackman, A., Campari, J., Conant, R. T., Delgado, C., Elias, P., Gopalakrishna, T., Hamsik, M. R., ... Fargione, J. (2017). Natural climate solutions. *Proceedings of the National Academy of Sciences of the United States of America*, *114*(44). <https://doi.org/10.1073/pnas.1710465114>
- Gupta, B., Shah, D. O., Mishra, B., Joshi, P. A., Gandhi, V. G., & Fougat, R. S. (2015). Effect of top soil wettability on water evaporation and plant growth. *Journal of Colloid and Interface Science*, *449*, 506–513. <https://doi.org/10.1016/J.JCIS.2015.02.018>
- Ha, E., Basu, N., Bose-O'Reilly, S., Dórea, J. G., McSorley, E., Sakamoto, M., & Chan, H. M. (2017). Current progress on understanding the impact of mercury on human health. *Environmental Research*, *152*. <https://doi.org/10.1016/j.envres.2016.06.042>
- Hansen, L. J., Fendt, S., & Spliethoff, H. (2022). Impact of hydrothermal carbonization on combustion properties of residual biomass. *Biomass Conversion and Biorefinery*, *12*(7). <https://doi.org/10.1007/s13399-020-00777-z>
- Heidari, M., Dutta, A., Acharya, B., & Mahmud, S. (2019). A review of the current knowledge and challenges of hydrothermal carbonization for biomass conversion. <https://doi.org/10.1016/j.joei.2018.12.003>
- Henriques, M. C., Loureiro, S., Fardilha, M., & Herdeiro, M. T. (2019). Exposure to mercury and human reproductive health: A systematic review. <https://doi.org/10.1016/j.reprotox.2019.02.012>
- Huezo, L., Vasco-Correa, J., & Shah, A. (2021). Hydrothermal carbonization of anaerobically digested sewage sludge for hydrochar production. *Bioresource Technology Reports*, *15*. <https://doi.org/10.1016/j.biteb.2021.100795>
- Hunsom, M., & Autthanit, C. (2013). Adsorptive purification of crude glycerol by sewage sludge-derived activated carbon prepared by chemical activation with H₃PO₄, K₂CO₃ and KOH. *Chemical Engineering Journal*, *229*. <https://doi.org/10.1016/j.cej.2013.05.120>
- IBI. (2015). Standardized Product Definition and Product Testing Guidelines for Biochar That Is Used in Soil. https://www.biochar-international.org/wp-content/uploads/2018/04/IBI_Biochar_Standards_V2.1_Final.pdf
- IEA. (n.d.). Heat values of various fuels - World Nuclear Association. <https://world-nuclear.org/information-library/facts-and-figures/heat-values-of-various-fuels.aspx>
- Ilyas, M., Ahmad, W., Khan, H., Yousaf, S., Yasir, M., & Khan, A. (2019). Environmental and health impacts of industrial wastewater effluents in Pakistan: A review. <https://doi.org/10.1515/reveh-2018-0078>
- Inglezakis, V. J., Zorpas, A. A., Karagiannidis, A., Samaras, P., Voukkali, I., & Sklari, S. (2014). European union legislation on sewage sludge management. *Fresenius Environmental Bulletin*, *23*(2 A).
- Ischia, G., & Fiori, L. (2021). Hydrothermal Carbonization of Organic Waste and Biomass: A Review on Process, Reactor, and Plant Modeling. <https://doi.org/10.1007/s12649-020-01255-3>
- Islam, M. A., Limon, M. S. H., Romić, M., & Islam, M. A. (2021). Hydrochar-based soil amendments for agriculture: a review of recent progress. *Arabian Journal of Geosciences*, *14*(2), 102. <https://doi.org/10.1007/s12517-020-06358-8>
- Järup, L. (2003). Hazards of heavy metal contamination. <https://doi.org/10.1093/bmb/ldg032>
- Jeder, A., Sanchez-Sanchez, A., Gadonneix, P., Masson, E., Ouederni, A., Celzard, A., & Fierro, V. (2018). The severity factor as a useful tool for producing hydrochars and derived carbon materials. *Environmental Science and Pollution Research*, *25*(2). <https://doi.org/10.1007/s11356-017-0366-7>
- Jellali, S., Zorpas, A. A., Alhashmi, S., & Jeguirim, M. (2022). Recent Advances in Hydrothermal Carbonization of Sewage Sludge. *Energies 2022, Vol. 15, Page 6714*, *15*(18), 6714. <https://doi.org/10.3390/EN15186714>

- Kambo, H. S., & Dutta, A. (2015). A comparative review of biochar and hydrochar in terms of production, physico-chemical properties and applications. <https://doi.org/10.1016/j.rser.2015.01.050>
- Kamerud, K. L., Hobbie, K. A., & Anderson, K. A. (2013). Stainless steel leaches nickel and chromium into foods during cooking. *Journal of Agricultural and Food Chemistry*, 61(39). <https://doi.org/10.1021/jf402400v>
- Kampschreur, M. J., Temmink, H., Kleerebezem, R., Jetten, M. S., & van Loosdrecht, M. C. (2009). Nitrous oxide emission during wastewater treatment. <https://doi.org/10.1016/j.watres.2009.03.001>
- Khosravi, A., Zheng, H., Liu, Q., Hashemi, M., Tang, Y., & Xing, B. (2022). Production and characterization of hydrochars and their application in soil improvement and environmental remediation. *Chemical Engineering Journal*, 430, 133142. <https://doi.org/10.1016/J.CEJ.2021.133142>
- Kim, H., Parajuli, P. B., Yu, F., & Columbus, E. P. (2011). *Economic Analysis and Assessment of Syngas Production using a Modeling Approach* (tech. rep.). ASABE. Louisville. <https://www.osti.gov/servlets/purl/1079601>
- Knapp, A. (2013). How Lead Caused America's Violent Crime Epidemic. <https://www.forbes.com/sites/alexknapp/2013/01/03/how-lead-caused-americas-violent-crime-epidemic/?sh=467886ac12c4>
- Krakat, N., Anjum, R., Dietz, D., & Demirel, B. (2017). Methods of ammonia removal in anaerobic digestion: a review. *Water Science and Technology*, 76(8), 1925–1938. <https://doi.org/10.2166/WST.2017.406>
- Kruse, A. (2009). Hydrothermal biomass gasification. *The Journal of Supercritical Fluids*, 47(3), 391–399. <https://doi.org/10.1016/J.SUPFLU.2008.10.009>
- Kulikova, Y., Babich, O., Tsybina, A., Sukhikh, S., Mokrushin, I., Noskova, S., & Orlov, N. (2022). Feasibility of Thermal Utilization of Primary and Secondary Sludge from a Biological Wastewater Treatment Plant in Kaliningrad City. *Energies*, 15(15). <https://doi.org/10.3390/en15155639>
- Lal, R. (2004). Soil carbon sequestration to mitigate climate change. <https://doi.org/10.1016/j.geoderma.2004.01.032>
- Lam, W. Y., Chatterton, J., Sim, S., Kulak, M., Mendoza Beltran, A., & Huijbregts, M. A. (2021). Estimating greenhouse gas emissions from direct land use change due to crop production in multiple countries. *Science of the Total Environment*, 755. <https://doi.org/10.1016/j.scitotenv.2020.143338>
- Lang, W., Blöck, T. M., & Zander, R. (1998). Solubility of NH₃ and apparent pK of NH₄⁺ in human plasma, isotonic salt solutions and water at 37°C. *Clinica Chimica Acta*, 273(1). [https://doi.org/10.1016/S0009-8981\(98\)00019-9](https://doi.org/10.1016/S0009-8981(98)00019-9)
- Langone, M., & Basso, D. (2020). Process waters from hydrothermal carbonization of sludge: Characteristics and possible valorization pathways. <https://doi.org/10.3390/ijerph17186618>
- Lawal, M., Wan Alwi, S. R., Manan, Z. A., & Ho, W. S. (2021). Industrial symbiosis tools—A review. *Journal of Cleaner Production*, 280, 124327. <https://doi.org/10.1016/J.JCLEPRO.2020.124327>
- Lee, X. J., Ong, H. C., Gan, Y. Y., Chen, W. H., & Mahlia, T. M. I. (2020). State of art review on conventional and advanced pyrolysis of macroalgae and microalgae for biochar, bio-oil and bio-syngas production. *Energy Conversion and Management*, 210, 112707. <https://doi.org/10.1016/J.ENCONMAN.2020.112707>
- Lehmann, J., Rillig, M. C., Thies, J., Masiello, C. A., Hockaday, W. C., & Crowley, D. (2011). Biochar effects on soil biota - A review. <https://doi.org/10.1016/j.soilbio.2011.04.022>
- Leng, L., Xiong, Q., Yang, L., Li, H., Zhou, Y., Zhang, W., Jiang, S., Li, H., & Huang, H. (2021). An overview on engineering the surface area and porosity of biochar. *Science of The Total Environment*, 763, 144204. <https://doi.org/10.1016/J.SCITOTENV.2020.144204>
- Leng, L., Yang, L., Leng, S., Zhang, W., Zhou, Y., Peng, H., Li, H., Hu, Y., Jiang, S., & Li, H. (2021). A review on nitrogen transformation in hydrochar during hydrothermal carbonization of biomass containing nitrogen. *Science of The Total Environment*, 756, 143679. <https://doi.org/10.1016/J.SCITOTENV.2020.143679>
- Li, D. C., & Jiang, H. (2017). The thermochemical conversion of non-lignocellulosic biomass to form biochar: A review on characterizations and mechanism elucidation. <https://doi.org/10.1016/j.biortech.2017.07.029>
- Li, F., Jiang, Z., Ji, W., Chen, Y., Ma, J., Gui, X., Zhao, J., & Zhou, C. (2022). Effects of hydrothermal carbonization temperature on carbon retention, stability, and properties of animal manure-

- derived hydrochar. *International Journal of Agricultural and Biological Engineering*, 15(1). <https://doi.org/10.25165/ijabe.20221501.6758>
- Li, H., Cao, M., Watson, J., Zhang, Y., & Liu, Z. (2021). In Situ hydrochar regulates Cu fate and speciation: Insights into transformation mechanism. *Journal of Hazardous Materials*, 410. <https://doi.org/10.1016/j.jhazmat.2020.124616>
- Liang, W., Nanou, P., Wray, H., Zhang, J., Lundstrom, I., Lundqvist, S., & Wang, C. (2022). Feasibility Study of Bio-Sludge Hydrochar as Blast Furnace Injectant. *Sustainability (Switzerland)*, 14(9). <https://doi.org/10.3390/SU14095510>
- Libra, J. A., Ro, K. S., Kammann, C., Funke, A., Berge, N. D., Neubauer, Y., Titirici, M. M., Fühner, C., Bens, O., Kern, J., & Emmerich, K. H. (2011). Hydrothermal carbonization of biomass residuals: A comparative review of the chemistry, processes and applications of wet and dry pyrolysis. *Biofuels*, 2(1). <https://doi.org/10.4155/bfs.10.81>
- Lin, Y., Ye, Y., Hu, Y., & Shi, H. (2019). The variation in microbial community structure under different heavy metal contamination levels in paddy soils. *Ecotoxicology and Environmental Safety*, 180, 557–564. <https://doi.org/10.1016/J.ECOENV.2019.05.057>
- Lin, Z., Wang, R., Tan, S., Zhang, K., Yin, Q., Zhao, Z., & Gao, P. (2023). Nitrogen-doped hydrochar prepared by biomass and nitrogen-containing wastewater for dye adsorption: Effect of nitrogen source in wastewater on the adsorption performance of hydrochar. *Journal of Environmental Management*, 334. <https://doi.org/10.1016/j.jenvman.2023.117503>
- Lin-fu, J. S. (1982). Children and Lead: New Findings and Concerns. *New England Journal of Medicine*, 307(10).
- Liu, D., Li, J., Zhao, B., Zhu, J., Chen, G., & Dong, L. (2020). Pb²⁺ Absorption Mechanism and Structure Characterization of Hydrochar and Pyrochar from Straw. *Nongye Jixie Xuebao/Transactions of the Chinese Society for Agricultural Machinery*, 51(12). <https://doi.org/10.6041/j.issn.1000-1298.2020.12.033>
- Liu, T., Guo, Y., Peng, N., Lang, Q., Xia, Y., Gai, C., & Liu, Z. (2017). Nitrogen transformation among char, tar and gas during pyrolysis of sewage sludge and corresponding hydrochar. *Journal of Analytical and Applied Pyrolysis*, 126. <https://doi.org/10.1016/j.jaap.2017.05.017>
- Liu, T., Liu, Z., Zheng, Q., Lang, Q., Xia, Y., Peng, N., & Gai, C. (2018). Effect of hydrothermal carbonization on migration and environmental risk of heavy metals in sewage sludge during pyrolysis. *Bioresource Technology*, 247. <https://doi.org/10.1016/j.biortech.2017.09.090>
- Liu, W., Jordan, C. M., Cherubini, F., Hu, X., & Fu, D. (2021). Environmental impacts assessment of wastewater treatment and sludge disposal systems under two sewage discharge standards: A case study in Kunshan, China. *Journal of Cleaner Production*, 287. <https://doi.org/10.1016/j.jclepro.2020.125046>
- Lu, B. Q., Willhammar, T., Sun, B. B., Hedin, N., Gale, J. D., & Gebauer, D. (2020). Introducing the crystalline phase of dicalcium phosphate monohydrate. *Nature Communications*, 11(1). <https://doi.org/10.1038/s41467-020-15333-6>
- Lu, L., Guest, J. S., Peters, C. A., Zhu, X., Rau, G. H., & Ren, Z. J. (2018). Wastewater treatment for carbon capture and utilization. <https://doi.org/10.1038/s41893-018-0187-9>
- Lucian, M., Merzari, F., Messineo, A., & Volpe, M. (2022). Hydrothermal Carbonization of Sludge Residues via Carborem C700 industrial Scale Continuous Operating Plant. *Chemical Engineering Transactions*, 92, 19–24. <https://doi.org/10.3303/CET2292004>
- Maaz, T. M. C., Hockaday, W. C., & Deenik, J. L. (2021). Biochar volatile matter and feedstock effects on soil nitrogen mineralization and soil fungal colonization. *Sustainability (Switzerland)*, 13(4). <https://doi.org/10.3390/su13042018>
- Maj, I., Kalisz, S., & Ciukaj, S. (2022). Properties of Animal-Origin Ash—A Valuable Material for Circular Economy. *Energies*, 15(4). <https://doi.org/10.3390/en15041274>
- Maletić, S., Isakovski, M. K., Sigmund, G., Hofmann, T., Hüffer, T., Beljin, J., & Rončević, S. (2022). Comparing biochar and hydrochar for reducing the risk of organic contaminants in polluted river sediments used for growing energy crops. *Science of The Total Environment*, 843, 157122. <https://doi.org/https://doi.org/10.1016/j.scitotenv.2022.157122>
- Malool, M. E., KeshavarzMoraveji, M., & Shayegan, J. (2022). Hydrothermal carbonization of digested sewage sludge coupled with Alkali activation: Integrated approach for sludge handling, optimized production, characterization and Pb(II) adsorption. *Journal of the Taiwan Institute of Chemical Engineers*, 133, 104203. <https://doi.org/10.1016/J.JTICE.2022.104203>

- Martins, S. (2003). *Unravelling the maillard reaction network by multiresponse kinetic modelling* (Doctoral dissertation) [WU-thesis no. 3402]. Wageningen University. Wageningen University.
- Marzbali, M. H., Kundu, S., Halder, P., Patel, S., Hakeem, I. G., Paz-Ferreiro, J., Madapusi, S., Surapaneni, A., & Shah, K. (2021). Wet organic waste treatment via hydrothermal processing: A critical review. *Chemosphere*, 279, 130557. <https://doi.org/10.1016/J.CHEMOSPHERE.2021.130557>
- Masoumi, S., Borugadda, V. B., Nanda, S., & Dalai, A. K. (2021). Hydrochar: A Review on Its Production Technologies and Applications. *Catalysts*, 11(8), 939. <https://doi.org/10.3390/catal11080939>
- Merzari, F., Goldfarb, J., Andreottola, G., Mimmo, T., Volpe, M., & Fiori, L. (2020). Hydrothermal carbonization as a strategy for sewage sludge management: Influence of process withdrawal point on hydrochar properties. *Energies*, 13(11). <https://doi.org/10.3390/en13112890>
- Merzari, F., Langone, M., Andreottola, G., & Fiori, L. (2019). Methane production from process water of sewage sludge hydrothermal carbonization. A review. Valorising sludge through hydrothermal carbonization. *Critical Reviews in Environmental Science and Technology*, 49(11). <https://doi.org/10.1080/10643389.2018.1561104>
- Metzger, M. (2005). The relationship between iron and ph. *Worldwide Drilling Resource, Janeiro*(January).
- Mierzwa-Hersztek, M., Gondek, K., Jewiarz, M., & Dziedzic, K. (2019). Assessment of energy parameters of biomass and biochars, leachability of heavy metals and phytotoxicity of their ashes. *Journal of Material Cycles and Waste Management*, 21(4). <https://doi.org/10.1007/s10163-019-00832-6>
- Mohammadi, A., Sandberg, M., Venkatesh, G., Eskandari, S., Dalgaard, T., Joseph, S., & Granström, K. (2019). Environmental analysis of producing biochar and energy recovery from pulp and paper mill biosludge. *Journal of Industrial Ecology*, 23(5). <https://doi.org/10.1111/jiec.12838>
- Mohammed, I. S., Na, R., Kushima, K., & Shimizu, N. (2020). Investigating the effect of processing parameters on the products of hydrothermal carbonization of corn stover. *Sustainability (Switzerland)*, 12(12). <https://doi.org/10.3390/su12125100>
- Monica, K. B., Parameswari, E., Davamani, V., Sivakumar, K., & Kalaiselvi, P. (2022). Hydrothermal Carbonization of Paper Mill ETP Sludge and Assessing its Potential Application in Agriculture. *Ecology, Environment and Conservation*. <https://doi.org/10.53550/eec.2022.v28i02s.078>
- Montgomery, D. C. (2013). *1.4 guidelines for designing experiments*. <https://app.knovel.com/hotlink/khtml/id:kt011B0NJ2/design-analysis-experiments/guidelines-designing>
- Mowla, D., Tran, H. N., & Allen, D. G. (2013). A review of the properties of biosludge and its relevance to enhanced dewatering processes. <https://doi.org/10.1016/j.biombioe.2013.09.002>
- Naderi, M., & Vesali-Naseh, M. (2021). Hydrochar-derived fuels from waste walnut shell through hydrothermal carbonization: characterization and effect of processing parameters. *Biomass Conversion and Biorefinery*, 11(5). <https://doi.org/10.1007/s13399-019-00513-2>
- Nanou, P., Sebastiani, F., de Legé, L., Pels, J., Driessen, W., & Kuipers, H. (2020). *Pilotonderzoek hydrothermale bewerking van zuiveringsslib met torwash®* (tech. rep.). STOWA. <https://www.stowa.nl/sites/default/files/assets/PUBLICATIES/Publicaties%5C%202020/STOWA%5C%202020-26%5C%20Torwash.pdf>
- Nelson, P. F., Buckley, A. N., & Kelly, M. D. (1992). Functional forms of nitrogen in coals and the release of coal nitrogen as NO_x precursors (HCN and NH₃). *Symposium (International) on Combustion*, 24(1), 1259–1267. [https://doi.org/https://doi.org/10.1016/S0082-0784\(06\)80148-7](https://doi.org/https://doi.org/10.1016/S0082-0784(06)80148-7)
- Nriagu, J. O. (1983). Saturnine gout among Roman aristocrats. Did lead poisoning contribute to the fall of the Empire? *The New England journal of medicine*, 308(11).
- Onay, O., & Kockar, O. M. (2003). Slow, fast and flash pyrolysis of rapeseed. *Renewable Energy*, 28(15), 2417–2433. [https://doi.org/10.1016/S0960-1481\(03\)00137-X](https://doi.org/10.1016/S0960-1481(03)00137-X)
- Ottosen, L. M., Kirkelund, G. M., & Jensen, P. E. (2013). Extracting phosphorous from incinerated sewage sludge ash rich in iron or aluminum. *Chemosphere*, 91(7), 963–969. <https://doi.org/10.1016/J.CHEMOSPHERE.2013.01.101>
- Ozgen, S., Cernuschi, S., & Caserini, S. (2021). An overview of nitrogen oxides emissions from biomass combustion for domestic heat production. *Renewable and Sustainable Energy Reviews*, 135. <https://doi.org/10.1016/j.rser.2020.110113>
- Padhye, L. P., Bandala, E. R., Wijesiri, B., Goonetilleke, A., & Bolan, N. (2022). Hydrochar: A Promising Step Towards Achieving a Circular Economy and Sustainable Development Goals. *Frontiers in Chemical Engineering*, 0, 33. <https://doi.org/10.3389/FCENG.2022.867228>

- Paiboonudomkarn, S., Wantala, K., Lubphoo, Y., & Khunphonoi, R. (2023). Conversion of sewage sludge from industrial wastewater treatment to solid fuel through hydrothermal carbonization process. *Materials Today: Proceedings*, 75, 85–90. <https://doi.org/https://doi.org/10.1016/j.matpr.2022.11.107>
- Pandey, A. K., & Prakash, R. (2019). Impact of Industrial Symbiosis on Sustainability. *Open Journal of Energy Efficiency*, 08(02). <https://doi.org/10.4236/ojee.2019.82006>
- Pearl GTL - overview. (n.d.). Retrieved June 2, 2022, from <https://www.shell.com/about-us/major-projects/pearl-gtl/pearl-gtl-an-overview.html>
- Peng, N., Li, Y., Liu, T., Lang, Q., Gai, C., & Liu, Z. (2017). Polycyclic Aromatic Hydrocarbons and Toxic Heavy Metals in Municipal Solid Waste and Corresponding Hydrochars. *Energy & Fuels*, 31(2), 1665–1671. <https://doi.org/10.1021/acs.energyfuels.6b02964>
- Peterson, A. A., Lachance, R. P., & Tester, J. W. (2010). Kinetic evidence of the maillard reaction in hydrothermal biomass processing: Glucose-glycine interactions in high-temperature, high-pressure water. *Industrial and Engineering Chemistry Research*, 49(5). <https://doi.org/10.1021/ie9014809>
- Qatarneh, A. F., Dupont, C., Michel, J., Simonin, L., Beda, A., Matei Ghimbeu, C., Ruiz-Villanueva, V., da Silva, D., Piégay, H., & Franca, M. J. (2021). River driftwood pretreated via hydrothermal carbonization as a sustainable source of hard carbon for Na-ion battery anodes. *Journal of Environmental Chemical Engineering*, 9(6). <https://doi.org/10.1016/j.jece.2021.106604>
- Rauret, G., López-Sánchez, J. F., Sahuquillo, A., Rubio, R., Davidson, C., Ure, A., & Quevauviller, P. (1999). Improvement of the BCR three step sequential extraction procedure prior to the certification of new sediment and soil reference materials. *Journal of Environmental Monitoring*, 1(1). <https://doi.org/10.1039/a807854h>
- Reißmann, D., Thrän, D., & Bezama, A. (2018). Hydrothermal processes as treatment paths for biogenic residues in Germany: A review of the technology, sustainability and legal aspects. <https://doi.org/10.1016/j.jclepro.2017.10.151>
- Ren, J., Wang, F., Zhai, Y., Zhu, Y., Peng, C., Wang, T., Li, C., & Zeng, G. (2017). Effect of sewage sludge hydrochar on soil properties and Cd immobilization in a contaminated soil. *Chemosphere*, 189. <https://doi.org/10.1016/j.chemosphere.2017.09.102>
- Reza, M. T., Freitas, A., Yang, X., & Coronella, C. J. (2016). Wet Air Oxidation of Hydrothermal Carbonization (HTC) Process Liquid. *ACS Sustainable Chemistry and Engineering*, 4(6), 3250–3254. <https://doi.org/10.1021/acssuschemeng.6b00292>
- Rodriguez, J. J., Ipiates, R. P., de la Rubia, M. A., Diaz, E., & Mohedano, A. F. (2021). Integration of hydrothermal carbonization and anaerobic digestion for energy recovery of biomass waste: An overview. <https://doi.org/10.1021/acs.energyfuels.1c01681>
- Ronsse, F., van Hecke, S., Dickinson, D., & Prins, W. (2013). Production and characterization of slow pyrolysis biochar: Influence of feedstock type and pyrolysis conditions. *GCB Bioenergy*, 5(2). <https://doi.org/10.1111/gcbb.12018>
- Roslan, S. Z., Zainudin, S. F., Mohd Aris, A., Chin, K. B., Musa, M., Mohamad Daud, A. R., & Syed Hassan, S. S. A. (2023). Hydrothermal Carbonization of Sewage Sludge into Solid Biofuel: Influences of Process Conditions on the Energetic Properties of Hydrochar. *Energies*, 16(5). <https://doi.org/10.3390/en16052483>
- Saadattalab, V., Wang, X., Szego, A. E., & Hedin, N. (2020). Effects of Metal Ions, Metal, and Metal Oxide Particles on the Synthesis of Hydrochars. *ACS Omega*, 5(11), 5601–5607. <https://doi.org/10.1021/acsomega.9b03926>
- Sangjumras, P., Udomsap, P., Kaewtrakulchai, N., Eiad-ua, A., Fuji, M., & Chutipaijit, S. (2018). Effects of transition metal during the hydrothermal carbonization on characteristics of carbon materials. *AIP Conference Proceedings*, 2010, 020014. <https://doi.org/10.1063/1.5053190>
- Sarkar, B., Mandal, S., Tsang, Y. F., Vithanage, M., Biswas, J. K., Yi, H., Dou, X., & Ok, Y. S. (2019). Sustainable sludge management by removing emerging contaminants from urban wastewater using carbon nanotubes. *Industrial and municipal sludge: Emerging concerns and scope for resource recovery*. <https://doi.org/10.1016/B978-0-12-815907-1.00024-6>
- Sarkar, D. K. (2015). Fuels and Combustion. *Thermal Power Plant*, 91–137. <https://doi.org/10.1016/B978-0-12-801575-9.00003-2>

- Schmidt, H., Bucheli, T., & Kammann, C. (2022). *Guidelines European Biochar Certificate for a sustainable production of biochar* (tech. rep.). https://www.european-biochar.org/media/doc/2/version_en_10_1.pdf
- Schmidt, H., & Wilson, K. (2014). The 55 uses of biochar. *the Biochar Journal 2014*. <https://www.biochar-journal.org/en/ct/2>
- Schneider, F., & Haderlein, S. B. (2016). Potential effects of biochar on the availability of phosphorus — mechanistic insights. *Geoderma*, 277, 83–90. <https://doi.org/10.1016/J.GEODERMA.2016.05.007>
- Scholz, M. (2006). Activated sludge processes. *Wetland Systems to Control Urban Runoff*, 115–129. <https://doi.org/10.1016/B978-044452734-9/50021-9>
- Sharma, H. B., Venna, S., & Dubey, B. K. (2021). Chapter 13 - Resource recovery and circular economy approach in organic waste management using hydrothermal carbonization. In V. Tyagi & K. Aboudi (Eds.), *Clean energy and resources recovery* (pp. 313–326). Elsevier. <https://doi.org/10.1016/B978-0-323-85223-4.00003-8>
- Sharma, R., Jasrotia, K., Singh, N., Ghosh, P., Srivastava, S., Sharma, N. R., Singh, J., Kanwar, R., & Kumar, A. (2020). A Comprehensive Review on Hydrothermal Carbonization of Biomass and its Applications. <https://doi.org/10.1007/s42250-019-00098-3>
- Shell. (2022). Blue hydrogen | Low-carbon energy | Shell Catalysts & Technologies | Shell Global. <https://www.shell.com/business-customers/catalysts-technologies/licensed-technologies/refinery-technology/shell-blue-hydrogen-process.html>
- Sheng, C., & Azevedo, J. L. (2005). Estimating the higher heating value of biomass fuels from basic analysis data. *Biomass and Bioenergy*, 28(5), 499–507. <https://doi.org/10.1016/J.BIOMBIOE.2004.11.008>
- Shi, Z., Usman, M., He, J., Chen, H., Zhang, S., & Luo, G. (2021). Combined microbial transcript and metabolic analysis reveals the different roles of hydrochar and biochar in promoting anaerobic digestion of waste activated sludge. *Water Research*, 205, 117679. <https://doi.org/10.1016/J.WATRES.2021.117679>
- Shimizu, T., & Toyono, M. (2007). Emissions of NO_x and N₂O during co-combustion of dried sewage sludge with coal in a circulating fluidized bed combustor. *Fuel*, 86(15), 2308–2315. <https://doi.org/10.1016/J.FUEL.2007.01.033>
- Singh, B., Dolk, M. M., Shen, Q., & Camps-Arbestain, M. (2017). Biochar pH, electrical conductivity and liming potential. *Biochar: A guide to analytical methods*.
- Staf, M., & Buryan, P. (2016). Slow pyrolysis of pre-dried sewage sludge. *Chemical Papers*, 70(11). <https://doi.org/10.1515/chempap-2016-0089>
- Stilo, A. (n.d.). Lead Poisoning and Rome. https://penelope.uchicago.edu/~grout/encyclopaedia_romana/wine/leadpoisoning.html
- Su, B.; Wang, G.; Li, R.; Xu, K.; Wu, J.; Li, D.; Liu, J., Su, B., Wang, G., Li, R., Xu, K., Wu, J., Li, D., & Liu, J. (2022). Co-Combustion Behavior of Paper Sludge Hydrochar and Pulverized Coal: Low Rank Coal and Its Product by Hydrothermal Carbonization. *Energies 2022, Vol. 15, Page 5619*, 15(15), 5619. <https://doi.org/10.3390/EN15155619>
- Sun, C., Guo, L., Zheng, Y., Yu, D., Jin, C., Zhao, Y., Yao, Z., Gao, M., & She, Z. (2021). The hydrolysis and reduction of mixing primary sludge and secondary sludge with thermophilic bacteria pretreatment. *Process Safety and Environmental Protection*, 156, 288–294. <https://doi.org/10.1016/J.PSEP.2021.10.026>
- Tarelho, L. A., Hauschild, T., Vilas-Boas, A. C., Silva, D. F., & Matos, M. A. (2020). Biochar from pyrolysis of biological sludge from wastewater treatment. *Energy Reports*, 6, 757–763. <https://doi.org/10.1016/J.EGYR.2019.09.063>
- Tasca, A. L., Puccini, M., Gori, R., Corsi, I., Galletti, A. M. R., & Vitolo, S. (2019). Hydrothermal carbonization of sewage sludge: A critical analysis of process severity, hydrochar properties and environmental implications. *Waste Management*, 93, 1–13. <https://doi.org/10.1016/j.wasman.2019.05.027>
- Tasca, A. L., Stefanelli, E., Raspolli Galletti, A. M., Gori, R., Mannarino, G., Vitolo, S., & Puccini, M. (2020). Hydrothermal Carbonization of Sewage Sludge: Analysis of Process Severity and Solid Content. *Chemical Engineering and Technology*, 43(12), 2382–2392. <https://doi.org/10.1002/ceat.202000095>

- Taskin, E., Branà, M. T., Altomare, C., & Loffredo, E. (2019). Biochar and hydrochar from waste biomass promote the growth and enzyme activity of soil-resident ligninolytic fungi. *Heliyon*, 5(7), e02051. <https://doi.org/10.1016/J.HELIYON.2019.E02051>
- Tchounwou, P. B., Yedjou, C. G., Patlolla, A. K., & Sutton, D. J. (2012). Heavy metal toxicity and the environment. <https://doi.org/10.1007/978-3-7643-8340-4>
- The Government of Japan. (2019). The Long-term Strategy under the Paris Agreement.
- Tran, T. K., Leu, H. J., Chiu, K. F., & Lin, C. Y. (2017). Electrochemical Treatment of Heavy Metal-containing Wastewater with the Removal of COD and Heavy Metal Ions. *Journal of the Chinese Chemical Society*, 64(5). <https://doi.org/10.1002/jccs.201600266>
- UNFCCC. (n.d.). Key aspects of the Paris Agreement. Retrieved June 14, 2022, from <https://unfccc.int/process-and-meetings/the-paris-agreement/the-paris-agreement/key-aspects-of-the-paris-agreement>
- Usman, K., Khan, S., Ghulam, S., Khan, M. U., Khan, N., Khan, M. A., & Khalil, S. K. (2012). Sewage Sludge: An Important Biological Resource for Sustainable Agriculture and Its Environmental Implications. *American Journal of Plant Sciences*, 03(12). <https://doi.org/10.4236/ajps.2012.312209>
- Vassilev, S. V., & Vassileva, C. G. (2009). A new approach for the combined chemical and mineral classification of the inorganic matter in coal. 1. Chemical and mineral classification systems. *Fuel*, 88(2). <https://doi.org/10.1016/j.fuel.2008.09.006>
- Vassilev, S. V., Vassileva, C. G., Song, Y. C., Li, W. Y., & Feng, J. (2017). Ash contents and ash-forming elements of biomass and their significance for solid biofuel combustion. <https://doi.org/10.1016/j.fuel.2017.07.036>
- Villamil, J. A., Diaz, E., de la Rubia, M. A., & Mohedano, A. F. (2020). Potential use of waste activated sludge hydrothermally treated as a renewable fuel or activated carbon precursor. *Molecules*, 25(15). <https://doi.org/10.3390/molecules25153534>
- Vlahov, A. (2021). XRD graphitization degrees: A review of the published data and new calculations, correlations, and applications. *Geologica Balcanica*, 50(1). <https://doi.org/10.52321/GeolBalc.50.1.11>
- Volpe, M., Fiori, L., Merzari, F., Messineo, A., & Andreottola, G. (2020). Hydrothermal carbonization as an efficient tool for sewage sludge valorization and phosphorous recovery. *Chemical Engineering Transactions*, 80. <https://doi.org/10.3303/CET2080034>
- Wan, W., Zhao, W., Wu, Y., Dai, C., Zhu, X., Wang, Y., Qin, J., Chen, T., & Lü, Z. (2020). A highly efficient biomass based electrocatalyst for cathodic performance of lithium–oxygen batteries: Yeast derived hydrothermal carbon. *Electrochimica Acta*, 349. <https://doi.org/10.1016/j.electacta.2020.136411>
- Wang, C., Wang, Y., & Herath, H. M. (2017). Polycyclic aromatic hydrocarbons (PAHs) in biochar – Their formation, occurrence and analysis: A review. *Organic Geochemistry*, 114, 1–11. <https://doi.org/10.1016/J.ORGGEOCHEM.2017.09.001>
- Wang, J., Cai, J., Wang, S., Zhou, X., Ding, X., Ali, J., Zheng, L., Wang, S., Yang, L., Xi, S., Wang, M., & Chen, Z. (2022). Biochar-based activation of peroxide: multivariate-controlled performance, modulatory surface reactive sites and tunable oxidative species. <https://doi.org/10.1016/j.cej.2021.131233>
- Wang, J., Odinga, E. S., Zhang, W., Zhou, X., Yang, B., Waigi, M. G., & Gao, Y. (2019). Polyaromatic hydrocarbons in biochars and human health risks of food crops grown in biochar-amended soils: A synthesis study. *Environment International*, 130, 104899. <https://doi.org/10.1016/J.ENVINT.2019.06.009>
- Wang, J., Lv, W., Ren, Q., Yan, L., Zhang, L., & Shi, Z. (2021). High-performance hard carbon anode prepared via an ingenious green-hydrothermal route. *Applied Surface Science*, 558. <https://doi.org/10.1016/j.apsusc.2021.149824>
- Wang, J., Yan, L., Ren, Q., Fan, L., Zhang, F., & Shi, Z. (2018). Facile hydrothermal treatment route of reed straw-derived hard carbon for high performance sodium ion battery. *Electrochimica Acta*, 291, 188–196. <https://doi.org/10.1016/j.electacta.2018.08.136>
- Wang, L., Chang, Y., & Li, A. (2019). Hydrothermal carbonization for energy-efficient processing of sewage sludge: A review. *Renewable and Sustainable Energy Reviews*, 108, 423–440. <https://doi.org/10.1016/j.rser.2019.04.011>

- Wang, L., Chang, Y., & Liu, Q. (2019). Fate and distribution of nutrients and heavy metals during hydrothermal carbonization of sewage sludge with implication to land application. *Journal of Cleaner Production*, 225, 972–983. <https://doi.org/10.1016/j.jclepro.2019.03.347>
- Wang, L., Fan, X., Wang, S., & Chang, Y. (2023). High fixed carbon and low ash hydrochar production from sewage sludge with addition of phloroglucinol: Theoretical modeling of reaction mechanism using density functional theory. *Fuel Processing Technology*, 244, 107703. <https://doi.org/https://doi.org/10.1016/j.fuproc.2023.107703>
- Wang, L., Zhang, L., & Li, A. (2014). Hydrothermal treatment coupled with mechanical expression at increased temperature for excess sludge dewatering: Influence of operating conditions and the process energetics. *Water Research*, 65. <https://doi.org/10.1016/j.watres.2014.07.020>
- Wang, R., Wang, C., Zhao, Z., Jia, J., & Jin, Q. (2019). Energy recovery from high-ash municipal sewage sludge by hydrothermal carbonization: Fuel characteristics of biosolid products. *Energy*, 186, 115848. <https://doi.org/10.1016/J.ENERGY.2019.07.178>
- Wang, T., Zhai, Y., Zhu, Y., Li, C., & Zeng, G. (2018). A review of the hydrothermal carbonization of biomass waste for hydrochar formation: Process conditions, fundamentals, and physicochemical properties. *Renewable and Sustainable Energy Reviews*, 90, 223–247. <https://doi.org/10.1016/J.RSER.2018.03.071>
- Wang, W., Chen, W. H., & Jang, M. F. (2020). Characterization of hydrochar produced by hydrothermal carbonization of organic sludge. *Future Cities and Environment*, 6. <https://doi.org/10.5334/fce.102>
- Wei, J., Liu, Y., Li, J., Yu, H., & Peng, Y. (2018). Removal of organic contaminant by municipal sewage sludge-derived hydrochar: Kinetics, thermodynamics and mechanisms. *Water Science and Technology*, 78(4), 947–956. <https://doi.org/10.2166/wst.2018.373>
- Wen, Q., Li, C., Cai, Z., Zhang, W., Gao, H., Chen, L., Zeng, G., Shu, X., & Zhao, Y. (2011). Study on activated carbon derived from sewage sludge for adsorption of gaseous formaldehyde. *Bioresource Technology*, 102(2). <https://doi.org/10.1016/j.biortech.2010.09.042>
- Wiedner, K., Naisse, C., Rumpel, C., Pozzi, A., Wieczorek, P., & Glaser, B. (2013). Chemical modification of biomass residues during hydrothermal carbonization - What makes the difference, temperature or feedstock? *Organic Geochemistry*, 54. <https://doi.org/10.1016/j.orggeochem.2012.10.006>
- Wray, H. (2022). Pre-treatment of wet and complex biomass. https://www.ieabioenergy.com/wp-content/uploads/2022/10/1-3_Wray-TNO.pdf
- Xing, P., Mason, P. E., Chilton, S., Lloyd, S., Jones, J. M., Williams, A., Nimmo, W., & Pourkashanian, M. (2016). A comparative assessment of biomass ash preparation methods using X-ray fluorescence and wet chemical analysis. *Fuel*, 182. <https://doi.org/10.1016/j.fuel.2016.05.081>
- Xu, Y., Bai, T., Yan, Y., & Ma, K. (2020). Influence of sodium hydroxide addition on characteristics and environmental risk of heavy metals in biochars derived from swine manure. *Waste Management*, 105. <https://doi.org/10.1016/j.wasman.2020.02.035>
- Xu, Z., Wang, J., Guo, Z., Xie, F., Liu, H., Yadegari, H., Tebyetekerwa, M., Ryan, M. P., Hu, Y. S., & Titirici, M. M. (2022). The Role of Hydrothermal Carbonization in Sustainable Sodium-Ion Battery Anodes. *Advanced Energy Materials*. <https://doi.org/10.1002/aenm.202200208>
- Yang, J., Ji, G., Gao, Y., Fu, W., Irfan, M., Mu, L., Zhang, Y., & Li, A. (2020). High-yield and high-performance porous biochar produced from pyrolysis of peanut shell with low-dose ammonium polyphosphate for chloramphenicol adsorption. *Journal of Cleaner Production*, 264, 121516. <https://doi.org/https://doi.org/10.1016/j.jclepro.2020.121516>
- Yang, L., Shuang, E., Liu, J., Sheng, K., & Zhang, X. (2022). Endogenous calcium enriched hydrochar catalyst derived from water hyacinth for glucose isomerization. *Science of the Total Environment*, 807. <https://doi.org/10.1016/j.scitotenv.2021.150660>
- Yi, S., Witt, B., Chiu, P., Guo, M., & Imhoff, P. (2015). The Origin and Reversible Nature of Poultry Litter Biochar Hydrophobicity. *Journal of Environmental Quality*, 44(3). <https://doi.org/10.2134/jeq2014.09.0385>
- Yin, S., Zhang, X., Suo, F., You, X., Yuan, Y., Cheng, Y., Zhang, C., & Li, Y. (2022). Effect of biochar and hydrochar from cow manure and reed straw on lettuce growth in an acidified soil. *Chemosphere*, 298. <https://doi.org/10.1016/j.chemosphere.2022.134191>

- Yue, Y., Yao, Y., Lin, Q., Li, G., & Zhao, X. (2017). The change of heavy metals fractions during hydrochar decomposition in soils amended with different municipal sewage sludge hydrochars. *Journal of Soils and Sediments*, 17(3), 763–770. <https://doi.org/10.1007/s11368-015-1312-2>
- Zang, Z., Li, Z., Lu, X., Liang, J., Wang, J., Cui, H. L., & Yan, S. (2021). Terahertz spectroscopy for quantification of free water and bound water in leaf. *Computers and Electronics in Agriculture*, 191, 106515. <https://doi.org/10.1016/J.COMPAG.2021.106515>
- Zhai, Y., Liu, X., Zhu, Y., Peng, C., Wang, T., Zhu, L., Li, C., & Zeng, G. (2016). Hydrothermal carbonization of sewage sludge: The effect of feed-water pH on fate and risk of heavy metals in hydrochars. *Bioresource Technology*, 218. <https://doi.org/10.1016/j.biortech.2016.06.085>
- Zhang, D., Angelotti, B., Schlosser, E., Novak, J. T., & Wang, Z. W. (2020). Using cerium chloride to control soluble orthophosphate concentration and improve the dewaterability of sludge: Part I. Mechanistic understanding. *Water Environment Research*, 92(3), 320–330. <https://doi.org/10.1002/WER.1142>
- Zhang, J. H., Lin, Q. M., & Zhao, X. R. (2014). The hydrochar characters of municipal sewage sludge under different hydrothermal temperatures and durations. *Journal of Integrative Agriculture*, 13(3). [https://doi.org/10.1016/S2095-3119\(13\)60702-9](https://doi.org/10.1016/S2095-3119(13)60702-9)
- Zhang, S., Sheng, K., Liang, Y., Liu, J., E, S., & Zhang, X. (2020). Green synthesis of aluminum-hydrochar for the selective isomerization of glucose to fructose. *Science of the Total Environment*, 727. <https://doi.org/10.1016/j.scitotenv.2020.138743>
- Zhang, X., Chen, S., Ai, F., Jin, L., Zhu, N., & Meng, X. Z. (2022). Identification of industrial sewage sludge based on heavy metal profiles: a case study of printing and dyeing industry. *Environmental Science and Pollution Research*, 29(8). <https://doi.org/10.1007/s11356-021-16569-5>
- Zhang, Y., Qin, J., & Yi, Y. (2021). Biochar and hydrochar derived from freshwater sludge: Characterization and possible applications. *Science of the Total Environment*, 763. <https://doi.org/10.1016/j.scitotenv.2020.144550>
- Zhang, Z., Zhu, Z., Shen, B., & Liu, L. (2019). Insights into biochar and hydrochar production and applications: A review. *Energy*, 171, 581–598. <https://doi.org/10.1016/J.ENERGY.2019.01.035>
- Zhu, F., Hoehn, R., Thakkar, V., & Yuh, E. (2016). Description of Hydrocracking Process. *Hydroprocessing for Clean Energy*, 51–78. <https://doi.org/10.1002/9781119328261.CH4>
- Zhu, K., Liu, Q., Dang, C., Li, A., & Zhang, L. (2021). Valorization of hydrothermal carbonization products by anaerobic digestion: Inhibitor identification, biomethanization potential and process intensification. *Bioresource Technology*, 341. <https://doi.org/10.1016/j.biortech.2021.125752>
- Zhu, Y., Wei, J., Liu, Y., Liu, X., Li, J., & Zhang, J. (2019). Assessing the effect on the generation of environmentally persistent free radicals in hydrothermal carbonization of sewage sludge. *Scientific Reports*, 9(1). <https://doi.org/10.1038/s41598-019-53781-3>
- Zhuang, X., Huang, Y., Liu, H., Yuan, H., Yin, X., & Wu, C. (2018). Relationship between physicochemical properties and dewaterability of hydrothermal sludge derived from different source. *Journal of Environmental Sciences (China)*, 69. <https://doi.org/10.1016/j.jes.2017.10.021>
- Zhuang, X., Liu, J., Zhang, Q., Wang, C., Zhan, H., & Ma, L. (2022). A review on the utilization of industrial biowaste via hydrothermal carbonization. *Renewable and Sustainable Energy Reviews*, 154, 111877. <https://doi.org/10.1016/j.rser.2021.111877>